

TWO-PHASE SENSORLESS BRUSHLESS DC MOTOR DESIGN AND CONTROL

Researched by:

EYNASS TURKI DIAB

HANI AL-SAYYED

Supervisor:

Dr. SAMEER HANNA KHADER



PALESTINE POLYTECHNIC UNIVERSITY

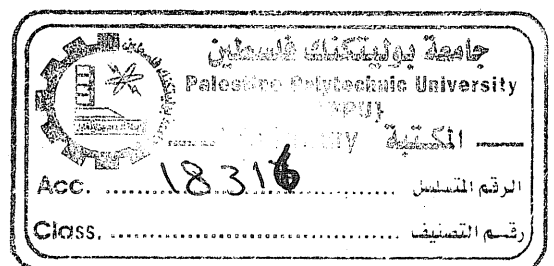
COLLEGE OF ENGINEERING AND TECHNOLOGY

DEPARTMENT OF ELECTRICAL AND COMPUTER ENGINEERING

INDUSTRIAL AUTOMATION ENGINEERING

HEBRON - PALESTINE

February, 2005



PALESTINE POLYTECHNIC UNIVERSITY
Hebron-Palestine

COLLEGE OF ENGINEERING AND TECHNOLOGY
DEPARTMENT OF ELECTRICAL AND COMPUTER ENGINEERING

Graduation Project Evaluation
TWO-PHASE SENSORLESS BRUSHLESS DC
MOTOR
DESIGN AND CONTROL


Researched by:

EYNASS TURKI DIAB

HANI MOHAMAD AL-SAYYED

According to the system of the College of Engineering and Technology, and to the recommendation of the Project Supervisor and with agreement of the testing group, this project is presented to Electrical and Computer Engineering Department as a part of requirements of B.Sc. degree in Electrical Engineering – Industrial Automation Engineering.

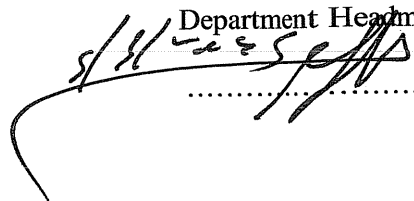
Project Supervisor signature


.....
ع.د. ت.ك. دياب

Testing Group signature

 28.2.2005
.....

Department Headmaster signature


.....

DEDICATION

To our parents who waited so long.

To our brothers and sisters.

To the spirits of the Martyrs on the land of Palestine and away from it.

To our instructors and friends.

To our supervisor Dr. Sameer Hanna Khader.

We dedicate this humble effort.

Eynass T. Diad

Hani M. AL_Sayyed

ACKNOWLEDGMENT

We wish to express our great thanks to the many people who have contributed directions and suggestions, particularly Dr. Sameer Hanna Khader who was, as always, the rock solid man behind completing the project. We highly appreciate the feedback offered by him.

We repeat our thanks to Dr. Abdel_Karim Daud, and Eng. Nizar Amro and Eng. Moudar Al_Swate and Eng. Hamza Jraiwy and Eng. Baha` Mahasneh and Mr. Ra`ed Abu Marghia, for their essential suggestions and contributions to this project.

Above all, we are indebted to all those instructors at Electrical Department in Palestine Polytechnic University.

Thanks are also due to our colleagues in the department who have helped us with their supporting comments to bring the project to existence by the grace of Allah.

ABSTRACT

This project describe mathematical method which look for optimized electromagnetic torque with reduced ripple in both single-phase and two-phase brushless dc motor with special rotor construction . The conventional two-phase two-pulse brushless dc motor requires special construction with aim to realize successful starting and ensuring relatively constant torque independent of the rotor position . Three methods are described:

1. Pulse Width Modulation (PWM) control strategy with skewed stator poles, which introduce unsymmetrical airgap magnetic, permance and thus additional reluctance torque eliminated low-order current harmonics.
2. PWM control strategy with symmetrical stator poles and shorted coil pitch.
3. Combined PWM and continuous control signal energized two-phase three-winding motor and unsymmetrical rotor construction, where it is expected producing electromagnetic torque with reduced ripples and increasing stability, independent of the rotor position.

The electromagnetic torque produced by motors using each of these methods is calculated by applying Coenergy method. The numerically obtained results are going to be verified with experimental results, and it is expected to obtained good coincidence between these results.

Table of Contents

| | |
|----------------------|-----|
| Detection..... | ii |
| Acknowledgement..... | iii |
| Abstract..... | iv |
| Continents..... | v |
| List of figure..... | xi |
| List of Tables..... | xv |

Chapter One: Introduction

| | |
|--|----|
| 1.1 Overview of brushless | 1 |
| 1.2. Introduction..... | 5 |
| 1.2.1. Construction and Principle of Operation..... | 5 |
| 1.2.1.1. Principle..... | 5 |
| 1.2.1.2. Basic Structures..... | 6 |
| 1.2.1.3. Comparison of conventional and brushless dc motors..... | 7 |
| 1.2.1.4. Stator..... | 7 |
| 1.2.1.5. Rotor..... | 9 |
| 1.2.2. Motor function..... | 10 |
| 1.3. Overview of Signal Feedback Devices..... | 11 |
| 1.3.1. Hall-Effect Sensors..... | 11 |
| 1.3.2. DC Tachometer (brush-type)..... | 11 |
| 1.3.3. Brushless Tachometer..... | 12 |
| 1.3.4. Resolver..... | 12 |
| 1.3.5. Synchro..... | 12 |
| 1.3.6. Tachsyn..... | 13 |
| 1.3.7. Encoder..... | 13 |
| 1.4. Time Plan..... | 14 |
| 1.5. Estimated Cost..... | 15 |

Chapter Two: Brushless DC Motor Classification

| | |
|--|----|
| 2.1. Introduction..... | 16 |
| 2.2. Brushless Motor Operation..... | 17 |
| 2.3. Brushless DC Motor Classification..... | 20 |
| 2.3.1. Introduction..... | 20 |
| 2.3.2. Multi-Phase BPM Motor..... | 20 |
| 2.3.3. Non-Linear Finite Element Analysis..... | 22 |
| 2.3.3.1. Three-Phase BPM Motor with 120° Conduction..... | 22 |
| 2.3.3.2. Three-Phase BPM Motor with 180° Conduction..... | 22 |
| 2.3.3.3. Two-Phase BPM Motor with 180° Conduction..... | 24 |
| 2.3.3.4. Five-Phase BPM Motor with 144° Conduction..... | 24 |
| 2.3.3.5. Five-Phase BPM Motor with 180° Conduction..... | 25 |
| 2.3.4. Conclusion..... | 25 |

Chapter Three: Classification of electrical motor

| | |
|---|----|
| 3.1. DC Motors..... | 26 |
| 3.1.1. Introduction to DC Motors..... | 26 |
| 3.1.2. Principle of Operation..... | 27 |
| 3.1.3. DC Motor Characteristics..... | 27 |
| 3.1.4. Types of DC Motors | 27 |
| 3.1.4.1. Series-wound motors..... | 28 |
| 3.1.4.2. Shunt-wound motors..... | 28 |
| 3.1.4.3. Compound-wound motors..... | 29 |
| 3.1.5. Summary..... | 29 |
| 3.2. AC Motors..... | 30 |
| 3.2.1. Introduction to AC Motors..... | 30 |
| 3.2.2. Principles of Operation..... | 30 |
| 3.2.3. Types of AC Motors..... | 30 |
| 3.2.3.1. Series (Universal) AC Motors | 31 |
| 3.2.3.2. Synchronous AC Motor..... | 31 |

| | |
|--|----|
| 3.2.3.3. Induction AC Motors..... | 31 |
| 3.3. Linear Motors..... | 31 |
| 3.3.1. Linear Synchronous Motors..... | 32 |
| 3.3.2. DC linear Motors..... | 32 |
| 3.4. Step (Stepper) Motors..... | 32 |
| 3.4.1. Introduction to Step Motors..... | 32 |
| 3.4.2. Types of Step Motors and how they work..... | 32 |
| 3.4.2.1. Variable Reluctance (VR) Motor..... | 33 |
| 3.4.2.2. PM Motor..... | 33 |
| 3.4.2.3. Hybrid Motor..... | 33 |
| 3.4.3. Summary..... | 33 |
| 3.5. Servo Motors..... | 34 |
| 3.5.1. Summary..... | 34 |

Chapter four: Control Brushless DC Motor

| | |
|--|----|
| 4.1. Introduction | 35 |
| 4.2. Different between sensor and sensorless | 36 |
| 4.2.1. Rotation-Sensor Technologies..... | 36 |
| 4.2.1.1. Hall-Effect Rotation Sensors..... | 36 |
| 4.2.1.2. Optical Encoders..... | 37 |
| 4.3. Sensorless Motor Control..... | 38 |
| 4.3.1. Existing Approaches..... | 38 |
| 4.3.1.1. Back-EMF sensing..... | 38 |
| 4.4. Sensor control of brushless dc motor..... | 39 |
| 4.4.1. General block diagram..... | 39 |
| 4.4.1.1 Open loop control system..... | 39 |
| 4.4.1.2. Closed loop control system..... | 40 |
| 4.5. Sensorless control of BLDC Motor..... | 41 |
| 4.5.1. Open loop control of BLDC motor with back emf strategy..... | 41 |
| 4.5.2. Closed loop control of BLDC motor with back emf strategy..... | 42 |

| | |
|---|----|
| 4.5.3. General block diagram of sensorless..... | 43 |
| 4.6. Back emf construction circuit (Sensorless)..... | 44 |
| 4.7. Efficiency..... | 48 |
| 4.8. Information about components..... | 49 |
| 4.8.1. High isolation current..... | 49 |
| 4.8.2. Typical applications..... | 50 |
| 4.8.3. Protection and interface of PC..... | 51 |
| 4.8.4. Resistors (R1 & R2) are for current limited..... | 52 |
| 4.8.5. Mosfet..... | 52 |
| 4.8.6. Tachogenerator..... | 52 |
| 4.8.7 Inverter Signals Isolation..... | 53 |
| 4.8.8. The converter..... | 55 |
| 4.8.8.1 Transformer..... | 55 |
| 4.8.8.2. Rectifier..... | 56 |
| 4.8.8.3. Inverter..... | 56 |
| 4.9. Total Circuit | 57 |
| 4.10. Flow Chart | 59 |

Chapter Five: Design and Simulation of Brushless DC Motor

| | |
|---|----|
| 5.1. Introduction..... | 60 |
| 5.2. Analysis..... | 61 |
| 5.2.1: Motor windings and the Phase current..... | 61 |
| 5.2.2: Electromagnetic Torque | 68 |
| 5.2.2.1. Unsymmetrical rotor construction..... | 68 |
| 5.2.2.2. Combined control method | 71 |
| 5.3. Results | 74 |
| 5.4. Conclusion..... | 79 |
| 5.5. Study and comparing some of electromagnetic parameters | 80 |

Chapter Six: Theoretical Background and constructions motor

| | |
|---|-----|
| 6.1 Introduction..... | 89 |
| 6.2 Equivalent Circuit and General Equations..... | 89 |
| 6.3 Performance of Brushless DC Motor..... | 91 |
| 6.3.1 Efficiency..... | 92 |
| 6.4 Calculation of construction motor..... | 92 |
| 6.4.1 Classification of Motors | 92 |
| 6.4.2 Calculation of Stator Parameters..... | 93 |
| 6.4.3 Calculation of magnetic..... | 95 |
| 6.5 Motor Construction..... | 102 |
| 6.5.1 Stator..... | 102 |
| 6.5.2 Permanent magnet rotor..... | 105 |
| 6.6 How the motor operates..... | 106 |

Chapter Seven: Software system design

| | |
|--|-----|
| 7.1 Initializations..... | 108 |
| 7.1.1 Determining the mission of each MOSFET of the inverter..... | 108 |
| 7.1.2 Calculating the hex codes for each phase in both directions..... | 109 |
| 7.2 Parallel Port..... | 109 |
| 7.2.1 Introduction to Parallel Port..... | 109 |
| 7.2.2 Parallel Port Hardware Properties | 109 |
| 7.2.3 Port Addresses | 111 |
| 7.2.4 How to Connect Circuits to Parallel Port..... | 112 |
| 7.2.5 How to Calculate Your Own Values to Send To Program..... | 113 |
| 7.2.6 Interfacing Circuit of Diode Clamped Multilevel inverter..... | 113 |
| 7.2.7 This table is explained as the following..... | 115 |
| 7.2.8 The program works as the following..... | 115 |
| 7.3 Calculation of PWM by Program..... | 117 |

| | |
|--------------------------------|-----|
| 7.3.1 The equation of PWM..... | 118 |
|--------------------------------|-----|

Chapter Eight :Conclusion and Recommendation

| | |
|----------------------------|-----|
| 8.1 Conclusion..... | 120 |
| 8.2 Results..... | 121 |
| 8.3 Recommendation..... | 125 |
| References..... | 126 |
| Appendix (A, B, C, D)..... | 126 |
| Appendix (A)..... | 128 |
| List of symbols..... | |
| Appendix (B)..... | 132 |
| Motor Construction..... | |
| Appendix (C)..... | 147 |
| Data Sheets..... | |
| Appendix (D)..... | 162 |
| Software Program..... | |

List of figures

Chapter One

| | |
|--|----|
| Figure (1.1): Disassembled view of a brushless dc motor..... | 6 |
| Figure (1.2): Brushless dc motor = Permanent magnet ac motor + Electronic commutator..... | 6 |
| Figure (1.3): Two-phase motor having auxiliary salient poles..... | 7 |
| Figure (1.4): Trapezoidal Back EMF..... | 8 |
| Figure (1.5): Sinusoidal Back EMF..... | 9 |
| Figure (1.6): Rotor Magnet Cross Section..... | 10 |

Chapter Two

| | |
|--|----|
| Figure (2.1.): Models used for simulation of 3-phase, 2-phase. And 5-phase BPM motors..... | 21 |
| Figure (2.2): Current waveforms..... | 21 |
| Figure (2.3): Static torque characteristic for 3-phase BPM motor..... | 22 |
| Figure (2.4): Motoring torque (static) | 23 |
| Figure (2.5): Motoring torque (static) for 3-phase BPM motor Supplied With 180° Pulses of current for 3-phase BPM motor supplied with 120° Conduction..... | 23 |
| Figure (2.6) Motoring torque (static) for 2-phase BPM motor supplied with 180°Pulses of current..... | 24 |
| Figure (2.7) Motoring torque (static) for 5-phase BPM motor supplied with Pulses of current° 144..... | 25 |

Chapter Three

| | |
|---|----|
| Figure (3.1): Typical speed –torque curve for series wound motor..... | 28 |
| Figure (3.2): Typical speed-torque curve for shunt wound motors..... | 28 |
| Figure (3.3): Typical speed-torque curve for compound wound motors..... | 29 |

Chapter Four

| | |
|--|----|
| Figure (4.1): Hall-Effect sensor..... | 36 |
| Figure (4.2): optical encoder sensing..... | 37 |
| Figure (4.3): Open loop control system..... | 39 |
| Figure (4.4): Closed loop control system..... | 40 |
| Figure (4.5): Open loop control of BLDC motor with back emf strategy..... | 42 |
| Figure (4.6): Closed loop control system..... | 42 |
| Figure (4.7): Control system Block diagram of sensorless..... | 43 |
| Figure (4.8): Emf signal and current waveform relationship..... | 44 |
| Figure (4.9): Control of back emf circuit diagram..... | 45 |
| Figure (4.10): waveforms of sensorless circuit | 46 |
| Figure (4.11): voltage wave (amp A)..... | 46 |
| Figure (4.12): voltage wave (amp A, B)..... | 46 |
| Figure (4.13): current wave (amp A)..... | 46 |
| Figure (4.14): voltage wave (amp A)..... | 47 |
| Figure (4.15): Pin configuration of HCPL7840 opt isolator..... | 49 |
| Figure (4.16): High current isolation circuit..... | 51 |
| Figure (4.17): optisolator circuit input from control circuit and Output to PC..... | 51 |
| Figure (4.18): Optoisolator circuit - input from PC And output to Mosfet..... | 52 |
| Figure (4.19): Tachogenerator diagram..... | 53 |
| Figure (4.20): One-phase bridge isolation of power circuit | 54 |
| Figure (4.21): Inverter diagram | 57 |
| Figure (4.22): The total system | 58 |

Chapter Five

| | |
|---------------------------------------|----|
| Figure (5.1): Motor construction..... | 62 |
|---------------------------------------|----|

| | |
|--|-------|
| Figure (5.2) :a) Magnetic permance at variable airgap and symmetrical located Slots and b) the obtained harmonic spectrum..... | 63 |
| Figure (5.3a): Electrical circuit..... | 64 |
| Figure (5.3b): Pulse generation wave form-illustration..... | 64 |
| Figure (5.4): Phase current of both coils S1 & S2..... | 65 |
| Figure (5.5): Phase voltage of coil S3..... | 66 |
| Figure (5.6): a) phase current of S3 at speed of n1 and b) Current harmonic spectrum Ic..... | 68 |
| Figure (5.7): Total Electromagnetic torque of coils S1 & S2..... | 71 |
| Figure (5.8): Total electromagnetic torque of S3..... | 73 |
| Figure (5.9): a) the total electromagnetic torque of both coils S1, S2 & S3; b) The torque harmonic spectrum..... | 73/74 |
| Figure (5.10): a) The mean torque; b) Torque-Current ratio; c) Torque ripples factor; and d) Current harmonic factor Versus signal width. β | 76/77 |
| Figure (5.11): a) Motor means torque; b) Torque-Current ratio. c) Torque ripples factor; and d) Current harmonic factor Versus slots width B5, mm..... | 78 |
| Figure (5.A5): a) Mean torque ratio; b) Torque-current ratio; c) 2nd torque harmonic ratio; and d) Torque ripples Ratio- versus the signal width β | 83/84 |
| Figure (5.A1): Magnetic permance at a) case#1; b) Case#2, and c) case#3..... | 84/85 |
| Figure (5.A2): harmonic spectrum of Magnetic permance for the same cases At a) case#case#2and c) case# 3..... | 85/86 |
| Figure (5.A3): The total electromagnetic torque at four cases: a) case#1; b) case#2; c) case#3; and d) case#4..... | 86/87 |
| Figure (5.A4): The harmonic spectrum of produced electromagnetic toque at the same cases:case#1; b) case#2; c) case#3; and d) case#4..... | 87/88 |

Chapter Six

| | |
|--|-----|
| Figure (6.1): Steady State Equivalent Circuit per phase..... | 90 |
| Figure (6.2): Cross section of the stator..... | 94 |
| Figure (6.3): Rotor cross section..... | 99 |
| Figure (6.4): Stator windings construction..... | 103 |
| Figure (6.5): One-phase connection..... | 103 |
| Figure (6.6): Coil 3 Connection..... | 104 |
| Figure (6.7): Stator construction..... | 104 |
| Figure (6.8): Rotor construction..... | 105 |
| Figure (6.9): the 2-phase BDC motor..... | 106 |
| Figure (6.10): The total electromagnetic torque of both phases 1, 2, & coil 3..... | 107 |

Chapter Seven

| | |
|--|-----|
| Figure (7.1): Parallel Port Pins..... | 110 |
| Figure (7.2): the interfacing circuit per phase..... | 114 |
| Figure (7.3): Wave of PWM as sinusoidal..... | 117 |
| Figure (7.4): The shape of PWM..... | 118 |

Chapter Eight

| | |
|--|-----|
| Figure (8.1): The relation of efficiency and Torque..... | 121 |
| Figure (8.2): The relation of efficiency and P_{out} | 122 |
| Figure (8.3): The relation of Speed and Torque..... | 122 |
| Figure (8.4): The wave of Current with ohme load..... | 123 |
| Figure (8.5): The Wave of PWM..... | 123 |
| Figure (8.6): The Wave of current with Phase one..... | 124 |
| Figure (8.7): The Wave of Current..... | 124 |

List of Tables

| | |
|---|-----|
| Table (1.1): Estimated cost..... | 15 |
| Table (5.1): The motor parameters..... | 77 |
| Cases as well shown on Table (5.A1)..... | 81 |
| Table (6.1): Properties of Motors | 93 |
| Table (6.2): Magnetic Parameter..... | 101 |
| Table (7.1): Inverter MOSFET's missions..... | 108 |
| Table (7.2): bidirectional motor operation codes..... | 109 |
| Table (7.3): Pin Assignments of the D-Type 25 pin Parallel Port Connector.... | 110 |
| Table (7.4): Port Addresses..... | 112 |
| Table (7.5): Represent the motor work using the program..... | 114 |
| Table (7.6): Definition Symbols..... | 119 |
| Table (8.1): the result | 121 |

Chapter One

Introduction

1.1 Overview.

1.2. Introduction.

1.3. Overview of Signal Feedback Devices.

1.4. Time Plan.

1.5. Estimated Cost.

Chapter One

Introduction

1.1 Overview

The brushed DC motor is one of the earliest motor designs. Today, it is the motor of choice in the majority of variable speed and torque control applications the design of the brushed DC motor is quite simple. A permanent magnetic field is created in the stator by either of two means

- Permanent magnets
- Electro-magnetic windings.

If the field is created by permanent magnets, the motor is said to be a "permanent magnet DC motor" (PMDC). If created by electromagnetic windings, the motor is often said to be a "shunt wound DC motor" (SWDC). Today, because of cost-effectiveness and reliability, the PMDC motor is the motor of choice for applications involving fractional horsepower DC motors, as well as most applications up to about three horsepower.

At five horsepower and greater, various forms of the shunt wound DC motor are most commonly used. This is because the electromagnetic windings are more cost effective than permanent magnets in this power range.

Caution: If a DC motor suffers a loss of field (if for example, the field power connections are broken), the DC motor will immediately begin to accelerate to the top speed which the loading will allow. This can result in the motor flying apart if the motor is lightly loaded. The possible loss of field must be accounted for, particularly with shunt wound DC motors.

Opposing the stator field is the armature field, which is generated by a changing electromagnetic flux coming from windings located on the rotor. The magnetic poles of the armature field will attempt to line up with the opposite magnetic poles generated by the stator field. If we stopped the design at this point,

the motor would spin until the poles were opposite one another, settle into place, and then stop -- which would make a pretty useless motor, However, we are smarter than that. The section of the rotor where the electricity enters the rotor windings is called the commutator. The electricity is carried between the rotor and the stator by conductive graphite-copper brushes (mounted on the rotor) which contact rings on stator. Imagine power is supplied.

The motor rotates toward the pole alignment point. Just as the motor would get to this point, the brushes jump across a gap in the stator rings. Momentum carries the motor forward over this gap. When the brushes get to the other side of the gap, they contact the stator rings again and -- the polarity of the voltage is reversed in this set of rings! The motor begins accelerating again, this time trying to get to the opposite set of poles. (The momentum has carried the motor past the original pole alignment point.) This continues as the motor rotates. In most DC motors, several sets of windings or permanent magnets are present to smooth out the motion.

In a traditional DC brush motor, the commutator and brushes supply current to the armature while allowing the rotor to rotate. However, the brushes create the major weakness of DC motors in that physical contact causes wear and tear, unwanted debris and degradation of performance.

This leads to the very popular idea of the DC brushless motor in which the commutation is done electronically rather than through physical contact. The technique works beautifully and the motor world has been predicting the demise of the brush motor for some time now. Even so, it shouldn't come as any surprise that the less expensive traditional brush motor is still the most popular. Brushless D.C. motors have received considerable attention throughout the industrial world since.

The early 1970's however their use is still very limited as we approach 1990's. Computer disc drives and small fans are exclusively D.C. permanent magnet brushless motors.

Brushless DC motors consist of two coaxial magnetic armatures separated by an air

Gap. In certain types of motor,

- The external armature, the stator, is fixed.
- The internal armature, the rotor, is mobile (the rotor can also be external in certain cases).

The stator is the induced part of the machine.

The rotor is the inductor of the machine.

In brushless DC motors, the internal armature, the rotor, is a permanent magnet. This armature is supplied by a constant current (DC).

The external armature (stator) is polyphased (2 phases in our case) and is covered by polyphased currents. The pulsation of these currents is ω .

We say that the machine is a synchronous machine because, if ω is the angular speed of the rotor, we have the relation:

$$\omega = \omega_r / p \dots \dots \dots (E1.1)$$

In a Brushless DC motor, the rotor is a permanent magnet, this type of motor has almost the same properties and physical laws as a DC current machine. An electric motor transforms electrical energy into mechanical energy. Two main characteristics of a brushless DC motor are:

- It has an electromotive force proportional to its speed
- The stator flux is synchronized with the permanent magnet rotor flux.

The back electromotive force (as we will see in this document) is the basis of one the ways of driving brushless DC motors.

The brushless DC motor combines many of the advantages of the permanent excited DC motor and the synchronous motor. It has no exciting losses, and no wear

out, long live, high reliability, low radio noise, low power consumption and less maintenance.

Also Brushless DC motors allow greater power density than brushed machines. In a brushless motor the heat generating windings are stationary thereby allowing more effective cooling of the machine. The rotor is manufactured using a rare earth permanent magnet material which leads to excellent performance efficiency. Many machines of this type are used for electric vehicle applications where a superior power to weight ratio is required – up to 1.5 kW/kg. Typically the units are water cooled and can achieve efficiencies as high as 98%.

Brushless DC motors offer the same performance characteristics as a conventional brushed dc machine. However, with a brushless machine the heat generating portion of the motor is stationary which allows for enhanced cooling of the motor and as a result brushless machines can typically produce a greater performance from a smaller frame size, the brushes of a conventional machine are replaced with a position feedback device which is used to provide information on the position of the rotor relative to the stator, with this information the motor can be commutated electronically

1.2. Introduction

Brushless Direct Current (BLDC) motors are one of the motor types rapidly gaining popularity. BLDC motors are used in industries such as Appliances, Automotive, Aerospace, Consumer, Medical, Industrial Automation Equipment and Instrumentation. As the name implies, BLDC motors do not use brushes for commutation; instead, they are electronically commutated. BLDC motors have many advantages over brushed DC motors and induction motors. A few of these are:

- Better speed versus torque characteristics
- High dynamic response
- High efficiency
- Long operating life
- Noiseless operation
- Higher speed ranges

In addition, the ratio of torque delivered to the size of the motor is higher, making it useful in applications where space and weight are critical factors. In this application note, we will discuss in detail the construction,

Working principle characteristics and typical applications of BLDC motors.

1.2.1. Construction and Principle of Operation

1.2.1.1. Principle

BLDC motors are a type of synchronous motor. This means that the magnetic field generated by the stator and the magnetic fields generated by the rotor rotate at the same frequency. BLDC motors don't experience the "slip" that is normally seen in induction motors. BLDC motors come in single-phase, 2-phase and 3-phase configurations. Corresponding to its type, the stator has the same number of windings. Out of these, 3-phase motors are the most popular and widely used. This application note focuses on 3-phase motors.

1.2.1.2. Basic Structures.

The construction of modern brushless motors is very similar to the ac motor, known as the permanent magnet synchronous motor. Fig.1 illustrates the structure of a typical.

Three-phase brushless dc motor the stator windings are similar to those in a polyphase ac motor and the rotor is composed of one or more permanent magnets. Brushless dc Motors are different from ac synchronous motors in that the former incorporates some Means to detect the rotor position (or magnetic poles) to produce signals to control the Electronic switches as shown in Fig.2. The most common position/pole sensor is the Hall element, but some motors use optical sensors.

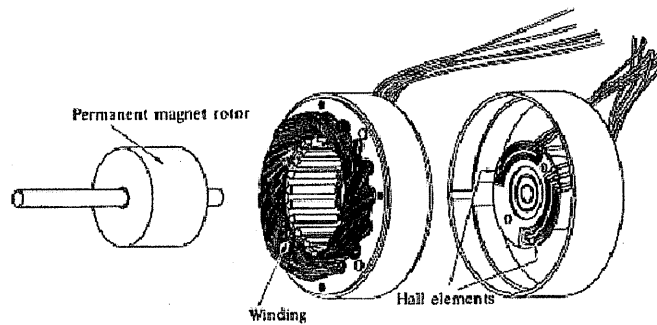


Figure (1.1): Disassembled view of a brushless dc motor.

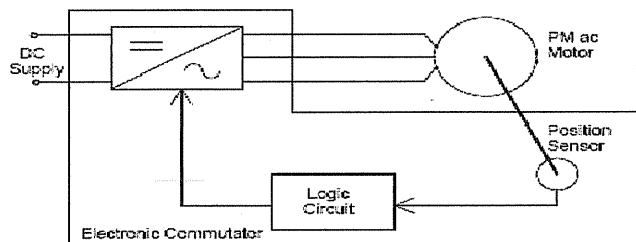


Figure (1.2): Brushless dc motor = Permanent magnet ac motor + Electronic commutator.

Although the most orthodox and efficient motors are three-phase, two-phase brushless Dc motors are also very commonly used for the simple construction and drive circuits.

Fig.3 shows the cross section of a two-phase motor having auxiliary salient poles

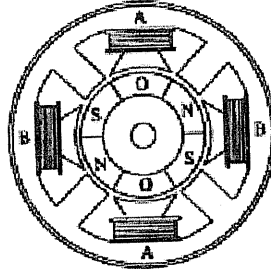


Figure (1.3): Two-phase motor having auxiliary salient poles.

1.2.1.3. Comparison of conventional and brushless dc motors

Although it is said that brushless dc motors and conventional dc motors are similar in their static characteristics, they actually have remarkable differences in some aspects. When we compare both motors in terms of present-day technology, a discussion of their differences rather than their similarities can be more helpful in understanding their proper applications.

1.2.1.4. Stator

The stator of a BLDC motor consists of stacked steel laminations with windings placed in the slots that are axially cut along the inner periphery (as shown in Figure 3). Traditionally, the stator resembles that of an induction motor; however, the windings are distributed in a different manner. Most BLDC motors have three stator windings connected in star fashion. Each of these windings are constructed with numerous coils interconnected to form a winding. One or more coils are placed in the slots and they are interconnected to make a winding. Each of these windings are distributed over the stator periphery to form an even numbers of poles. There are

two types of stator windings variants: trapezoidal and sinusoidal motors. This differentiation is made on the basis of the interconnection of coils in the stator windings to give the different types of back Electromotive Force (EMF). Refer to the "What is Back EMF?" section for more information. As their names indicate, the trapezoidal motor gives a back EMF in trapezoidal fashion and the sinusoidal.

Motor's back EMF is sinusoidal, as shown in Figure 4 and Figure 5. In addition to the back EMF.

The phase Current also has trapezoidal and sinusoidal variations in the respective types of motor. This makes the torque output by a sinusoidal motor smoother than that of a trapezoidal motor. However, this comes with an extra cost, as the sinusoidal motors take extra winding interconnections because of the coils distribution on the stator periphery, thereby increasing the copper intake by the stator windings depending upon the control power supply capability the motor with the correct voltage rating of the stator.

Can be chosen. Forty-eight volts, or less voltage rated motors are used in automotive, robotics, small arm movements and so on. Motors with 100 volts, or higher ratings, are used in appliances, automation and in Industrial applications.

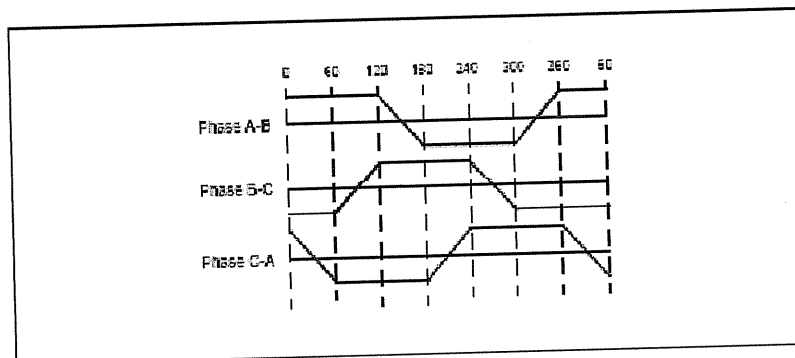


Figure (1.4): Trapezoidal Back EMF.

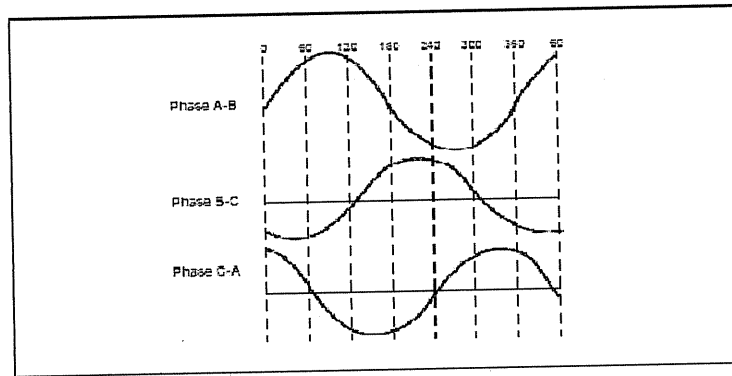


Figure (1.5): Sinusoidal Back EMF.

1.2.1.5. Rotor

The rotor consists of permanent magnet and can vary from two to eight pole pairs with alternate North (N) and South (S) poles. Based on the required magnetic field density in the rotor, the proper magnetic material is chosen to make the rotor. Ferrite magnets are traditionally used to make permanent magnets. As the technology advances, rare earth alloy magnets are gaining popularity. The ferrite magnets are less expensive but they have the disadvantage of low flux density for a given volume. In contrast, the alloy material has high magnetic density per volume and enables the rotor to compress further for the same torque. Also, these alloy magnets improve the size-to-weight ratio and give higher torque for the same size motor using ferrite magnets. Neodymium (Nd), Samarium Cobalt (SmCo) and the alloy of Neodymium, Ferrite and Boron (NdFeB) are some examples of rare earth alloy magnets. Continuous research is going on to improve the flux density to compress the rotor further. Figure 6 shows cross sections of different arrangements of magnets in a rotor.

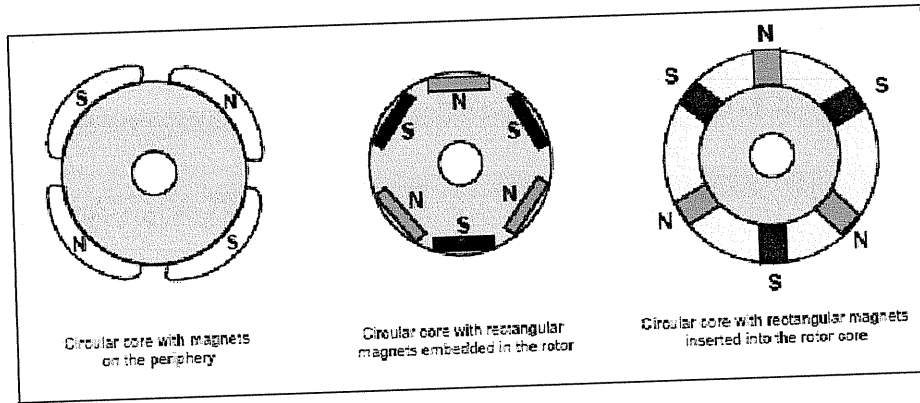


Figure (1.6): Rotor Magnet Cross Section.

1.2.2. Motor function

The dc servomotor is the oldest and probably the most commonly used actuator for servo systems. The name arises because a constant (or dc) voltage applied to the motor will produce motor movement. Over a linear range these motors exhibit a torque that is proportional to the current flowing in the winding. The chief disadvantage of the brush dc motor is the brush, which performs the mechanical commutation. These brushes are the first part of the motor to fail, severely limiting the reliability of dc brush motors when compared with other actuators. Another motor that operates similarly to a dc brush motor is the dc brushless motor (a dc voltage will cause it to rotate). Its method of commutation, however, is much different. Whereas the dc motor accomplishes switching mechanically with brushes, the dc brushless motor contains Hall Effect sensors that electronically control the switching. As a result, dc brushless motors have much greater life and reliability.

1.3. Overview of Signal Feedback Devices.

A wide variety of feedback devices are used in DC servo systems and brushless servo systems. This note outlines the devices, their uses, and their merits in a brushless servo system.

1.3.1. Hall-Effect Sensors

Hall-effect devices are used to sense magnetic fields. They are used in some brushless servo systems to provide commutation information to the brushless servo controller. For three phase brushless servo motors, three Hall-effect devices are used to provide commutation signals. In some motors, a magnetized wheel is attached to the rear of the motor shaft. In other motors, the actual rotor magnets are used in lieu of a magnetized wheel. The three Hall-effect devices sense the magnet field of the wheel or the rotor magnets as the motor shaft rotates and produce three square wave signals phased 120° apart. These three signals are used by the brushless controller to generate currents in the proper motor phases for optimum torque production. The Hall-effect device itself is an electronic component and has a temperature rating of 155°C .

1.3.2. DC Tachometer (brush-type)

The DC tachometer is used to sense motor velocity. It generates an analog DC voltage that is proportional to shaft velocity. The polarity of the output voltage is determined by the direction of rotation. The tachometer can be viewed as a DC servo motor operated as a DC generator. Brushes and a commutator couple the output voltage from the rotating winding to the stationary terminal connections. The DC tachometer is an electromagnetic device and contains no electronics.

1.3.3. Brushless Tachometer

Like the DC tachometer, this device is used to sense motor velocity. It provides an analog DC voltage proportional to speed with its polarity determined by the direction of rotation. However, unlike the DC tachometer, the brushless tachometer does not have brushes or a commutator. Commutation is done electronically which eliminates brushes and their potential problems. The commutation electronics are typically located in the tachometer package mounted on the rear of the motor. The brushless tachometer was developed specifically for use with brushless motors.

1.3.4. Resolver

The resolver is an electromagnetic device that is excited with a high frequency carrier signal. The resolver output is a two phases, amplitude modulated signal. These signals are processed by a resolver-to-digital converter (RDC) located in the controller. There are no electronics located in the resolver package mounted on the motor. The RDC produces an analog velocity signal and a digital position word. The digital position word is used for motor commutation and can also be used for motor positioning. The resolver is functionally equivalent to Hall-effect sensors plus brushless tachometer plus absolute encoder.

1.3.5. Synchro

The synchro is essentially a three phase version of the resolver. Synchro signals can be processed by an RDC by first running the three phase synchro signals through a Scott-T transformer. This transformer converts the three phase signals to two phase signals which can be used by the RDC. In industrial servo applications, the resolver is far more prevalent than the synchro. This is due primarily to the lower cost of the resolver and its ability to directly interface to the RDC electronics. Synchros require the Scott-T transformer to interface to the RDC which adds cost and complexity.

1.3.6. Tachsyn

The Tachsyn is a modification of a synchro or resolver. It is an electromagnetic device which provides rotor position information as well as velocity information. The rotor position information is in the same form as that produced by Hall-effect sensors. The velocity information is an analog DC voltage proportional to speed. The Tachsyn functionally replaces Hall-effect sensors plus a brushless tachometer. The Tachsyn signals must be processed to produce the analog tachometer signal and the commutation signals. The processor electronics are located in the controller rather than in the Tachsyn package mounted on the motor.

1.3.7. Encoder

An encoder is an electro-optical position sensor. It is available in absolute or incremental versions with the incremental version more commonly used. An incremental encoder consists of a glass, Mylar, or metal disk with alternating opaque and transparent stripes. Light from an LED or lamp is passed through the disk onto a photo sensor which detects the alternating opaque and transparent stripes. Encoder outputs are typically two phase digital signals in quadrature (90° out of phase). Rotational direction information is obtained by sensing which output phase is leading. Absolute encoders operate on similar principles but have multiple tracks to generate absolute position.

Information the processing electronics used to convert the optical signals to digital signals is contained in the encoder package mounted on the motor.

1.4. Time Plan

Designing and controlling this two-phase brushless DC motor And preparing this project to achieve the final result of project by controlling and designing of Brushless DC motor and preparing of closed loop and back EMF and how the system work to gather. This must be done in a limited time for the project.

These procedures are divided into steps to be done with the time required for each step. These steps are:

1. Gathering information about the brushless DC motor and all its types with a comparison and study the principal of operation for these types, and analyzing of brushless DC motor. This is estimated to take about three weeks.
2. Complete of preparing of the aims of project and put the special schedule of project and preparing of a proposal about the project "draft form". This is estimated to take one week.
3. Designing the general block diagram of the project with closed loop control system and designing the motor with its windings (phases) and creating them. This is estimated to take four weeks.
4. Constructing the converter used and gathering the devices and elements and connected the circuit to gather. This is estimated to take two weeks.
5. Designing the microprocessor-based system as a controller for the open and closed loop speed control system. This is estimated to take two weeks.
6. Constructing the overall system and putting it into operation and doing various experiments and tests and analyzing the results by making simulation of the system. This is estimated to take also three weeks.

So, the overall project time can be estimated in four months to get ready.

1.5. Estimated Cost

In this project we need many items and equipment to built electrical and power circuit and built motor construction, now we can summary it in this table as below

Table (1.1): Estimated cost

| Equipment | Cost (nsh) | Total (nsh) |
|---------------------|------------|-------------|
| Electronic Material | 1230 | = |
| Material PM | 600 | = |
| Tr-r (220/15-20)V | 210 | = |
| Mechanical Material | 200 | = |
| Box | 150 | = |
| Rotor Construction | 150 | = |
| Plats | 160 | = |
| Print | 350 | = |
| = | = | 3050 |

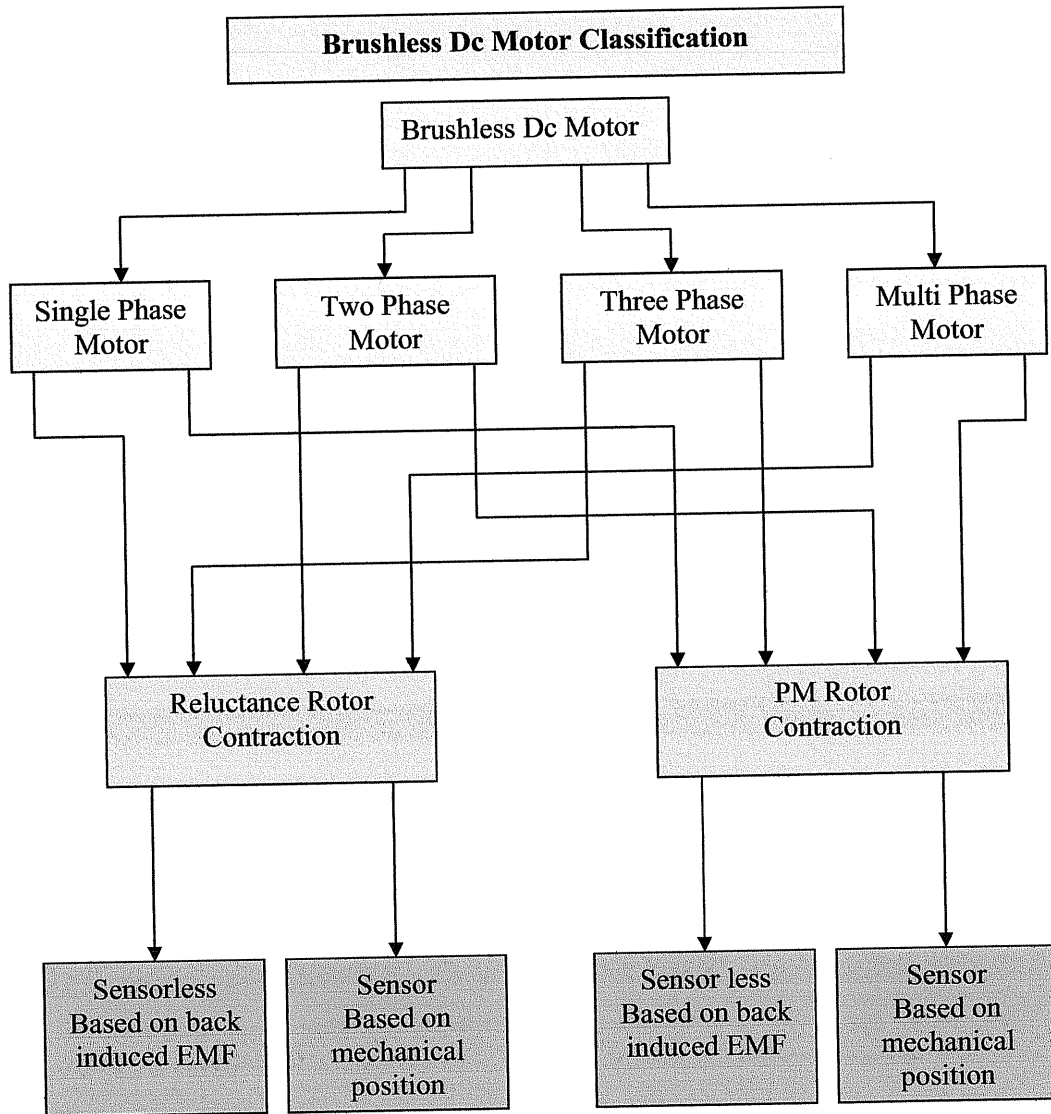
Chapter Two

Brushless DC Motor Classification

2.1. Introduction.

2.2. Brushless Motor Operation.

2.3. Brushless DC Motor Classification.



Chapter Two

Brushless DC Motor Classification

2.1. Introduction

A synchronous motor with a permanent magnet in the rotor and operated in self-controlled mode (using a rotor position sensor and an inverter to control current in the stator windings) is generally known as a brushless dc motor. The brushless DC motor is an inside-out brushed DC motor; because the armature is in the stator and the magnets are in the rotor, and its operating characteristics are similar to those of the conventional brushed DC motor. The position sensor and the solid-state switches in the inverter perform the role of the brushes and the mechanical commutator of the conventional DC motor.

The brushless DC motor operates in a manner similar to the self-controlled synchronous motor. The thyristors in the inverter controlling the motor current are commutated by the back EMF of the motor. At low speed, the back of EMF may not be sufficient to commutate the thyristors. A brushless DC machine is one in which the commutation is done by means of electronic. This concept is not new, but the improvements in magnet materials and the reduction of cost of integrated circuits and electronic power switches have made brushless DC machines marketable recently.

There advantages are low noise and radio interference, no requirement for commutator maintenance and brush replacement, and no dust due to brush wear. There big disadvantage at this writing in cost.

The electronic driving part of a brushless DC motor performs the function of a commutator: maintaining a 90 electrical-degree displacement between the rotor and stator magnetic poles, and acting as a rectifier/inverter between the dc terminals and the alternating current and voltages of the armature winding. Most computers use brushless DC motors since they are clean (no brushes to create carbon dust or to wear

out) and are now smaller and less expensive than even shaded pole AC motors. In reality, inside the hub of the motor are three sets of windings and a set of permanent magnets with sensors. As the magnets on the hub rotate past the sensors, the windings are turned on as needed to produce the torque needed. With 12V on it, it spins at about 2800rpm.

Our complete brushless DC motor capability provides solutions to prime mover requirements in a wide variety of applications. These motors are designed for use in high-speed continuous-operation applications, where they operate with low noise levels, low heat, and high reliability. Electronic commutation ensures exceptionally long life and speed control over a broad range. Efficiencies of 80-90% are achievable. We can custom design of these motors to meet your specific BDC motor requirements. They are available as housed units and rotor/stator parts sets.

2.2. Brushless Motor Operation

DC motors come in 2 basic design formats, as described by their names, "brush" or "brushless". There are many other pseudo names used, like "moving magnet motor" etc. In fact I know of one manufacturer where the magnets are stationary - while the "can" rotates around the shaft, but it's still a brushless motor! So all these alternative names end up doing is to confuse the less knowledgeable among us.

There are many different design styles that are possible with the actual construction of a DC motor, but generally they can be classified as being either brush or brushless in form - remember this discussion is limited to R/C car type and sized motor only.

The basic difference between the two types, is that one has brushes and a commutator, and the other does not hence "brush" Now, if you know how a brush motor works, then you will appreciate that the purpose of the brushes and commutator are to provide a correctly timed (remember that bit for later, it's important!) current to the windings on the armature. When this current flows, a

magnetic field is generated in the winding coils which interacts with the magnetic fields already present in the motor, emitting from the static magnets attached to the motor shell

Now if a brushless motor has no brushes, then you may ask yourself, exactly how does the brushless motor work!

There is one major physical constructional difference that characterizes these motors. To enable one to design a motor without brushes requires that the windings remain stationary (in most brushless designs anyway), therefore the brushes are now redundant. To make the winding stationary they are now located around the "outside" of the motor and the permanent magnets are now moved onto the central shaft, unlike the brush motor which is totally the opposite.

Since we no longer have brushes, exactly how does the correctly timed (there's that important bit again!) current flow through the windings then? Well the process of providing the current to the windings (technically known as commutation) in the brushless motor is now provided by the motor controller (ESC) by electronically switching the power flow to the individual motor winding coils directly. This controller, which since it has a much more complicated task to do on top of the "power flow control and switching", tends to be a much more complex piece of electronic equipment, much more so than the typical, and rather simple, ESC as used by racers with brushed motor.

A brushless motor controller, due to the number of features, and the processes it has to perform, requires quite a lot of real-time processing power, even more so for an R/C car due to the fine control requirements required over the motor output. The reason that the brushless motor has not been successful to date, in cars, is not because of a lack of motors, the brushless motor concept is many, many years old. I built my first experimental one nearly 30 years ago! No, the problem has always been the availability of such a relatively large amount of fast processing power in a small and affordable package. However, with the advent of relatively cheap processing power now being available via CMOS, VLSI and Digital technology, coupled with modern

manufacturing processes, we are now able to create controllers today with enough processing power in a really small package, of a capability that was unheard of even 2-3 years ago. My first controller was almost as big as the boat the motor was installed in, and was a very simple affair by today's standards as well.

This development has allowed designers to create controllers that, although they will never be quite as small as a (simpler) brush motor ESC, non-the-less they are now quite small and lightweight, enough to be used in R/C cars.

Main reasons for choosing brushless motor "faster\better\quicker"

***First:**

There is no friction in the motor other than that of the 2 shaft bearings and this is almost non-existent (BEC1 and BEC2 bearings are used). This results in much higher levels of efficiency and higher rpm's since the max rpm is no longer limited to the brushes ability to maintain contact with the comm., as in a brush motor.

***Second:**

This is that important bit! Since the controller is in fact now a digital microprocessor-a miniature dedicated computer. It is possible to configure the controller, through sophisticated programming and sensor circuits, to alter the timing of the motor dynamically in real-time, according to its rpm and load, similar to that of the modern Electronic Engine Management and Control System found in almost every modern, full scale, car. Which is a very important and huge power improving capability?

2.3. Brushless DC Motor Classification

This chapter analyzes the behavior of 2-phase, 3-phase, and 5-phase Brushless Permanent Magnet (BPM) motors when supplied by the suitable variable speed drives. The objective is to evaluate the suitability of these BPM motors for different applications.

2.3.1. Introduction

The availability of high-energy permanent magnets and recent advances in power electronics are leading to a large diffusion of permanent magnet motors in a variety of applications. Finite element analysis is a very useful tool for predicting and estimating the effect of different design parameters [1-2] on motor performance. Several recent projects [3-4] show the studies made on 3-phase, 4-pole, BPM motor, which is the most popular configuration. This project extends these analyses to compare a 3-phase BPM motor with 2-phase and 5-phase BPM motors with equal amount of copper and magnetic materials; a general dynamic model for multi-phase BPM motors in conjunction with the corresponding inverter is used to simulate the multiphase BPM motors.

2.3.2. Multi-Phase BPM Motor

A motor with higher number of phases has several advantages over conventional 3-phase motor drives [5]. These are: reducing the Ampere turns, increasing the frequency of torque pulsation, increasing the current per phase without increasing the voltage per phase and higher reliability [6]. On the other hand, a 2-phase BPM motor requires lesser number of Hall effect sensors and has better copper utilization [7]. In this paper, in order to have a fair comparison between the various BPM motors, the amount of iron and copper are maintained constant for all motors by changing the number of turns and slot width accordingly. Fig (2.1-b) and (2.1-c) show the cross-sectional views of the designed 2-phase and 5-phase BPM motors respectively based on the 3-phase BPM motor shown in Fig (2.1-a).

The 3-phase, 4-pole BPM motor with 120° current excitation is taken as the reference for evaluating the performance of 2-phase and 5-phase BPM motors with different current excitations. A surface mount Ferrite (FM -8D) magnet rotor with parallel magnetic polarization for each magnet is used in all motors.

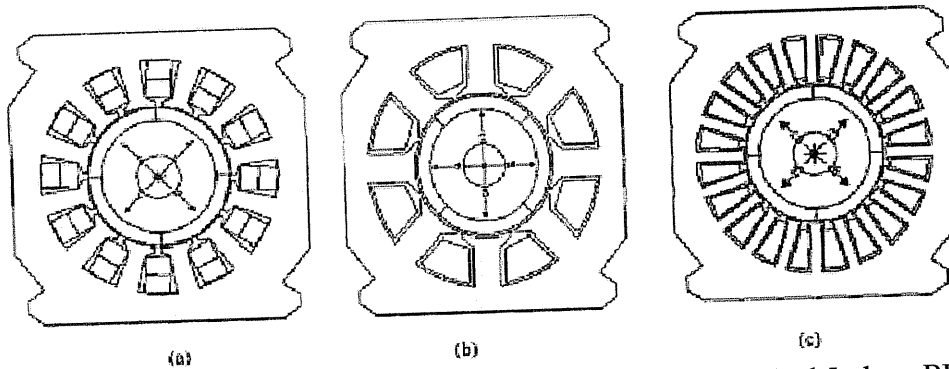


Figure (2.1.): Models used for simulation of 3-phase, 2-phase. And 5-phase BPM motors.

The various current waveforms used to excite the motors are shown in Fig. (2.2) Notice that the current amplitudes are adjusted to keep their (RMS) values equal. Of primary interest in these comparisons are the average torques and torque ripple. Next, the effects of variation in the number of phases on the flux density in the stator tooth and stator back-iron are studied.

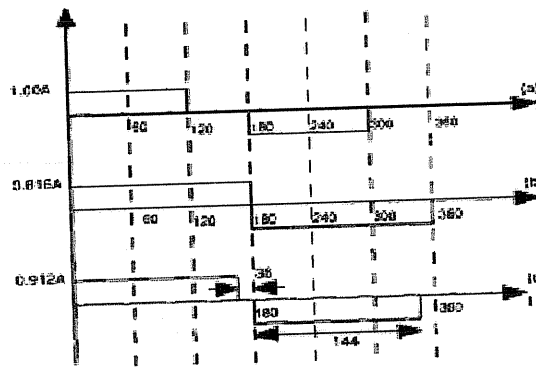


Figure (2.2): Current waveforms
 a) 120° conduction (b) 180° conduction (c) 144° conduction.

2.3.3. Non-Linear Finite Element Analysis

2.3.3.1. Three-Phase BPM Motor with 120° Conduction

Fig (2.3) shows a plot of the static torque versus rotor position in both generating (0°-90°) and motoring modes (90°- 180°) while only two phases are excited. The effect of stator slot opening on the static torque waveform is observed as notches on the static torque characteristics. The notch at the maximum/minimum torque position is also due to slot opening.

Fig. (2.4) shows the static torque characteristic at rated current with 120° pulse of current excitation for 3-phase operation. Notice that the frequency of torque ripple is six times the supply frequency as 180° mechanical corresponds to 360° electrical

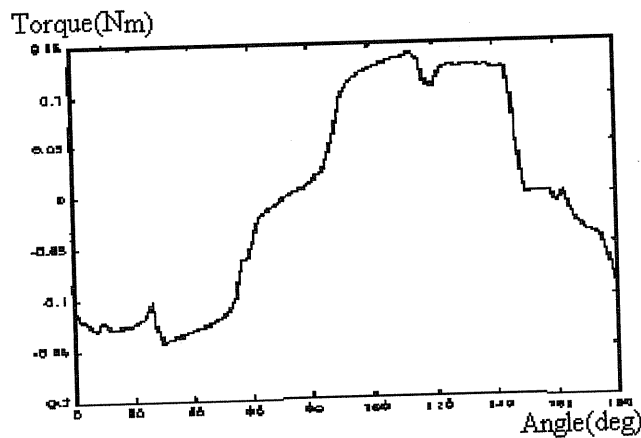


Figure (2.3). Static torque characteristic for 3-phase BPM motor

2.3.3.2. Three-Phase BPM Motor with 180° Conduction

In this case, the peak value of the current as shown in Fig. (2.2-b) is lesser than in Fig. (2.2-a) which means smaller peak current ratings and reduction in total switching loss.

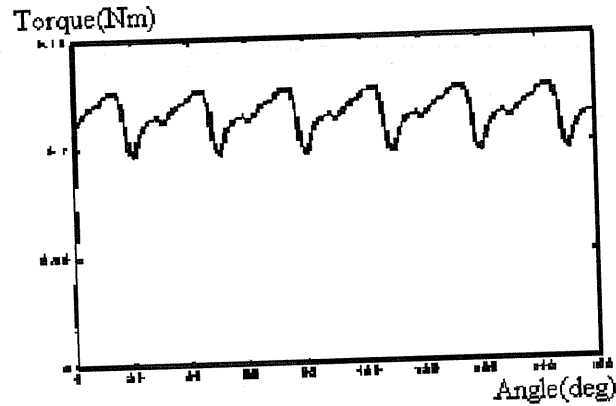


Figure (2.4) Motoring torque (static) for 3-phase BPM motor supplied with 120° Conduction

Fig (2.5) shows the static torque characteristics for the 3- phase motor with 180° pulse of current conduction. Notice an increase in the peak torque by a factor of 1.09 and an increase by a factor of 1.05 in the average torque. Also, in this case the converter needs to be modified to accommodate the neutral current as the three phase currents do not add up to zero.

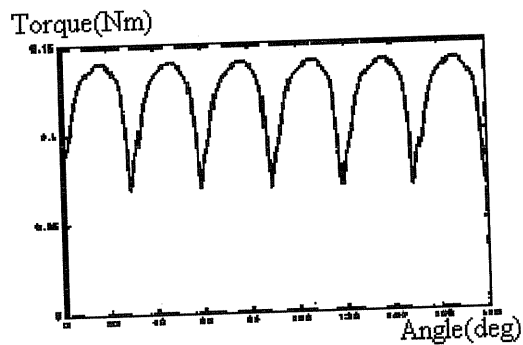


Figure (2.5) Motoring torque (static) for 3-phase BPM motor supplied with 180° Pulses of current.

2.3.3.3. Two-Phase BPM Motor with 180° Conduction

In this case, the 2-phase BPM motor is supplied with the square wave current waveform shown in Fig. (2.2-b). Static torque waveform for the 2-phase motor with square wave excitation is illustrated in Fig. (2.6). Notice that the torque ripple frequency is four times the supply frequency. In this case also, the peak current and hence switching loss are lower. Peak torque has increased by a factor of 1.19 and the average torque has increased by a factor of 1.18

2.3.3.4. Five-Phase BPM Motor with 144° Conduction

The 5-phase BPM motor with the same amount of copper and magnetic material is excited with 144° pulses of current as shown in Fig. (2.2-c). Static torque waveform phase motor with 144° excitation is shown in Fig. 7. Notice that the torque ripple frequency is ten times the supply frequency. The peak current is lower by a factor of 1.09. This reduces the switching losses per device. However, the number of devices increases. Peak torque has increased by a factor of 1.12 and the average torque has increased by a factor of 1.17

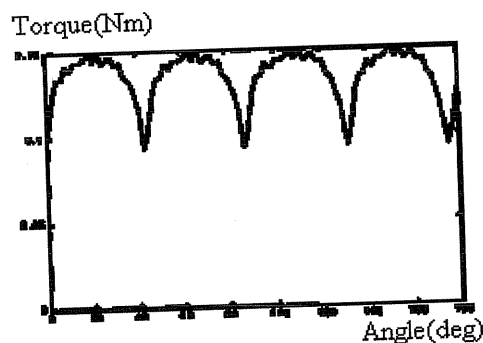


Figure (2.6) Motoring torque (static) for 2-phase BPM motor supplied with 180°Pulses of current

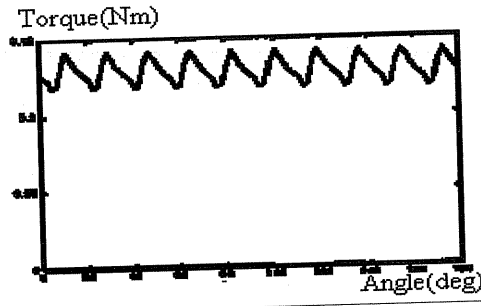


Figure (2.7) Motoring torque (static) for 5-phase BPM motor supplied with Pulses of current^o 144

2.3.3.5. Five-Phase BPM Motor with 180° Conduction

Static torque characteristic for the 5-phase motor with 180° excitation is shown in Fig. 8. Peak current requirement is reduced by a factor of 1.22. Average torque has increased by a factor of 1.07 and peak torque has increased by a factor of 1.13.

2.3.4. Conclusion

This chapter evaluates the 2-phase and 5-phase BPM motors with respect to 3-phase 120° conduction BPM motor. Finite element analysis was used to determine the flux density in the back iron and tooth of the designed motors. It was shown that the iron utilization is better in 5-phase BPM motor. Also, static torque versus rotor angular position has also been calculated using the finite element package. A dynamic model capable of determining the dynamic torque in Matlab environment has been developed. Dynamic torque pulsations for these motors have been obtained. It was shown that the 5-phase BPM motor with 144° conduction develops the minimum torque pulsations.

A two phase BPM motor has been designed and fabricated based on an existing 3-phase BPM motor. Experimental results confirm the results obtained from FEM simulations for 2-phase and 3-phase BPM motors. A 5-phase BPM motor is under fabrication.

Chapter Three

Classification of electrical motor

3.1. DC Motors.

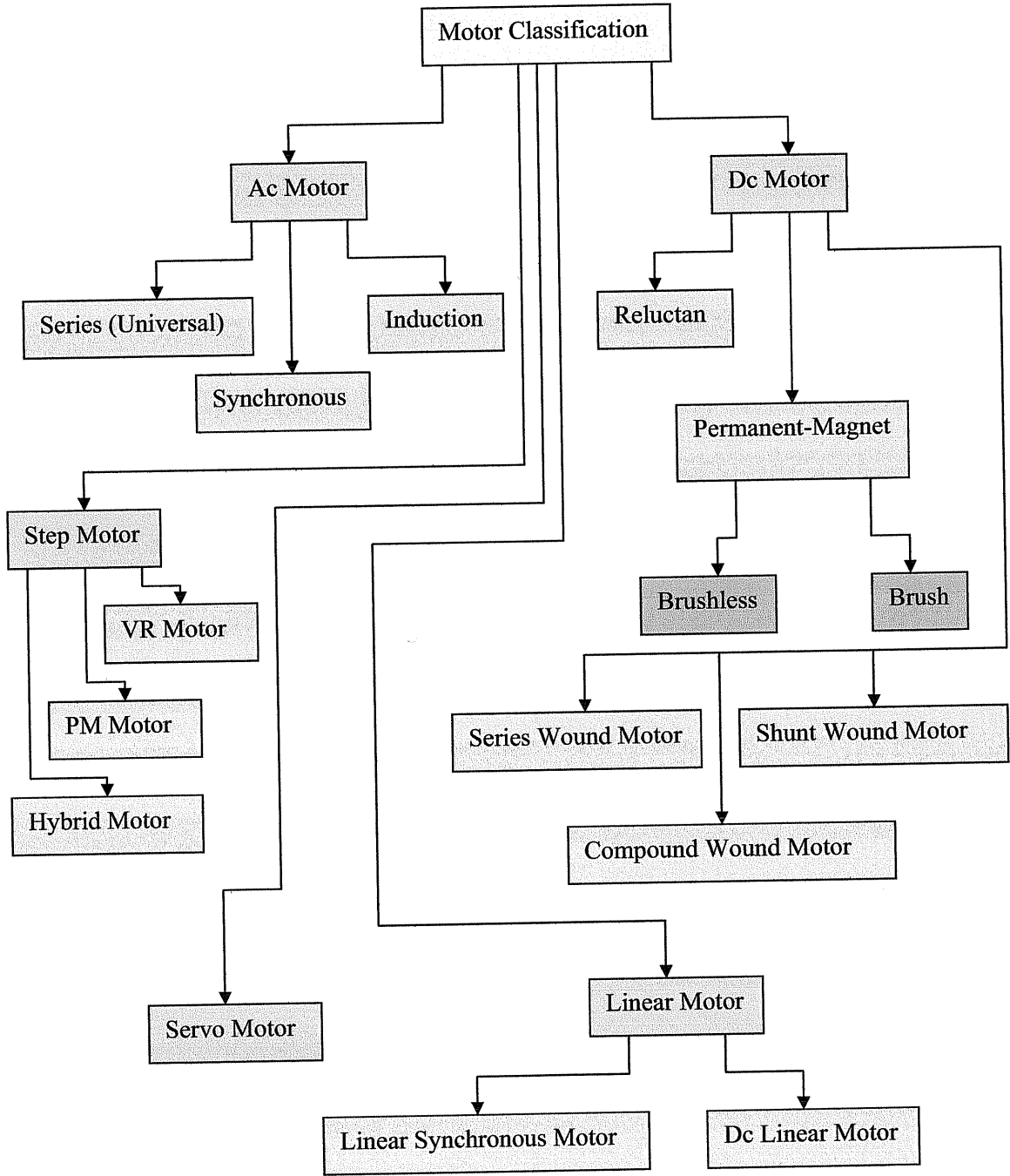
3.2. AC Motors.

3.3. Linear Motors.

3.4. Step (Stepper) Motors.

3.5. Servo Motors.

Classification of Motors



Chapter Three

Classification of electrical motor

Electrical motor can be classified as follow:

3.1. DC Motors

3.1.1. Introduction to DC Motors

A direct-current motor is a device for converting dc electrical energy into rotating mechanical energy. This process can be reversed, as in a dc generator, to convert mechanical to electrical power. Direct-current equipment lends itself to automatic processes, by giving automated machinery controllable, adjustable speeds, high starting torques, as well as responsive braking. The easy of control and high torque capability makes the DC motor attractive for many machinery applications. All motors, weather AC or DC power line, have several basic characteristics in common. They include:

1. A stator, which is the frame and other stationary components (provides the fixed Magnetic field could be a permanent magnet or an electromagnet).
2. A rotor or armature, which is the rotating shaft and its associated parts (many Coils of wire are wound on a cylindrical shaft).
3. Auxiliary equipment, such as a brush/commutator assembly for DC motors and a Starting circuit for AC motors.

3.1.2. Principle of Operation

The basic principle that drives the DC motor is Faraday's Law; which states that electrical current is produced when there is relative motion between a conductor and magnetic field. Of course the law is stated for a generator, however the opposite is also true, and motion is produced when a current carrying wire is in the presence of magnetic field. The motion is determined by two factors, the direction of the current and the direction of the magnetic field. The right-hand rule for motors is used when determining the direction of the motion.

3.1.3. DC Motor Characteristics

Motors that operate from DC power sources have many applications where speed control is desirable. They can be categorized into three major sectors series, shunt, or compound machines, depending on the method of connecting the armature and field windings. Permanent magnet DC motors are also used for certain applications.

3.1.4. Types of DC Motors

There are four basic types of commercially available motors:

1. permanent-magnet motors
2. Series-wound motors
3. shunt-wound motors
4. compound-wound motors

The armature or rotor is a common component of all of the motors including AC motors. Most use a drum-like armature.

Since most of the armatures in these motors are the same, they are often categorized by how the field poles are magnetized and wired. It is important to understand how the different fields are generated and the pros and cons of each.

Permanent-magnet motors.

3.1.4.1. Series-wound motors

The manner in which the armature and circuit field circuits of a dc motor are connected determines its basic characteristics. This is true for the series-wound motor, which has the armature and field circuit wired in series, as shown in Figure (3.1). There is only one path for the current to flow from the DC voltage source. Therefore, the field is wound of relatively few turns of large diameter wire, giving the field a low resistance. Changes in the mechanical load applied to the shaft causes changes in the current through the field if the load increases.

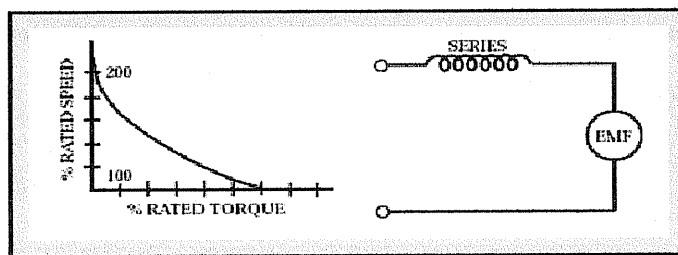


Figure (3.1): Typical speed –torque curve for series wound motor

3.1.4.2. Shunt-wound motors

Shunt-wound motors are more commonly used than any other type of dc motor. In this configuration the armature and field coils are wired in parallel, Figure (3.2). The field coils, which are wound with many turns of small-diameter wire, have a relatively high resistance. Due to the fact that this high resistive field is in parallel with the armature, very low current will pass through the field coils. Most of the current, about 95%, drawn by the shunt motor flows through the armature circuit.

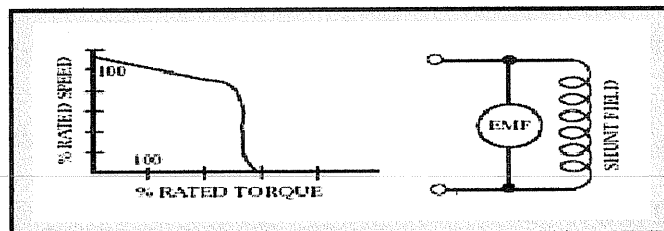


Figure (3.2): Typical speed-torque curve for shunt wound motors

3.1.4.3. Compound-wound motors

The compound-wound motor has two sets of field windings, one in series with the armature and one in parallel. It combines the desired characteristics of the series and shunt-wound motors into one motor. There are two methods of connecting compound motors: cumulative and differential. A cumulative compound motor has series and shunt fields that aid each other, while in differential compound motor they oppose each other. The two types vary in torque and speed in a different manner when the armature current is increased.

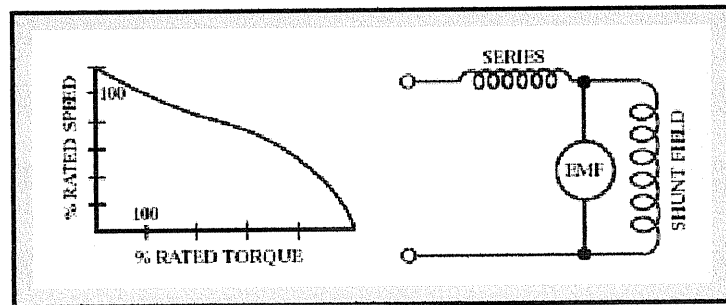


Figure (3.3): Typical speed-torque curve for compound wound motors

3.1.5. Summary

- Permanent-magnet dc motors – inexpensive motor with good speed control but With low torque
- Series-wound dc motors – high torque but changes in load dramatically change The rotational speed
- Shunt-wound dc motors – good speed regulation with slight variations with a Changing load, good overall more (widely used in industry)
- Compound-wound motors – has the best characteristics of both the series and Shunt-wound motors, but is very expensive.

3.2. AC Motors

3.2.1. Introduction to AC Motors

AC motors utilize either monophase or polyphase alternating current as their power source as opposed to the direct current of DC motors. AC motors are widely used and preferred over DC motors due to the wide availability of AC power. Virtually every country in the world produces AC power in their power plants. AC motors are well suited for applications where constant speed is desired. The speed of the AC motor is dependent on the frequency of the current applied to its terminals so some sort of controller is required to alter its operating speed and this can be varied only within certain limits.

3.2.2. Principles of Operation

Most AC motors rely on the principle of rotating magnetic electric fields in order to operate. The magnetic field in the stator rotates, causing the rotor to turn in both synchronous and induction types of AC motors. The magnetic field in the rotor, chases the electrically induced rotating magnetic field in the stator by being attracted and repelled by it. This rotating magnetic field causes a torque to be produced on the rotor and causes it to turn.

3.2.3. Types of AC Motors

There are three basic types of AC motors that are widely used:

1. Series motors.
2. Synchronous motors.
3. Induction motors.

3.2.3.1. Series (Universal) AC Motors

A series AC motor, sometimes termed a universal motor, is the only type of motor that can be powered by either AC or DC. The construction of this motor is very much the same as that of a series-wound DC motor. The only differences are the special metals, laminations, and windings that are used.

3.2.3.2. Synchronous AC Motor

Synchronous motors are able to run at a constant speed under any load condition. The synchronous motor operates when three-phase AC power causes a strong magnetic field to be set up around the rotor. The rotor is energized by DC that causes it to be attracted to the rotating magnetic field of the stator. This produces a high torque as the rotor turns in step with the rotating magnetic field of the stator. A major disadvantage of the synchronous motor is the fact it possesses no starting torque.

3.2.3.3. Induction AC Motors

Induction AC motors are the simplest type of AC motors and are therefore the most commonly used. This is due to the fact that they are simple and rugged and consequently are cheap to manufacture. They also have lower operating costs due to the fact that the rotor does not have to be connected to an external voltage source.

3.3. Linear Motors

Linear motors are increasingly popular solutions for today's automation applications. Driving this rise in popularity are application advantages inherent in linear motor systems. When compared to more traditional mechanical systems, some advantages of linear motors include significantly improved throughput, system accuracy and system life.

3.3.1. Linear Synchronous Motors

A linear synchronous motor (LSM) is the linear counterpart of the rotary synchronous motor. The armature winding of the motor is located in a laminated magnetic core installed along the guideway and is fed, section by section from rectifier-inverter power stations.

3.3.2. DC linear Motors

The main proposed purpose for DC linear motors has been for short-stroke applications. They use a mild steel core of circular cross section with a single-layer surface winding to form the primary (armature) this provides a normal and thrust force.

3.4. Step (Stepper) Motors

3.4.1. Introduction to Step Motors

A step motor is a device that processes digital signals in order to obtain a specific angular displacement. As the name implies, the motor accomplishes its displacement by rotating in steps. Each signal input into the motor results in the incremental rotation of the rotor.

3.4.2. Types of Step Motors and how they work

Step motors are electromagnetic rotary actuators that mechanically convert digital pulses into incremental shaft rotations. The number of pulses input into motors is directly proportional to the number of steps taken by the motor, thus determining the amount of rotation. The frequency of the pulses also determines the speed at which the shaft rotates. There are three types of stepping motors. Each accomplishes the same tasks in similar manners but use slightly different

components. The variable reluctance, VR, permanent magnet, PM and hybrid motor are the three different stepping motor types.

3.4.2.1. Variable Reluctance (VR) Motor

VR motors are comprised of two main parts, the rotor and stator. The rotor and stator are free of magnetic charge when the motor is not being used. This enables the motor to be “freewheeled”, which is a term that describes its ability to be spun with no resistance other than friction from bearings. Freewheeling is possible only with VR stepping motors.

3.4.2.2. PM Motor

Permanent magnet stepping motors are also comprised of a rotor and stator but the rotors in these motors carry a permanent magnetic charge. These motors cannot be freewheeled due to the rotor’s magnetic charge. Another distinguishing characteristic of PM motors is their rotor. The rotor of the PM motor has no teeth unlike the other stepping motors. The permanent magnetic field that the rotor contains eliminates the need for teeth.

3.4.2.3. Hybrid Motor

A hybrid stepping motor has characteristics of both PM and VR motors. In a hybrid Motor the rotor is a permanent magnet but it has blades like VR motors. The result is a motor that has very high torque and very small, precise step increments.

3.4.3. Summary

- VR motors are the most basic types of stepping motors. They produce little Torque but are able to freewheel.
- PM motors produce larger amounts of torque but have little precision.
- Hybrid motors have both high torque and excellent precision.

3.5. Servo Motors

A servo motor is an AC or DC powered motor that uses feedback and controllers to achieve a specific angular location. Servo motors can achieve the same levels of accuracy as stepping motors, but must use a closed loop feedback system whereas stepping motors operate using open loop systems.

3.5.1. Summary

- Servo motors use closed loop feedback systems.
- Servo systems are more expensive than stepping motor systems due to the need for a controller.
- Servo motors achieve their desired location faster than stepping motors.

Chapter four

Control Brushless DC Motor

- 4.1. Introduction.**
- 4.2. Different between sensor and sensorless.**
- 4.3. Sensorless Motor Control.**
- 4.4. Sensor control of brushless dc motor.**
- 4.5. Sensorless control of BLDC Motor.**
- 4.6. Back EMF construction circuit (Sensorless).**
- 4.7. Efficiency.**
- 4.8. Information about components.**
- 4.9. Total Circuit.**
- 4.10. Flow Chart.**

Chapter four

Control of Brushless DC Motor

4.1. Introduction

In this project, a novel back EMF sensing scheme, direct back EMF detection, for sensorless BLDC drives is presented. For this scheme, the motor neutral voltage is not needed to measure the back EMFs. The true back EMF of the floating motor winding can be detected during off time of PWM because the terminal voltage of the motor is directly proportional to the phase back EMF during this interval. Also, the back EMF voltage is referenced to ground without any common mode noise. Therefore, this back EMF sensing method is immune to switching noise and common mode voltage. As a result, there are no attenuation and filtering necessary for the back EMFs sensing.

This unique back EMF sensing method has superior performance to existing methods which rely on neutral voltage information, providing much wider motor speed range at low cost.

Based on the fundamental concept of the direct Back EMF detection, improved circuitry for low speed / low voltage and high voltage applications are also proposed in the project, which will further expand the applications of the sensorless BLDC motor drives.

Starting the motor is critical and sometime difficult for a BLDC sensorless system. A practical start-up tuning procedure for the sensorless system with the help of a dc tachometer is described in the project. This procedure has the maximum acceleration performance during the start-up and can be used for all different type applications.

4.2. Different between sensor and sensorless

4.2.1. Rotation-Sensor Technologies

1. Hall-effect magnetic sensors
2. Optical encoders

Brushless dc motors on the market contain both Hall-effect and optical rotation sensors.

4.2.1.1. Hall-Effect Rotation Sensors

1. Sensors detect the magnetic poles of the motor rotor.
2. Resolution limited by number of sensors.
3. Accuracy limited by positioning accuracy and gain tolerance of the sensors.

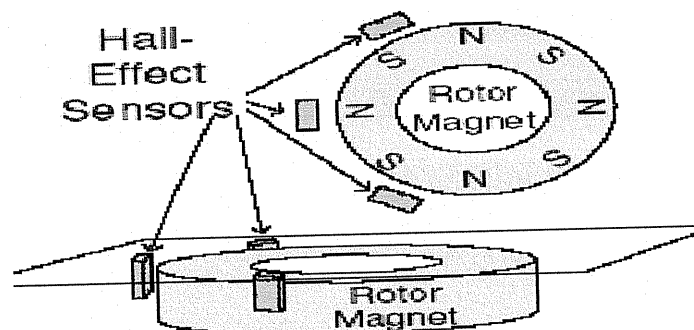


Figure (4.1): Hall-Effect sensor

❖ Advantages:

1. Low cost.
2. Simple, reliable.
3. Absolute position sensing for commutation.

❖ **Disadvantages:**

- 1- Low resolution
- 2- Low accuracy may cause torque ripple.
- 3- System often requires additional high-resolution rotation sensor.

4.2.1.2. Optical Encoders:

Optical unit shines light beams through the slots in the code wheel, detecting interruptions as the slots pass. Slots moving through the sensor are counted electronically; this gives the accumulated angle of rotation.

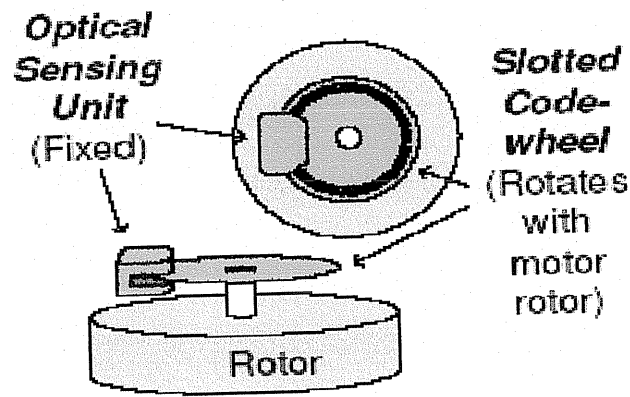


Figure (4.2): optical encoder sensing

❖ **Advantages:**

- 1- High resolution precision.

❖ **Disadvantages**

- 1- High cost.
- 2- Incremental position sensing (requires initialization).
- 3- Electronics needed for decoding/accumulation.
- 4- Sensitivity to contamination and ambient light
- 5- May require alignment/adjustment.

4.3. Sensorless Motor Control

4.3.1. Existing Approaches

1. Back-EMF sensing.
2. Added sense windings on motor.
3. Measure motor winding impedance changes.
 - Probing” with current pulses.
 - High-frequency sense carrier.

4.3.1.1. Back-EMF sensing

- Senses induced voltage from rotor rotation.
- Simple.
- Signal amplitude is proportional to motor speed, so this does not work when motor is stopped or rotating slowly.
- Very commonly used in disk drives and fans.

❖ Advantages

1. Removes board allocation for rotation-sensor hardware.
2. Moves sensing function into electronics, eliminating moving parts, mechanical adjustments, maintenance.
3. Position information comes directly from electromagnetic characteristics of motor, so sensing is always in alignment.

4.4. Sensor control of brushless dc motor

4.4.1. General block diagram

Our control system is divided into two parts, open loop control system and closed loop control system.

4.4.1.1 Open loop control system:

This system used when the user need to load the motor with a fixed loads and torques for some operations, where the speed must calibrate at constant required value. But if the load increases on the motor for any reason, then the speed will decrease and will not return to the previous calibrated value. Fig (4.3) shows open loop control system.

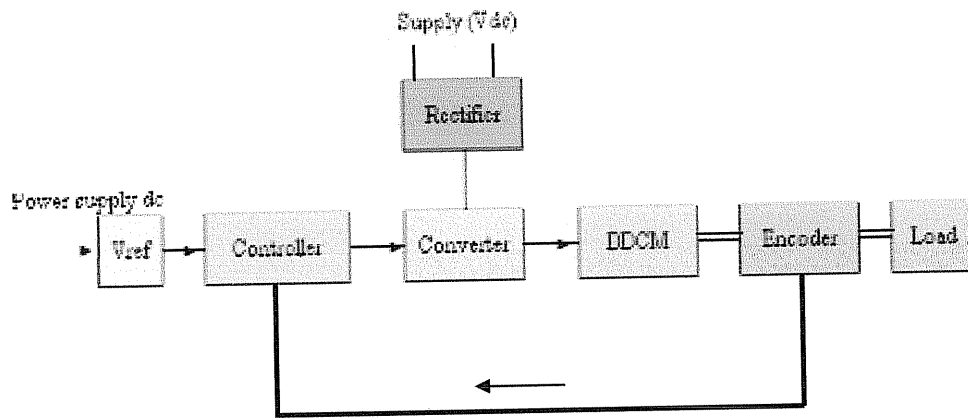


Figure (4.3): Open loop control system with sensor.

This system consists of seven main component, the PC which contain the controller and Vref generating circuit, Rectifier which gives us the dc needed voltage, the converter which used for generating the needed phase voltages from the rectifier ,the brushless dc motor ,the encoder which detects and senses the position of the rotor per one rotation, and finally the load .

This control system has no feed back for speed value control, but it has a closed loop for rotor position sensing in order the motor operates.

4.4.1.2. Closed loop control system

This system used when the user need to load the motor with a load needs constant speed and variable torques for some operations, where the speed should be calibrates at constant value. If the load increases on the motor for any additional load torque, then the speed will be the same or fixed at the calibrated speed. Fig (4.4) shows the block diagram of the closed loop control system.

In the closed loop control system there is a feedback signal taken from the output and then compared to a reference predetermined needed value, where the actual speed is measured by tachogenerator.

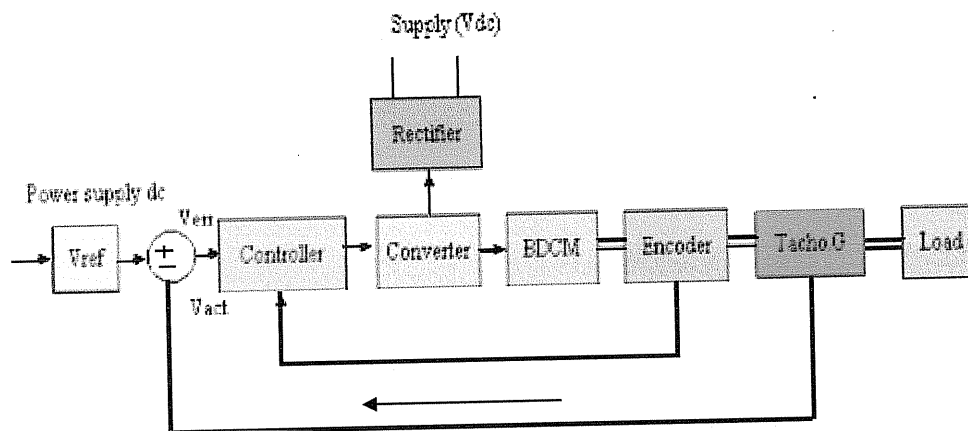


Figure (4.4): Closed loop control system with sensor.

This system consists of eight main components, the PC which contain the controller, V_{ref} generating circuit and the comparator, Rectifier which gives us the dc needed voltage, the converter which called inverter which used for generating the needed phase voltages from the rectifier, the brushless dc motor, the encoder which detects and senses the position of the rotor per one rotation, Tachogenerator which is the speed sensor which enables us to compare the actual speed with the reference speed, and finally the load.

4.5. Sensorless control of BLDC Motor

As explained before, the rotor position must be known in order to drive a brushless dc motor. If any sensors are used to detect rotor position, then sensed information must be transferred to a control unit.

The first type is the position sensing using back EMF of the motor, and the second one is position estimation using motor parameters, terminal voltages, and currents. The second type scheme usually needs DSPs to do the complicated computation, and the cost of the system is relatively high. So the back EMF sensing type of sensorless scheme.

A few other schemes for sensorless BLDC motor control were also reported in the literature give the literature number. The back EMF integration approach has the advantage of reduced switching noise sensitivity and automatically adjustment of the inverter switching instants to changes in the rotor speed. The back EMF integration still has accuracy problems at low speeds.

The rotor position can be determined based on the stator third harmonic voltage component .The main disadvantage is the relatively low value of the third harmonic voltage at low speed.

4.5.1. Open loop control of BLDC motor with back emf strategy

From the fact that the back emf signal is strictly proportional to the speed, the control of back emf signal will control the speed of the motor since BLDC produces this signal while operating. Fig (4.5) shows the block diagram of the open loop control system.

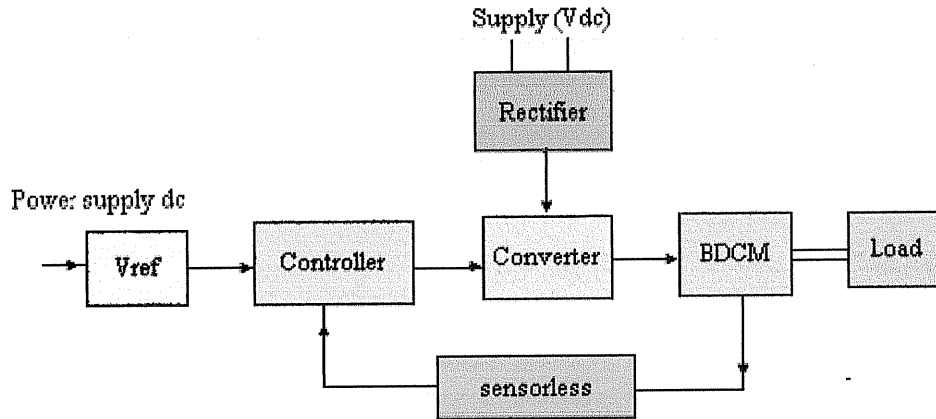


Figure (4.5): Open loop control of BLDC motor with back emf strategy

This system consists of seven main components, the PC which contains the controller and Vref generating circuit, Rectifier which gives us the dc needed voltage, the converter which used for generating the needed phase voltages from the rectifier and goes to brushless dc motor. The sensorless that detects and senses the position of the rotor per one rotation, and finally the load.

4.5.2. Closed loop control of BLDC motor with back emf strategy

In the closed loop control system there is a feedback signal taken from the output and then compared to a reference predetermined needed value, where the actual speed is measured by tachogenerator. Fig (4.6) shows the block diagram of the closed loop control system.

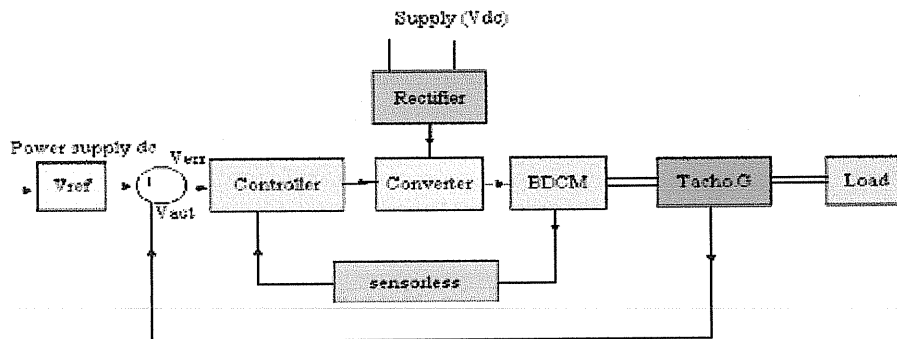


Figure (4.6): Closed loop control of BLDC motor with back emf strategy.

This system consists of eight main components, the PC which contain the controller, Vref generating circuit and the comparator, Rectifier which gives us the dc needed voltage, the converter which called inverter which used for generating the needed phase voltages from the rectifier and go to brushless dc motor, the sensorless which detects and senses the position of the rotor per one rotation, Tachogenerator which is the speed sensor which enables us to compare the actual speed with the reference speed, and finally the load.

4.5.3. General block diagram of sensorless

The way the back emf signal control the motor speed is by controlling the current applied to the motor which is depending on the phase angle between the back emf signal and the current signal. Fig (4.7) shows Control system Block diagram of sensorless.

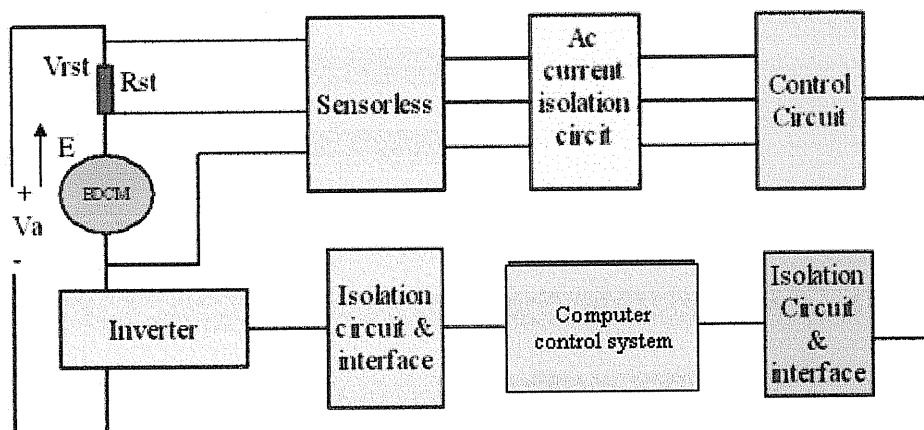


Figure (4.7): Control system Block diagram of sensorless.

General block diagram for the motor system and the control system attached for it. The phase angle between the current waveform and the emf waveform is determined according to the control requirements.

Note: the finger (4.7) will be discussed later in same chapter and explain this black and continents.

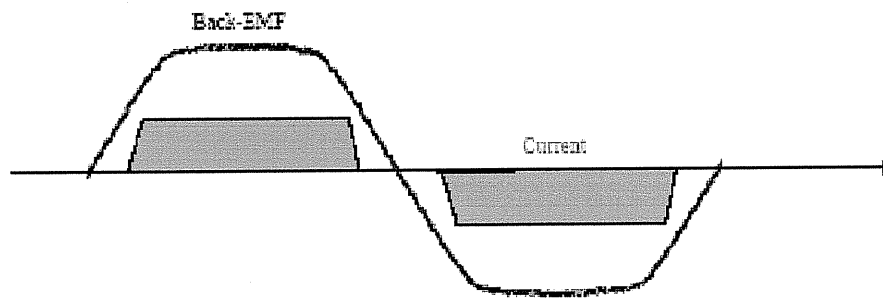


Figure (4.8): Emf signal and current waveform relationship

4.6. Back emf construction circuit (Sensorless)

In later, we assumed that the back e.m.f of the motor is given, but now, we will design a circuit that can produce this e.m.f. This will be done first because the back e.m.f cannot be measured in any way using the measurement devices, second, if we ignore the effect of the motor current, the phase that is fed will stay giving the signal to the PC controller that outputs the signals for the inverter to feed the same phase. So, the current must be taken into account for the sensorless circuit.

The sensorless circuit must satisfy equation (E4.1) to produce the induced voltage. Figure (4.9) shows the sensorless circuit we designed. It consists of an analog inverter, amplifier, subtract, comparator, and an opt isolator.

There are two signals must be taken from the motor circuit; the current signal and the terminal voltage across the second phase of the motor. These two signals must have a common ground, and must be connected to the ground of the sensorless circuit.

As shown, the current signal has a positive value, but the terminal voltage signal has a negative value. So, this signal must be inverted. We constructed this analog inverter with gain of 1 so as not to affect the amplitude of the signal.

The current here must be multiplied by the motor armature resistance. But here we use a (0.1Ω) resistor to sense the current, so the current must be multiplied by $(R_a/0.1)$ and this is the gain of the amplifier.

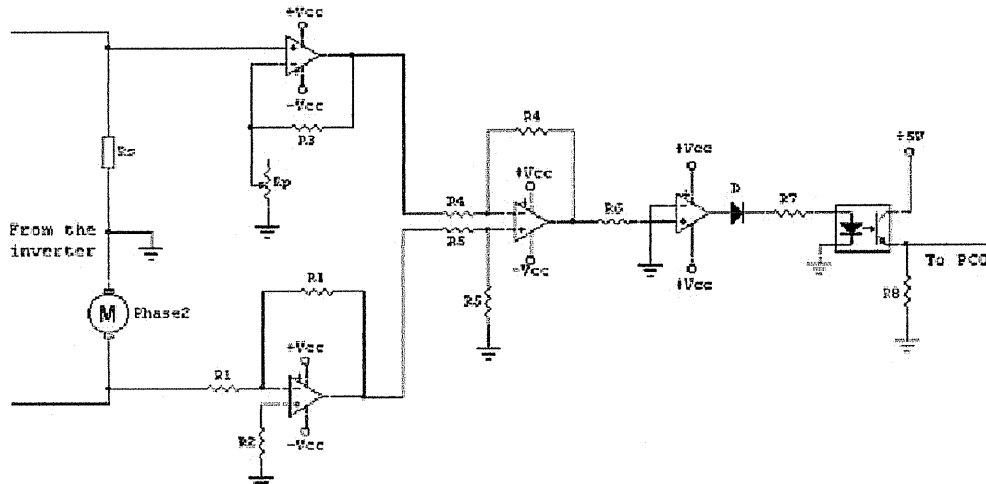


Figure (4.9): Control of back emf circuit diagram.

The sensing resistance has a small value so as to prevent the original current from decrease and to reduce losses of the sensing resistance. The sensorless circuit amplifies the current signal to have a final value equals $(I_a * R_a)$, i.e. the circuit multiplies the current signal by a gain equals to $(R_a/0.1)$, and then the circuit subtracts the amplified current signal from the phase voltage to obtain the pure e.m.f signal.

After that, this signal is compared with the ground to give a logic 1 or 0. Each has an interval of 180 degrees. If e.m.f is greater than or equal to 0 then it will give a pulse of 180 degree with amplitude (5V). When e.m.f becomes less than 0, this means that the South Pole of the permanent magnet is passes under first phase, then the comparator will give a zero voltage. Figure (4.10) shows the waveforms of the circuit and the output signal.

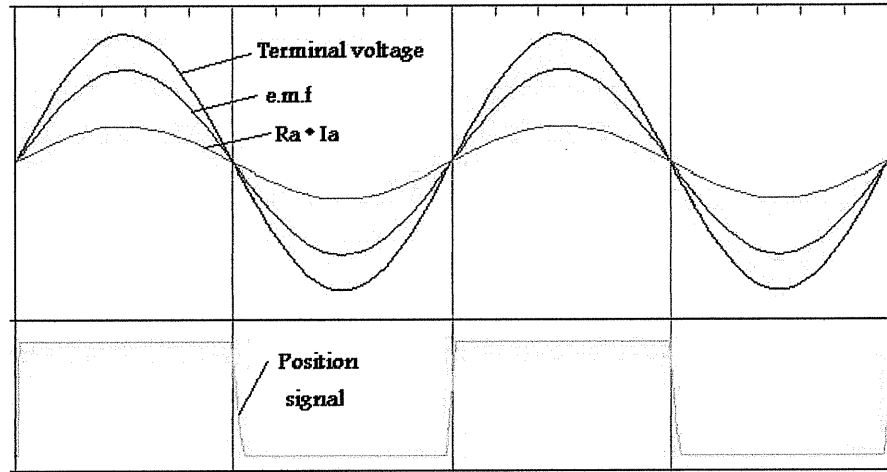


Figure (4.10): waveforms of sensorless circuit

Now the sequence of construction back emf is shown below:

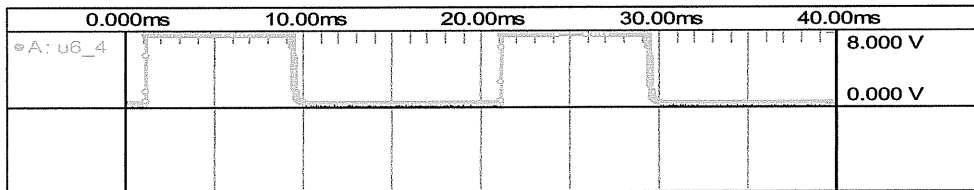


Figure (4:11): voltage wave (amp A)

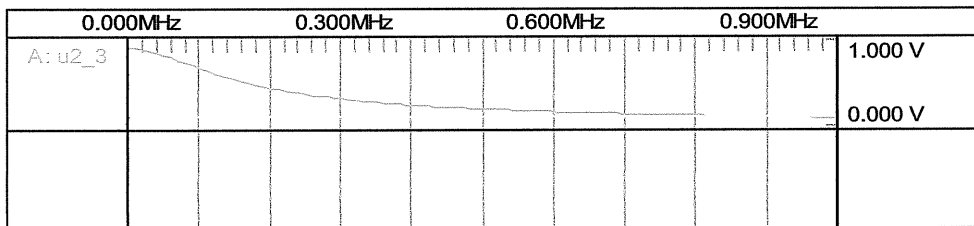


Figure (4.12): voltage wave (amp A, B)

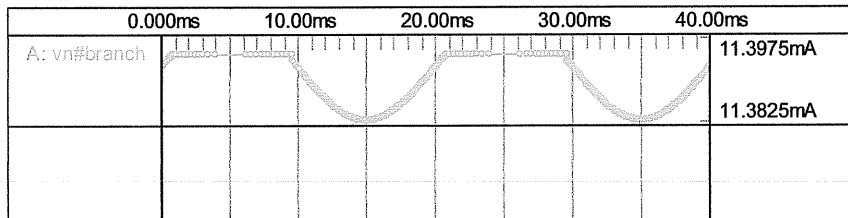


Figure (4.13): current wave (amp A)

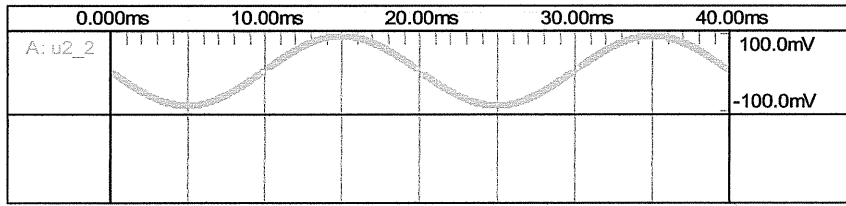


Figure (4:14): voltage wave (amp A)

The outputs of the isolating circuit are enabled directly to the inputs of the two operational amplifiers.

Ideal direct voltage source V . then at any instant the following equation can be written for the dock. Terminal voltage:

In summary the sensorless circuit satisfies the following equation:

$$e.m.f = V_{ph} - ((I_a * R_s) * G) \dots\dots\dots (E4.1)$$

Where:

V_{ph} : one-phase voltage.

R_s : current sensing resistor.

$G = R_a/R_s$ is the amplification constant.

So, equation (E4.2) becomes

$$e.m.f = V_{ph} - I_a * R_a \dots\dots\dots (E4.2)$$

The output pulses of the sensorless circuit are entered to an isolation circuit, and hence, to the PC system which can understand and then manipulates these signals as it manipulates the sensor signal as mentioned above.

Using this equation together with the e.m.f. and torque equations, the Torque/speed characteristic can be derived as:

$$W = W_0 [1 - T/T_0] \dots\dots\dots (E4.3)$$

Where the no-load speed is:

$$W = V/K\phi \text{ rad/sec} \dots\dots\dots (E4.4)$$

And the stall torque is given by:

$$T_0 = K\phi - I_0 \dots\dots\dots (E 4.5)$$

4.7. Efficiency

Efficiency is defined as the ratio of output power and input power, i.e.

$$\eta = \left(\frac{P_{in}}{P_{out}} \right) \times 100 \% \dots\dots\dots (E4.6)$$

Where:

$$P_{in} = m \cdot V \cdot I, \text{ and } P_{out} = T_{load} \cdot \omega_r.$$

In term of the power flow,

$$P_{in} = P_{cu} + P_{Fe} + P_{mec} + P_{out} \dots\dots\dots (E4.7)$$

Where:

$P_{cu} = m \cdot R \cdot I^2$ is the copper loss due to winding resistance, P_{Fe} the iron loss due to hysteresis and eddy currents, and P_{mec} the mechanical loss due to wind age and friction.

The purpose of this circuit is to construct back emf by subtract $(R_a \cdot I)$ from (V_a) .

The values of the resistors can be calculated as follows:

$$EMF = V_{ph} - ((I_a * R_s) * G) \dots \dots \dots (E4.8)$$

$$G = R_a / R_s \dots \dots \dots (E4.9)$$

Where:

V_{ph} : one-phase voltage.

R_s : current sensing resistor.

G : amplification constant.

4.8. Information about components

1.8.1. High isolation current

Since the current of the motor could be high it's necessary to provide current isolation between the motor system and the control circuit, such isolation and protection will prevent damage in the control circuit .The isolation is implemented at the inputs of the construction circuit.

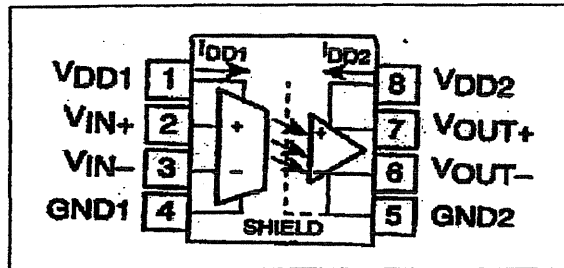
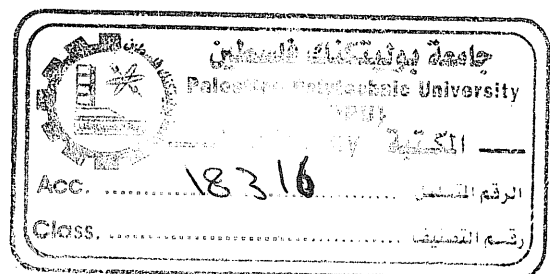


Figure (4.15): Pin configuration of HCPL7840 opt isolator

Optical isolator is a device that uses a short optical transmission path to accomplish electrical isolation between elements of a circuit. The optical path may be air or a dielectric waveguide. The transmitting and receiving elements of an optical isolator may be contained within a single compact module.



The optical isolator has many functions such as the dispatching of a signal, message, or other form of information; The propagation of a signal, message, or other form of information by any means, such as by telegraph, telephone, radio, television, or facsimile via any medium, coaxial cable, microwave, optical fiber, or radio frequency, in communications systems, a series of data units, such as blocks, messages, or frames; The transfer of electrical power from one location to another via conductors.

An optical isolator uses a short optical transmission path to accomplish electrical isolation between elements of a circuit. So, it is necessary for using in the motor system and control circuit to isolate the elements of the system and protect it from high current that damage the control circuit.

Stability is another advantage of isolation circuit. It is needed to accurately monitor motor in high noise motor control environments, providing for smoother control.

In various types of motor control applications, high accuracy and linearity are paramount under transient conditions. So, we must use isolation circuit between motor and control circuit, between control circuit and PC, between PC and power circuit.

4.8.2. Typical applications.

Motor phase current sensing, general-purpose industrial current sensing, high voltage power source sensing etc

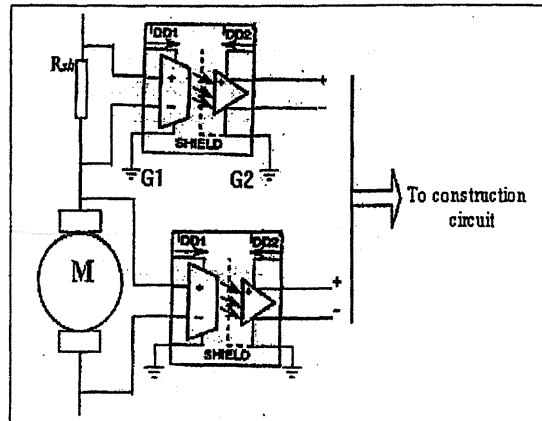


Figure (4.16): High current isolation circuit

4.8.3. Protection and interface of PC

Connecting the output of the construction circuit directly to the PC may cause dangerous damage to the PC unit if high current passes to the input port or if large amplitude signal is enabled to the input. So we should interface the construction circuit to the input port of the PC by mean of optoisolator. This device will prepare the signal to the PC in which the input signal amplitude is 5V.

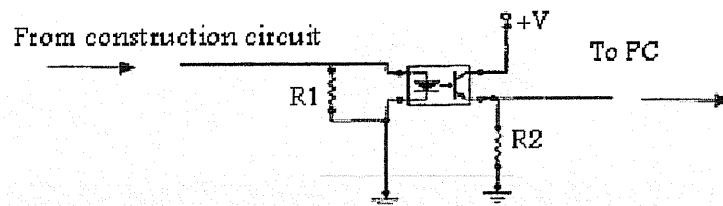


Figure (4.17): optisolator circuit input from control circuit and output to PC.

4.8.4. Resistors (R_1 & R_2) are for current limited

It's the same construction of the fig (4.17) above, but some differ of the input and output as the input from PC and output from the mosfet

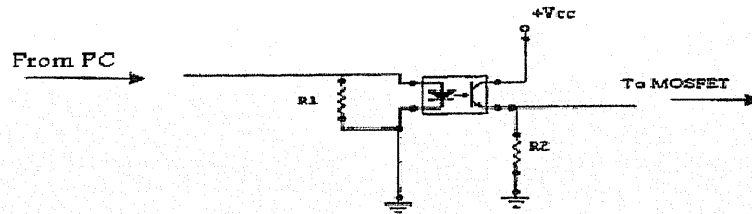


Figure (4.18): Opt isolator circuit - input from PC and output to Mosfet

4.8.5. MOSFET

We used the Mosfet transistor in control circuit because its characteristics and operation it used as the power switches and it very high speed to turn on or off.

4.8.6. Tachogenerator

An electromechanical generator is a device capable of producing electrical power from mechanical energy, usually the turning of a shaft. When not connected to a load resistance, generators will generate voltage roughly proportional to shaft speed. With precise construction and design, generators can be built to produce very precise voltages for certain ranges of shaft speeds, thus making them well-suited as measurement devices for shaft speed in mechanical equipment.

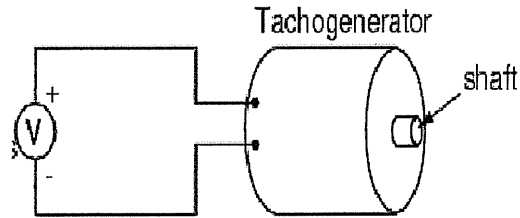


Figure (4.19): Tachogenerator diagram

Tachogenerators can also indicate the direction of rotation by the polarity of the output voltage. When a permanent-magnet style DC generator's rotational direction is reversed, the polarity of its output voltage will switch. In measurement and control systems where directional indication is needed, tachogenerators provide an easy way to determine that.

4.8.7 Inverter Signals Isolation.

Our inverter consists of 12 MOSFETs for operating the designed brushless motor bidirectional rotation. 4 MOSFETs for each phase are required and arranged as a bridge. The MOSFETs require signals to turn it on to conduct the current of each phase of the motor.

These signals come from the PC system. They must be isolated from the power circuit (the inverter). The N-channel MOSFET needs a positive gate voltage applied between the gate and the source of the MOSFET without existing any resistance between the source and the ground of the gate voltage supply. So the load that is driven must be on the drain side of the MOSFET.

But in our project, we used the bridge, to locate the phases between two MOSFETs which are operated together. The inverter isolation is shown in figure (4.20) for one phase.

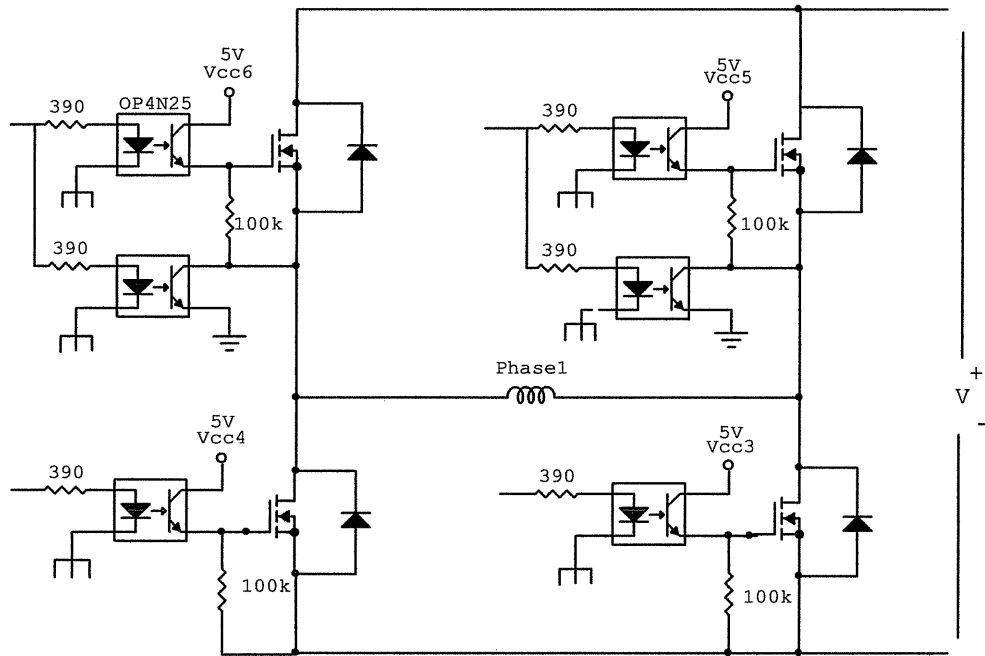


Figure (4.20): One-phase bridge isolation of power circuit

The lower MOSFET signals of the bridge could be applied directly with the same voltage supply, because the source pins of the MOSFETs could be grounded with the voltage supply. But if we connect the same voltage supply for the upper MOSFETs, we will make a short on the sources of the upper MOSFETs with the ground of the power supply, so the load and the lower MOSFETs will be canceled. Thus, the upper MOSFETs must have another voltage supply.

Also, for an individual MOSFET of the upper side must have an individual voltage supply in order not to make short of the MOSFET source pins i.e. shorting the phases of the motor. This problem is solved by the following tips.

- The MOSFET gate must be in two modes only; grounded with the source or should have a voltage greater than the threshold voltage of the gate-source. So a resistance is located between the gate and source pins to satisfy this tip.

- We designed isolation for the voltage source and also its ground, so two optocouplers are used for each MOSFET to avoid shorting the phases as shown in figure (4.20).
- So, in this way, we could use the same voltage supply for all upper MOSFETs for the two phases and coil 3.
- When the power supply is disconnected from the motor, it works as a generator and it reverses the current. This reverse current may destroy the MOSFETs; we have connected for each MOSFET a reversing diode to pass the reverse current without letting it to pass through the MOSFETs.
- The inputs of the optocouplers come from the PC system through a current-limiting resistor.
- In this way, we avoided using the multiple voltage supplies to give the protection for the inverter and the isolation circuit.

4.8.8. The converter

The converter used in our project consists of three components: a transformer, rectifier and an inverter.

4.8.8.1 Transformer

Voltage and current within the power supply are determined as the power supply starts up, and also when it stabilizes. These results will be displayed graphically.

The following steps are required to design the power supply parameters:

1. The parameters for the transformer, such as the no-load voltage, frequency and source impedance will be calculated from the nominal voltage, current, and regulation.
2. The type of rectifier we use is a solid-state rectifier.
3. We choose filter parameters which represent our chosen filter configuration.
4. Finally, we analyze and calculate the voltages and currents within the power supply. And we assume that the primary voltage for the transformer is 220V.

4.8.8.2 Rectifier

The rectifier converts the AC voltage into a dc voltage, and here we need a DC source because our dc motor operates at a dc voltage. We use the rectifier to obtain the dc source, because it will provide us with the dc voltage at any time, and it's easier to obtain the dc voltage than any other sources.

4.8.8.3 Inverter

The inverter provides the required sequence of the phase voltages that operates the motor in the 4 quadrants. In our project we mean by the inverter, the electronic circuit which gives us the required DC pulses for the motor.

This inverter consists of 12 MOSFETs. Two of them used to feed the first phase in clockwise direction operation, two of them used to feed also the first phase but in the opposite direction, and the other remaining MOSFETs used to feed the second phase in the same manner as the first phase and $T_9, T_{11}, T_{10}, T_{12}$ works to give the PWM.

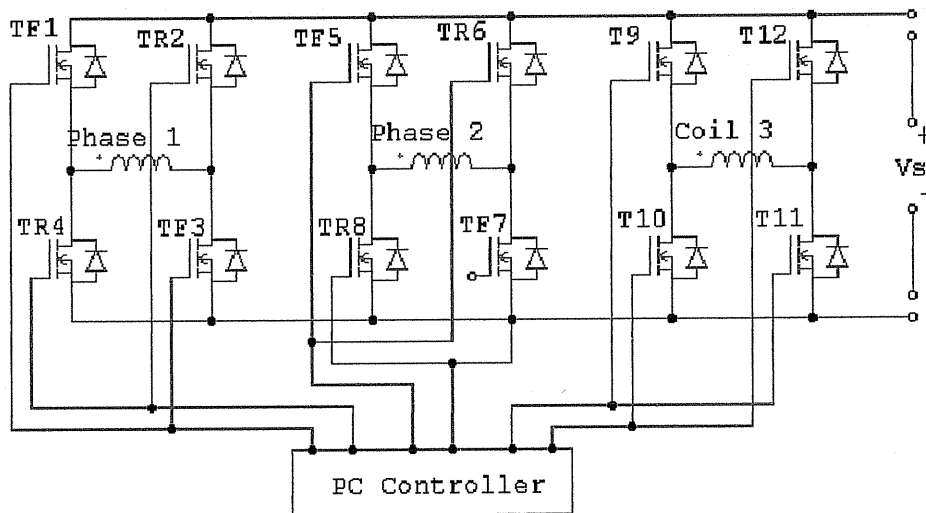


Figure (4.21): Inverter diagram

These MOSFETs receive its base pulses from a computer that provides the suitable signals for the transistors for the four quadrants operation. MOSFETs T_{F1} and T_{F3} feed phase1 of the motor in forward direction. T_{F5} and T_{F7} feed phase2 of the motor in forward direction. T_{R2} and T_{R4} feed phase (1) of the motor in reverse direction. T_{R6} and T_{R8} feed phase (2) of the motor in reverse direction and with forward direction in feed phase (1) the T_9 and T_{11} operation to get PWM. And with feed phase (2) worked the T_{10} and T_{12} work to give the PWM, and in opposed direction T_{10}, T_{12} work with phase (1) and T_9, T_{11} work with phase (2).

4.9. Total Circuit

In this section we illustrate the total circuit as a block, which represents the total system including the controller system and the drive system. Figure (4.23) shows the total system.

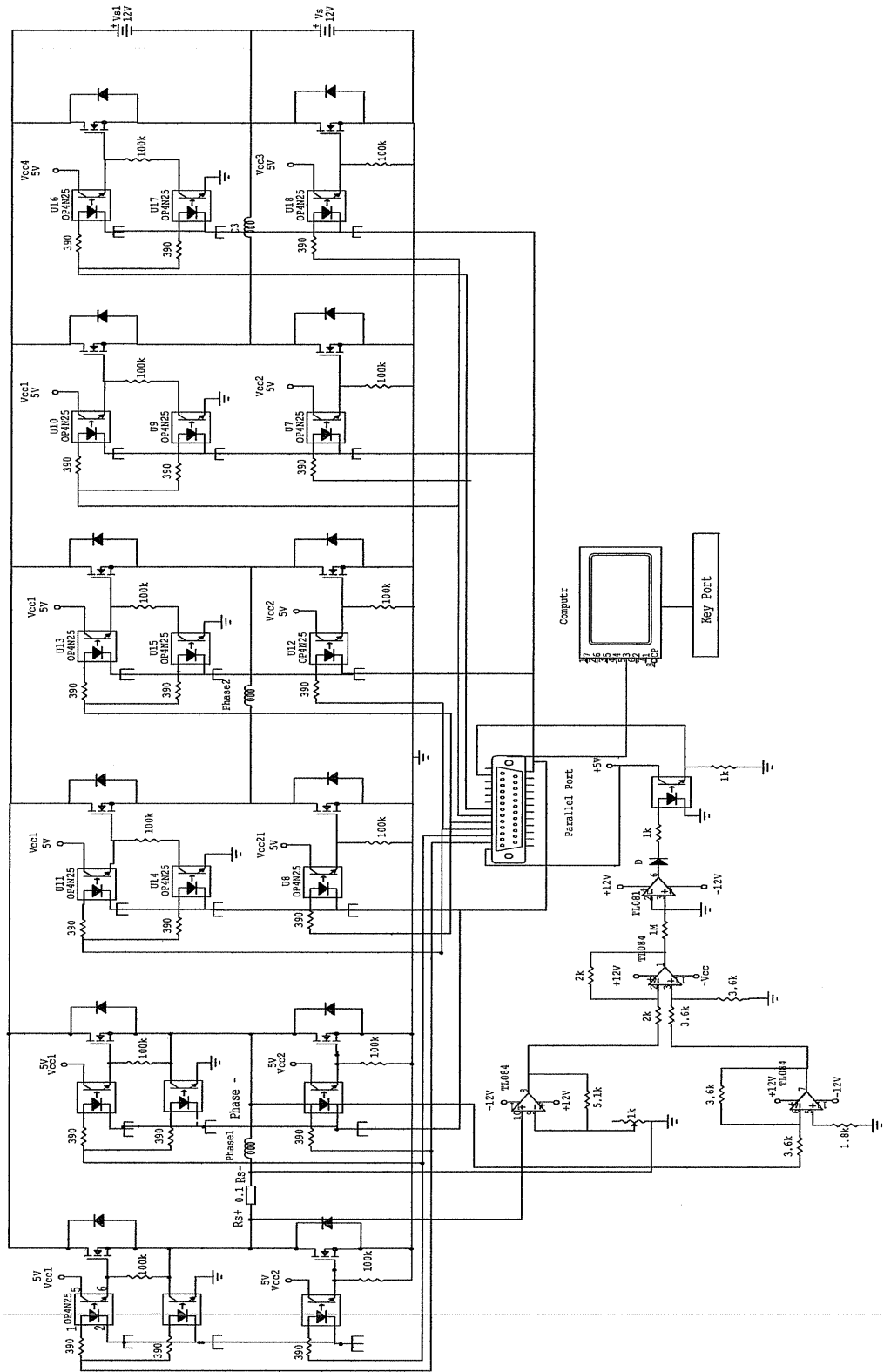
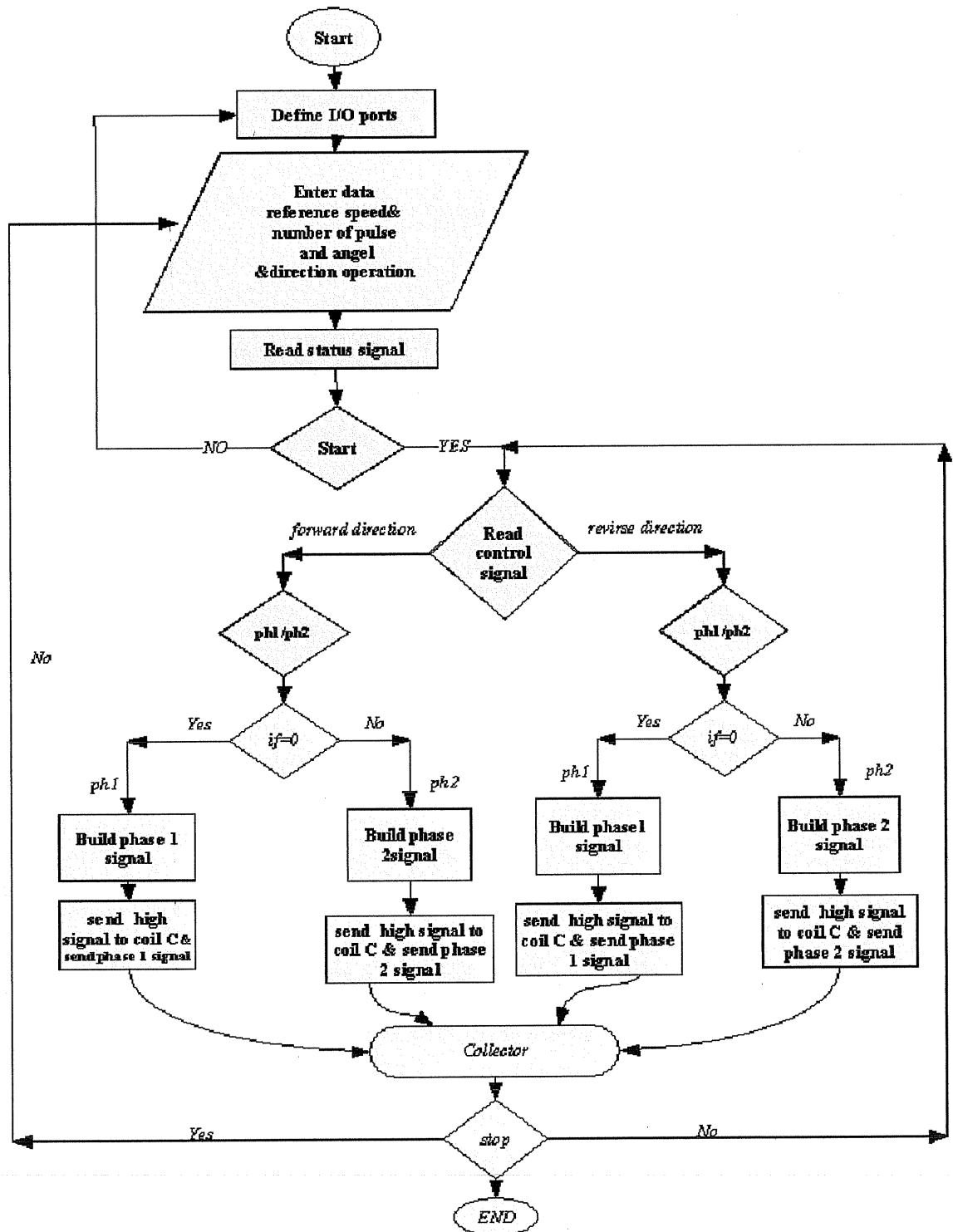


Figure (4.22): The total system

4.10. Flow Chart



Chapter Five

Design and simulation of Brushless DC Motor

5.1. Introduction.

5.2. Analysis.

5.3. Results.

5.4. Conclusion.

5.5. Study and compare some of electromagnetic parameters.

Chapter Five

Design and simulation of Brushless DC Motor

5.1. Introduction

Unlike a conventional dc motor, brushless dc motors has an “inside-out” construction [1, 2], i.e. the field poles rotate and the armature is stationary. The field poles consist of permanent magnets mounted on the outside of the rotor surface, and the armature is wound on a slotted or a salient pole laminated sheets. The armature coils are switched by transistors instead of the commutator. This arrangement has several advantages over small conventional DC motor or AC motor such as:

- 1) High efficiency.
- 2) Adaptability for speed control.
- 3) High speed operation.
- 4) Long operation life and absent rotor losses in additional with operation from low voltage dc supply.

A typical small-power application is in dc fans for cooling electronic equipments and closed spaces. Brushless dc motor fans are smaller in size and weight than ac fans using shaded pole or Universal motors.

Ability to work with the available 24-v or 12-v dc supply makes the brushless dc motor fans convenient for use in electronic equipment, computers, mobile equipment, vehicles, and spindle drives for disk memories, because of its high reliability, efficiency, and ability to reverse rapidly. Brushless dc motors in the fractional horsepower range have been used in various types of actuators in advanced aircraft and satellite systems [3, 4].

Together with applying permanent magnet excitation, it is necessary to obtain an additional torque components, which could be obtained due to difference in

magnetic permanent in both quadrant and direct axis, therefore, reluctance torque is developed and torque –null regions are eliminated [5, 6]. Unsymmetrical air gap rotor construction are introduced to reduce the torque ripples and to increase the mean torque.

The low level of fluctuation in the magnitude and orientation of the armature-current patterns that is a standard feature of well designed DC machines is normally absent in inverter-fed synchronous motors.

This stems from a relatively small number of switched armature-winding portions in the vast majority of synchronous motors and from the changes in phase angle between current and voltage that occur as load and speed varies. Fluctuations due to the latter usually occur relatively slowly and can be minimized by the use of current-forcing techniques or by appropriate control of switching instants.

5.2. Analysis

5.2.1: Motor windings and the Phase current

Brushless dc motors could be applied for various types of windings: single-phase single pulse, two-phase two pulse, three-phase three pulse or six pulse dc motors. The interest on two-phase brushless dc motor comes due to reduction of the driving circuit and total cost of the motor.

—The elementary two-phase Brushless dc motor circuit usually consists of a permanent magnet rotor and stator with two windings located on the same magnetic axis, and drives by two power transistors controlled by sensing units, each transistor is switched on for 180° . The torque produced by the interaction of the rotor magnetic field and the winding current nulls each 180° . The presence of null points in electromagnetic torque are the main limitation for widespread application because of the following several reasons: **first**, the motor will not start from the null position, **second**, high ripples in the electromagnetic torque, therefore the speed will

fluctuate with rotor position , and **third**, high current at low speed and additional losses . This disadvantage makes the motor impractical for commercial use unless one of the following solutions is taken to overcome the main drawbacks:

- I. Polyphase motor: this motor has no torque nulls and relatively constant torque. This motor is not a subject of this project.
- II. Unsymmetrical rotor construction: the rotor teeth are performed with predetermined high and width, this made with purpose to obtain unsymmetrical magnetic permanent around the rotor surface.

Taking into account motor design data and rotor construction illustrated on fig (5.1), which is the subject of present study.

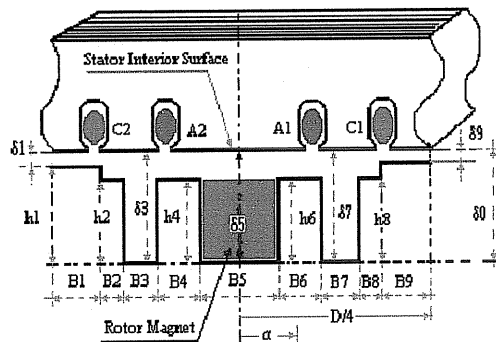


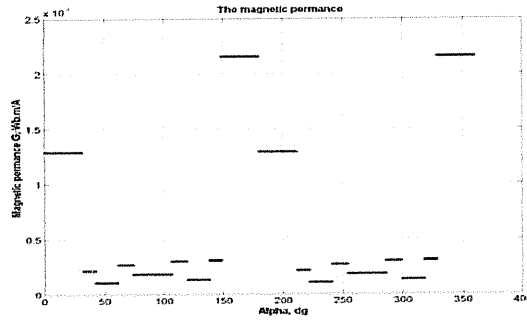
Figure (5.1): Motor construction

The magnetic permanent yield due to the difference in the stator construction could be changed depending on the Rotor slots width and depth. Fig (5.2(a)) illustrates the magnetic permanent distribution in the stator air gap with respect to rotor main tooth width, the obtained harmonic spectrum is shown on fig (5.2(b)), where it is clearly shown that by introducing some asymmetry in the rotor construction high order harmonic of magnetic permanent are realized, which are a required condition for avoiding null points.

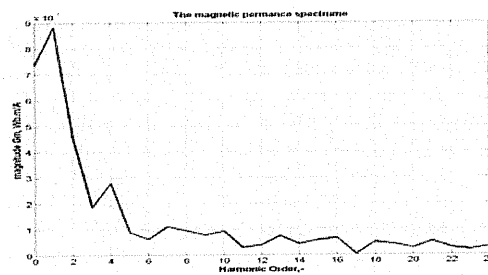
By applying above mentioned construction the motor will produce two torque components:

1. Electromagnetic torques which form is expected to be sinusoidal positive change.

2. And a reluctance.



a)



b)

Figure (5.2.a: Magnetic permanent at variable airgap and symmetrical located slots; and b) the obtained harmonic spectrum

Component with nulls of the torque does not coincide with the nulls of the electromagnetic torque. The torque ripples could be reduced furthermore by representing an innovative way to resolve the two-phase limitation and to achieve relatively ripples-free torque. One of these solutions is presented in this project, which is called a combination control method is introduced.

III Combination control: This type of motor control presents two solutions at the same time – first one unsymmetrical rotor construction is introduced with purpose to avoid torque-nulls points. – Second one PWM control drives additional bi-directional stator switching circuit as well shown on fig. (5.3(a)), where the time-switching diagram is shown on fig. (5.3(b)). Third winding S3 on the figure has uniform distribution in the stator periphery with aim to obtain

approximately sinusoidal flux distribution in the airgap. Third coil has less number of windings comparing with another two coils.

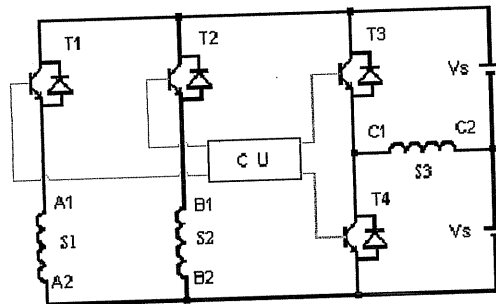


Figure (5.3a): Electrical circuit

III.1 -Switching pulse generation – Transistors T1 and T2 are switched continuously for 180° each one and connect the supply voltage to the coils S1 and S2 in

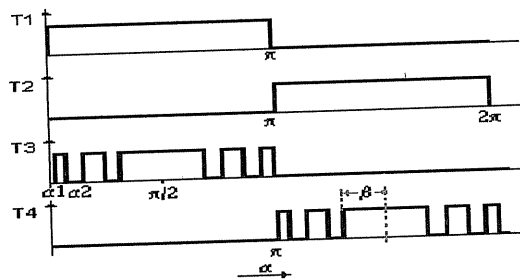


Figure (5.3b): Pulse generation wave form-illustration

Complementary sequence, Transistors T3 and T4 are switched the supply voltage to the third coil with polarity and time-duration determined from the applied PWM control strategy.

III.2 - Phase current calculation – the motor phase current differs in coils S1,S2 and S3, where the current in first two coils has continuous character and approximately constant value at steady state operation, the current in third coil takes form nearly to the sinusoidal phase current depending on the pulse PWM control strategy , induced counter EMF and magnetic permanent .

*- **Phase (coil) currents** $I_A(\omega t)$ and $I_B(\omega t)$ in integral form is presented as follow for one phase only, the second phase have the same relations:

$$\int_0^{\pi} i_{dA}(\omega) = \int_0^{\pi} \frac{V_{ds} - e_A(\omega)}{L_A(\omega)} d\omega + \int_0^{\pi} \frac{R_A i_A(\omega)}{L_A(\omega)} d\omega + \int_0^{\pi} \frac{i_A(\omega)}{L_A(\omega)} \left[\frac{d}{d\omega} L_A(\omega) \right] d\omega \dots\dots\dots (E5.1)$$

The obtained results are displayed on fig (5.4) for both phases, where each phase operates 180° only. It is clearly shown that the phase current depends on the rotor position.

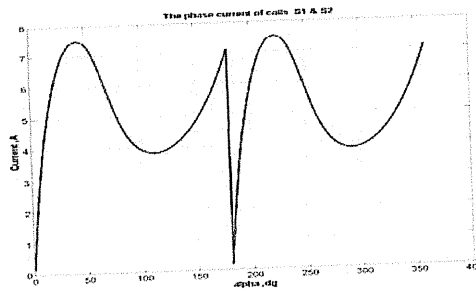


Figure (5.4): Phase current of both coils S1 & S2

**** Phase (coil) current $I_C(\omega t)$:**

The coil current $i_3(\alpha)$ could be calculated after determination the modulation function $h(\alpha)$ as well described in [Y7]. The pulse duration of generated train of pulses depends on the selected harmonic that must be eliminated while existing on the quarter wave interval from α_{min} to α_{max} ,

The Fourier series of required odd quarter –wave signal could be presented by assuming the following harmonic function [7, 8]:

$$h(\alpha) = \sum_{n=1}^{\infty} A_n \sin(n\alpha)$$

$$A_n = \frac{4}{n\pi} \sum_{k=1}^{N_p} (-1)^{k+1} \cos(n\alpha_k) \dots\dots\dots (E5.2)$$

Where:

N_p - odd or even numbers, and

$\alpha_{min} < \alpha_1 < \alpha_2 \dots < \alpha_k < \pi/2$.

If $n_1, n_2 \dots n_{N_p}$ are the harmonic to be eliminated.

From $h(\alpha)$ then the following set of algebraic equations must be satisfied to reduce the coefficients of each harmonic to be eliminated to zero:

$$0 = \sum_{k=1}^{\infty} (-1)^{k+1} \cdot \cos(n_1 \alpha_k)$$

$$0 = \sum_{k=1}^{\infty} (-1)^{k+1} \cdot \cos(n_{N_p} \alpha_k) \dots \dots \dots (E5.3)$$

The obtained algebraic matrix is solved, where a set of pulse patterns are calculated α_k , and the obtained waveforms for certain speed and frequency is presented in fig (5.5).

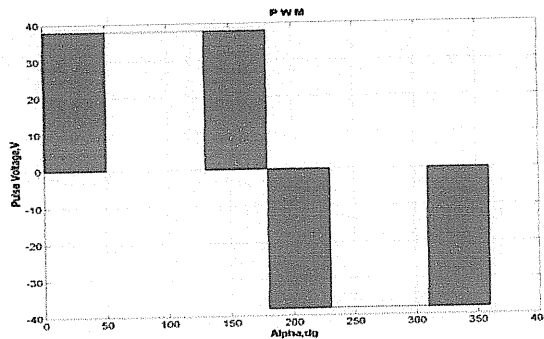


Figure (5.5): Phase voltage of coil S3

By applying KVL, and taking into account motor equivalent circuit with concentrated parameters the motor voltage equation for the third coil is:

$$\begin{aligned}
 V_d &= V_s \cdot h(\alpha) \\
 V_d &= R_C i_C(\alpha) + \frac{d}{d\alpha} \lambda_C(\alpha) + e_C(\alpha) \\
 e_C(\alpha) &= E m_C \sin(\alpha) \\
 \lambda_C(\alpha) &= L_C(\alpha) \cdot i_C(\alpha) \quad \dots\dots\dots (E5.4)
 \end{aligned}$$

Taking into account the leakage inductance of third coil and its dependency on the rotor position:

$$L_C(\alpha) = L_0 + \sum_{q=1}^{\infty} L_{2m} \cos(2q\alpha) \quad \dots\dots\dots (E5.5)$$

Now eq. (4) can be expressed as follow:

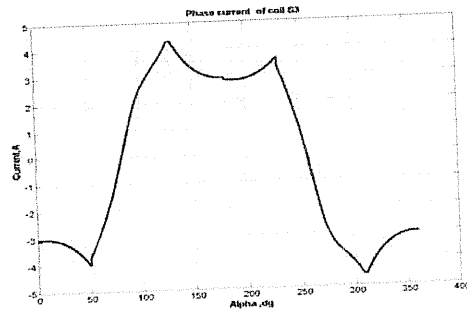
$$V_d - e_C(\alpha) = R_C i_C(\alpha) + L_C(\alpha) \cdot \frac{d}{d\alpha} i_C(\alpha) + i_C(\alpha) \cdot \frac{d}{d\alpha} L_C(\alpha) \quad \dots\dots\dots (E5.6)$$

By applying the principle of implicit integration, which form is present below:

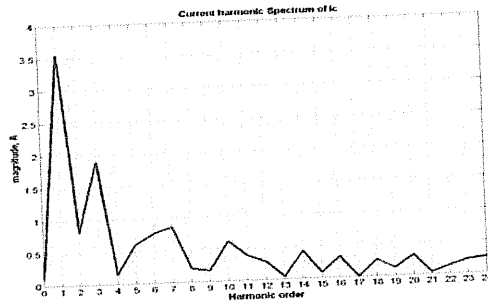
$$\int_{\alpha_1}^{\alpha_2} i_C(\alpha) d\alpha = \int_{\alpha_1}^{\alpha_2} \frac{V_d - e_C(\alpha)}{L_C(\alpha)} d\alpha + \int_{\alpha_1}^{\alpha_2} \frac{R_C i_C(\alpha)}{L_C(\alpha)} d\alpha + \int_{\alpha_1}^{\alpha_2} \frac{i_C(\alpha)}{L_C(\alpha)} \left[\frac{d}{d\alpha} L_C(\alpha) \right] d\alpha \quad \dots\dots\dots (E5.7)$$

The results of solving eq. (7) for various modulation index, modulation frequency and speed are graphically displayed on fig(5.6(a)). The obtained coil current $i_C(\alpha)$ can be expressed in Fourier series by applying FFT procedure, where the obtained results are displayed on fig (5.6(b)):

$$i_C(\alpha) = \sum_{v=1}^{\infty} I_{mv} \cdot \sin(\omega t - \psi_v) \quad \dots\dots\dots (E5.8)$$



(a)



(b)

Figure (5.6: a phase current of S3 at speed of n_1 ;
And b) current harmonic spectrum I_c .

5.2.2: Electromagnetic Torque

In this section two-types of two-phase two-pulse brushless dc motors are going to be described:

5.2.2.1. Unsymmetrical rotor construction:

The torque consists of two components[X2, (4)] - reluctance torque T_r and electromagnetic torque T_e . This torque is going to be called “original “in this study.

The reluctance torque: this torque is independent of the excitation of the stator coil and depends upon the permanent of the airgap as seen by the rotor

magnets. As stators consist of laminated sheets with slots, the rotor consist of massive iron core with special slots having different geometrical construction. The permanent in the airgap varied periodically with the rotor position, being maximum at the axis of the stator poles. Consider the rotor construction shown on fig.1, the reluctance torque is calculated using coenergy method as follow:

$$T_{RA} = \frac{d}{d\alpha} W_{RA}(\alpha) = 0.5 F_{SA} \cdot \frac{d}{d\alpha} G(\alpha)$$

where

$$F_{SA} = N_{phA} I_A K_{wA}$$

$$G(\alpha) = G_0 + \sum_{g=2}^{\infty} G_{mg} \cos [N_{tg} (\alpha - \beta_g)]$$

$$N_{tg} = g \cdot N_t$$

..... (E5.9)

The final expression for reluctance torque is:

$$T_{RA} = (F_{SA})^2 (G_2 \sin 2(\alpha - \beta_2) + 2 G_4 \sin 4(\alpha - \beta_4))$$

..... (E5.10)

The obtained reluctance torque expression indicates that null points torque occurs at $\alpha \neq 90^\circ, 180^\circ, \dots$, which is good indicator for realizing self starting torque.

The electromagnetic Torque: this component of torque is obtained due to the interaction between stator coil current and rotor magnets , where the mathematical expression taking into account coenergy method [9,10] for determination the electromagnetic torque is presented as follow :

$$T_{EA} = \frac{d}{d\alpha} W_{EA}(\alpha) = F_{SA} \cdot \phi_R(\alpha)$$

..... (E5.11)

Where,

$$\phi_R(\alpha) = \int_{-\frac{\pi}{2}}^{\frac{\pi}{2}} F_R \cdot \cos(\theta - \alpha) \cdot G(\alpha) d\alpha$$

Is the produced rotor flux in the airgap, which depends on the magnetic permanent and rotor MMF produced from the permanent magnet intensity and length.

The mathematical expression is given below:

$$\phi_R(\alpha) = F_R A \cos \alpha + F_R B \sin \alpha$$

where

$$A = 2 G_0 + \frac{2}{3} G_2 \cos 2 \beta_2 - \frac{2}{15} G_4 \cos 4 \beta_4$$

$$B = \frac{4}{3} G_2 \sin 2 \beta_2 - \frac{8}{15} G_4 \sin 4 \beta_4$$

$$F_R = L_m H_m$$

..... (E.512)

The final expression for electromagnetic torque for one coil S1 or S2 is :

$$T_{EA} = F_{SA} F_R A \sin \alpha - F_{SA} F_R A \cos \alpha$$

..... (E5.13)

The total motor torque, presents sum of both torques taking into account eq.(10) and eq.(13), has an expression expressed below , with graphically results illustrated on fig.7 for certain speed n_1 , where its clearly shown that the motor achieved self starting condition. At the same time the generated torque

$$T_{TA} = T_{EA} + T_{RA} \quad \text{..... (E5.14)}$$

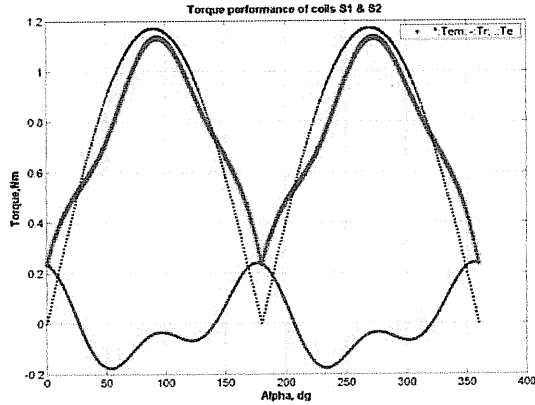


Figure (5.7): Total Electromagnetic torque of coils S1 & S2.

Ripples are relatively high, which is the main drawback of this design version. These ripples could be reduced extremely by applying the combination control method, where the produced torque is described hereinafter.

5.2.2.2. Combined control method

These methods is concentrated in producing additional torque by third coil S3, and have a purpose to eliminate the weak regions of the original torque. Further more , the produced torque will play significant role in ripples reduction overall the speed range , average torque increasing, and finally as a result from this procedure achieving more speed stability with minimized fluctuations, which is important criteria in electrical drive technology . The torque expression is presented below taking into account coenergy method:

$$T_{TC} = \frac{d}{d\alpha} W_{EC} (\alpha)$$

$$W_{EC} (\alpha) = \frac{1}{2} [F_{SC} (\alpha, \omega t)]^2 \cdot G(\alpha) + F_{SC} (\alpha, \omega t) \phi_R (\alpha)$$

..... (E5.15)

The stator MMF produced by third coil S3 with current $i_c(\omega t)$ flow through distributed winding in the stator periphery has space time variation with stepped character and minimized space-time ripples . Writing the trigonometrically terms as sums and difference leads to the following expression:

$$F_{SC}(\alpha, \omega t) = \frac{N_{phC} I_{m1}}{\pi} \sum_{v=1}^{\infty} \sum_{\gamma=1}^{\infty} \frac{K_{vi} K_{\omega\gamma}}{\gamma} X(v, \gamma) \cos(v\omega t - \gamma\alpha) + Y(v, \gamma) \cos(v\omega t + \gamma\alpha)$$

where

$$X(v, \gamma) = 1 + \cos(v - \gamma) \frac{\pi}{2}$$

$$Y(v, \gamma) = 1 + \cos(v + \gamma) \frac{\pi}{2} \quad K_{vi} = \frac{I_{mv}}{I_{m1}}$$

..... (E5.16)

Since the coil current $i_c(\omega t)$ depends on the rotor position and induced back EMF, the electromagnetic torque produced by this coil T_{TC} will changes alternatively, which means that in some regions will added to the original torques and subtracted in another regions . As a result from this adding and subtraction the produced total electromagnetic torque is expected to be with reduced ripples. Hereinafter mathematical expression explaining the dependency of T_{TC} on many parameters taking into account eq. (15) and eq. (16) :

$$T_{TC} = T_{EC1} + T_{EC2} + T_{EC3} + T_{EC4}$$

where

$$T_{EC1} = F_{SC}(\alpha, \omega t) \cdot G(\alpha) \frac{d}{d\alpha} F_{SC}(\alpha, \omega t)$$

$$T_{EC2} = \frac{1}{2} [F_{SC}(\alpha, \omega t)]^2 \cdot \frac{d}{d\alpha} G(\alpha)$$

$$T_{EC3} = F_{SC}(\alpha, \omega t) \cdot \frac{d}{d\alpha} \phi_R(\alpha)$$

$$T_{EC4} = \phi_R(\alpha) \cdot \frac{d}{d\alpha} F_{SC}(\alpha, \omega t)$$

..... (E5.17)

The obtained torque components of eq.(17) are graphically displayed on fig.8 at the same conditions, where this torque has reach harmonic spectrum when operates alone, but will improve the total motor torque when acts together with the original torque .

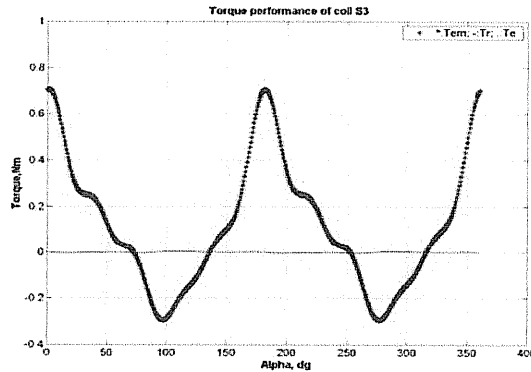
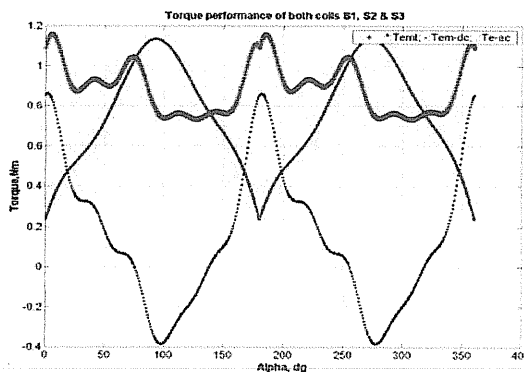


Figure (5.8): Total electromagnetic torque of S3

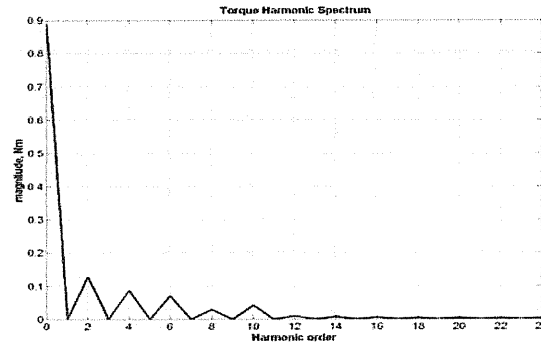
The total torque produced by three coils is the sum of eq. (14) and eq. (17) As follow:

$$T_{EM} = T_{TA} + T_{TC} \dots\dots\dots (E5.18)$$

The torque results are graphically displayed on fig. (5.9a) for certain motor speed of n1 and the torque harmonic spectrum is displayed on fig. (5.9b). from displayed .results it is shown that the put up tasks have been achieved.



(a)



(b)

Figure (5.9: a) The total electromagnetic torque of both coils S1, S2 & S3; b) The torque harmonic spectrum .

5.3. Results

Refer to the motor design parameters listed in table.1, and rotor design listed in the appendix, the discussed results in previous section can supported with additional conclusive parameters [11, 12] as follow :

Torque- Current ratio: this parameters presents the ratio of obtained mean torque to the root-mean square current :

$$T_{CR} = \frac{T_{AV}}{I_{TRMS}}$$

where

$$I_{TRMS} = \sqrt{\sum_{v=1}^{\infty} (I_{VRMS})^2} \dots\dots\dots (E5.19)$$

1. Torque ripple factor : this parameters presents the ratio of the torque ripples to motor mean torque :

$$T_{RR} = \frac{T_R}{T_{AV}}$$

where

$$T_R = \sqrt{T^{-1} \int_0^{\circ T} (T_{EM} - T_{AV})^2 d\alpha} \dots\dots\dots (E5.20)$$

2. Current harmonic factor : this parameters presents the ratio of total rms current to the fundamental :

$$H_{FI} = \sqrt{\left(\frac{I_{TRMS}}{I_{RMS}}\right)^2 - 1} \dots\dots\dots (E5.21)$$

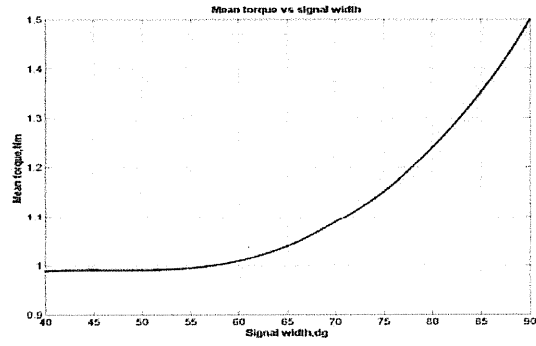
These parameters are going to be discussed for the following cases:

Case#1:

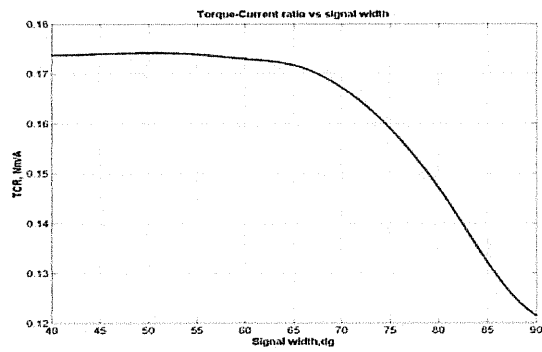
The width of control signal β (see fig.3b) could be varied, where the obtained results are graphically illustrated on fig10. From these results it is clearly shown that the motor mean (average) torque strongly increased by increasing β , but this increasing at the expense of torque-current ratio decreasing especially at certain value of $\beta > 65^\circ$. Furthermore the torque ripples factor reached it is minimized value at certain $\beta = 65^\circ$, while the current harmonic factor reached it is maximum value. This means that the pulse width must satisfy two contradict requirements high TCR and relatively low HFI.

Case#2:

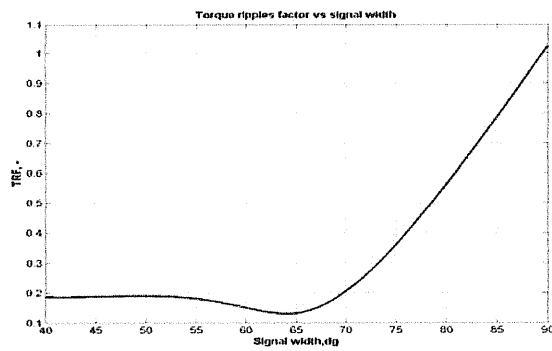
The width of main rotor slot B5 (see fig.1) could be varied, where the obtained results are graphically illustrated on fig11. From these results it is clearly shown that the motor mean torque strongly decreases by increasing B5, also TCR decreases in the same manner. The torque ripples and the current harmonic factor have acceptable values at B5=5...10 mm comparing with these results obtained for B5 >10 mm. The torque ripples raised significantly at certain value of B5 >12 mm, which means that the rotor construction must designed for B5 < 12mm.



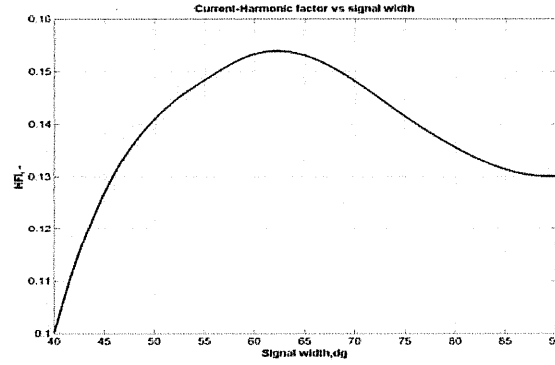
(a)



(b)



(c)

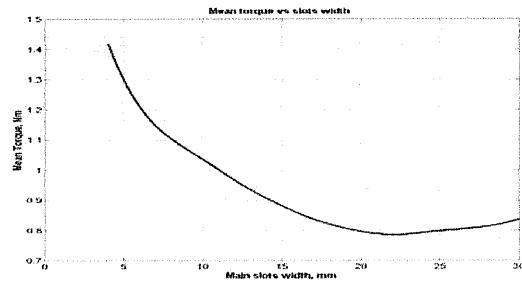


(d)

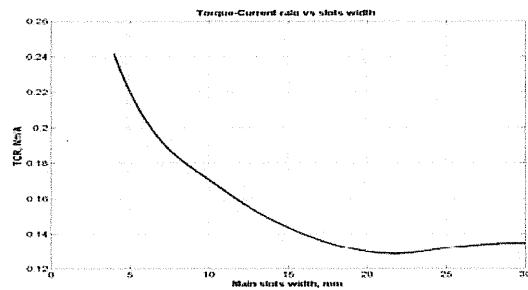
Figure(5.10: a)The mean torque ; b)Torque-Current ratio ; c) Torque ripples factor ; and d) Current harmonic factor versus signal width. β .

Table (5.1): The motor parameters

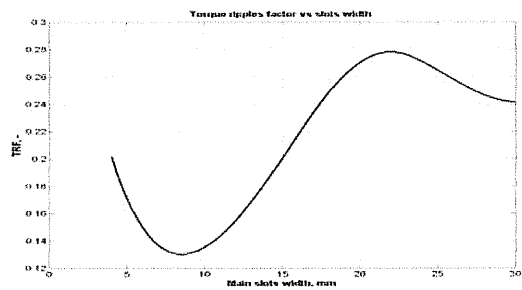
| | |
|--|-----|
| Phase voltage V_s , V | 38 |
| The induced counter voltage in coil S1 E_{mA} , V | 33 |
| The phase resistance of coils S1 & s2 R_A , Ω | 0.3 |
| The phase resistance of coil S3 R_C , Ω | 8.5 |
| The number of conductors of S1 & S2, N_{phA} , conductors/pole | 60 |
| The number of conductors of S3, N_{phC} , conductors/pole | 80 |
| The pole pairs number P | 2 |
| The induced voltage frequency f_1 , Hz | 50 |
| The modulation frequency f_m , kHz | 20 |
| The modulation ratio M | 0.9 |
| The stator interior diameter D , mm | 54 |
| The number of stator slots / pole S | 4 |
| The stator active length L_δ , mm | 65 |
| The permanent magnet coercive force (intensity) H_m , kA/m | 40 |



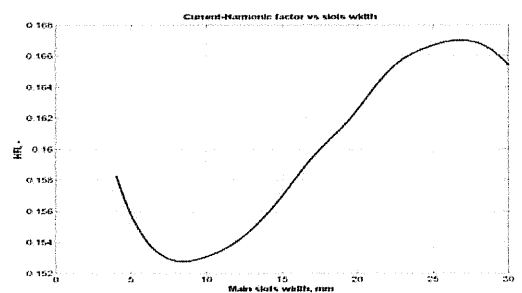
(a)



(b)



(c)



(d)

Figure(5.11: a) Motor mean torque ; b) Torque-Current ratio ; c) Torque ripples factor ; and d)Current harmonic factor versus slots width B5, mm.

5.4. Conclusion

1. The applied innovative design of two phases/ three coils two-pulse brushless DC motor with combined control produced electromagnetic torque having self-starting and reduced fluctuation. This is due to the dissymmetry in the rotor construction where the reluctance torque nulls do not occur at the same angles of the electromagnetic torque.
2. By introducing the PWM control of third coil the torque ripples are further decreases, because of the generated train of pulses with variable width. Once torque ripples decreases, the additional stability in the motor torque could be achieved, dissipated power reduction and motor utility increasing. The motor electromagnetic performances are directly depends on the continuous width of the PWM signal β , where by increasing this angle the Torque-current ration keeps relatively acceptable result .
3. Discussed results related to rotor slots width, where illustrated graphically mentioned that by increasing the width of main rotor slot B5, the consumed phase current increases with purpose to cover the required MMF. At the same time the mean torque decreases because of additional reduction in the magnetic permanent. The rotor has optimized slots width B5, which will be the design value in the future application of this motor.
4. The proposed design allow two operation modes depending on the required operation conditions and discussed results in the appendix :
 - first mode: when the main criteria is to obtain constant stable torque with somewhat reduced mean torque, minimized ripples and fluctuations, thus three coils must energized with appropriate switching signals .
 - second mode: when the main criteria is to obtain mean torque as great as possible, despite of the further increasing in the motor pulses and fluctuation, thus only two coils S1 and S2 are to be energized .

- Each described construction has certain advantages and disadvantages associated to moment of inertia, vibration and noises, which mean's that choosing the required construction must take these parameters into consideration

5.5. Study and comparing some of electromagnetic parameters

In this section Permanent magnet rotor should be described with purpose to study and compare some of electromagnetic parameters with reference values. This study is going to be realized as follow:

1-Design parameters and relations

In the following study rotor design cases are going to be described, taking into account table A.1, which give a relations between the rotor parameters with respect to width and depth of each one, where displayed on fig(5.1) and taking into account the following main data :

- the active uniform air gap width $\delta=0.5$ mm
- the permanent magnet high $h_m=6$ mm
- the outside rotor diameter $D=53$ mm

2-Design classifications

Four design classifications are going to be described depending on the required criteria:

- Production large mean torque at the expense of significant pulsation?
- Or production relatively less mean torque, but with reduced pulsations and good speed stability? These tasks should be described in details in four design

Cases as well shown on table (5.A1):

| Case No | Rotor construction | | | Displayed results on figure |
|--|--------------------|-----------------------------|--------------------------------|------------------------------|
| | Slots width mm | Slots depth mm | Air gap width mm | |
| Case#1 Uniform rotor construction with 2 coils S1&S2 | B1 =14B | $h1 = \delta 0 - \delta 1$ | $\delta 1 = 2 \delta$ | A1-a A2-a A3-a A4-a |
| | B5 =6B | $h5 =hm$ | $\delta 5 =hm + \delta 1$ | |
| | B3 =2B | -- | $\delta 3 = \delta 1 + hm$ | |
| | B2 =0 | $h2 =h8$ | $\delta 9 =2 \delta$ | |
| | B9 =14B | -- | -- | |
| | B8 =0 | $h5 =h6$ | -- | |
| Case#2 Uniform rotor construction with 3 coils S1,S2&S3 | B4 =B | $h4 =h6$ | -- | A1-a A2-b A3-b A4-b |
| | B1 =0B | $h1 = \delta 0 - \delta 1$ | $\delta 1 = 2 \delta$ | |
| | B5 =6B | -- | $\delta 5 =hm + \delta 1$ | |
| | B9 =10B | -- | $\delta 9 = \delta 1$ | |
| Case#3 Uniform rotor construction with multi slots,3coils and constant width of air gap | B2 =0 | $h2 =h8$ | $\delta 9 =2 \delta$ | A1-b A2-c A3-c A4-c |
| | B1 =6B | $h1 = \delta 0 - \delta 1$ | $\delta 1 =2 \delta$ | |
| | B2 =2B | $h 2 =h1 - \delta 1$ | $\delta 2 =h1 - h2 + \delta 1$ | |
| | B3 =3.5B | - | $\delta 3 =h2 + 2 \delta 1$ | |
| | B4 =2.5B | $h 4 = \delta 0 - \delta 1$ | $\delta 2 =h1 - h2 + \delta 1$ | |
| | B5 =6B | - | $\delta 5 =hm + \delta 1$ | |
| | B6 =2.5B | $h 6 =h4$ | $\delta 6 =x4 * \delta 4$ | |
| | B7 =3.5B | - | $\delta 7 =x3 * \delta 3$ | |
| | B8 =2B | $h 8 =h2$ | $\delta 8 =x2 * \delta 2$ | |
| B9 =6B | | $\delta 9 =x1 * \delta 1$ | | |
| $X1 = X2 = X3 = X4 = 1$ | | | | |
| Case#4 Rotor | B1 =6B | $h1 = \delta 0 - \delta 1$ | $\delta 1 =2 \delta$ | A1c A2-d A3-d A4-d |
| | B2 =2B | $h 2 =h1 - \delta 1$ | $\delta 2 =h1 - h2 + \delta 1$ | |
| | B3 =3.5B | - | $\delta 3 =h2 + 2 \delta 1$ | |
| | B4 =2.5B | $h 4 = \delta 0 - \delta 1$ | $\delta 2 =h1 - h2 + \delta 1$ | |
| | B5 =6B | - | $\delta 5 =hm + \delta 1$ | |
| | B6 =2.5B | $h 6 =h4$ | $\delta 6 =x4 * \delta 4$ | |
| | B7 =3.5B | - | $\delta 7 =x3 * \delta 3$ | |
| | B8 =2B | $h 8 =h2$ | $\delta 8 =x2 * \delta 2$ | |
| | B9 =6B | - | $\delta 9 =x1 * \delta 1$ | |
| $X1 = 0.6 ; X2 = 0.7 ; X3 = 0.8 ; X4 = 0.9 ;$ | | | | |

$$B = \frac{\pi \cdot D}{2 \cdot N_B}, \quad N_B - \text{number of circle sectors.}$$

$$G_x = \frac{B_x \cdot L_\delta}{\delta_x} \cdot \mu_0 \quad - \text{the magnetic permance}$$

$$x=1, 2, 3..9$$

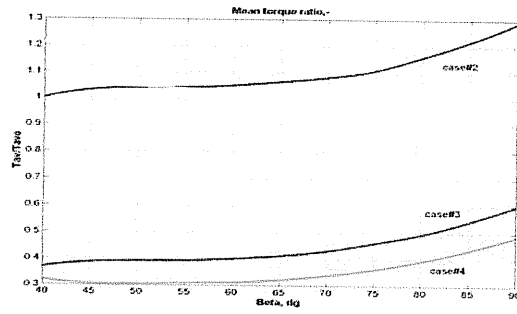
2- Result analyzing

from graphically displayed results(fig.A2, fig.A3 & fig.A4), it is necessary to make comparison analysis between some of important parameters for various values of PWM control signal, taking case#1 as reference case. From this analysis the results displayed on fig.A5, give clear mental about the behaviors when the PWM signal width varied in the range shown on the figure.

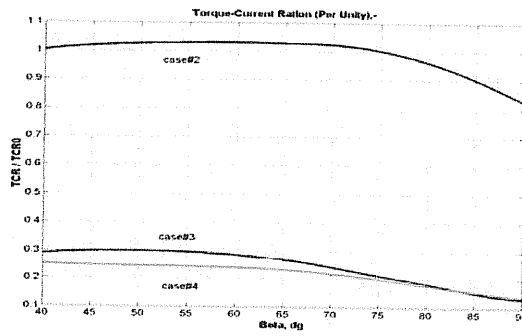
The main conclusions which could be made are:

- The uniform air gap produced great mean torque, but with significant high ripples and great stored energy could be produced due to high inductance, therefore as a result, additional power factor reduction and protective circuits must take into consideration.
- The ripple-free torque could be obtained at 4th case when the air gap has variable width, but this advantage is on the expense of reduced mean – torque value.
- In both cases the acceptable results could be obtained at certain values of $\beta < 65^\circ$.
- When great torque is required independent of the generated ripples only S1 & S2 are switched on, otherwise when the requirements are precise, relatively ripple- free torque, S3 is introduced in operation.
- Since this project describes nulls-torque avoiding and reduction of the torque pulsation, 4th case construction should be described in the further study with respect to torque ripples, current harmonic factor, torque ripples and other parameters. Also the on going study should describe the

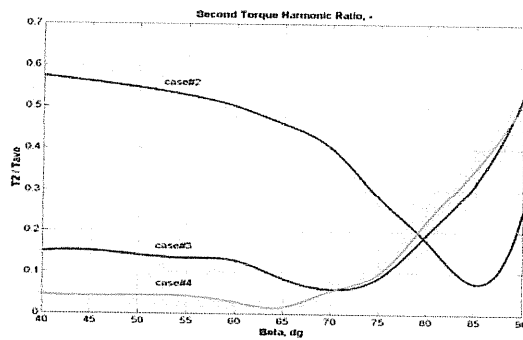
dependence of above mentioned parameters on the main slots width at optimized value of



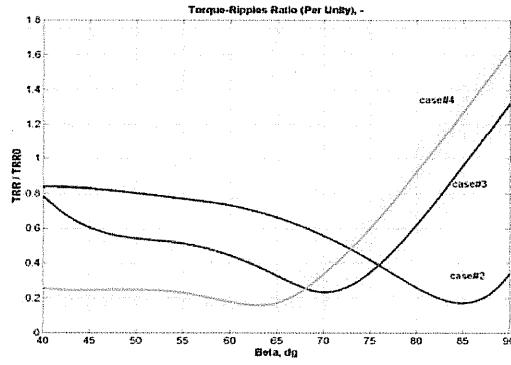
(a)



(b)

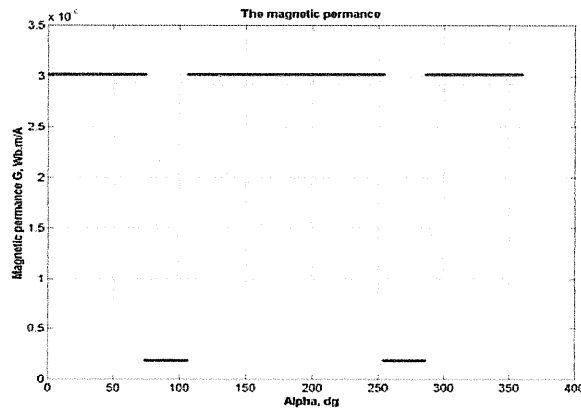


(c)

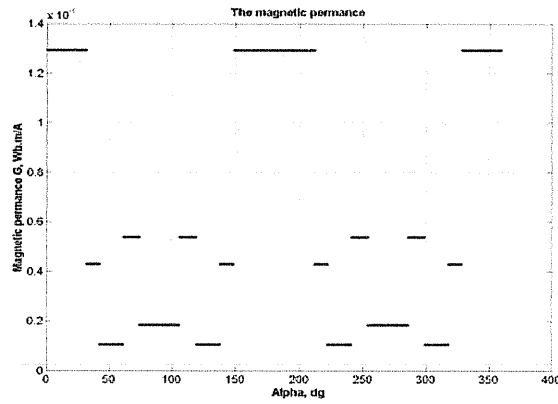


(d)

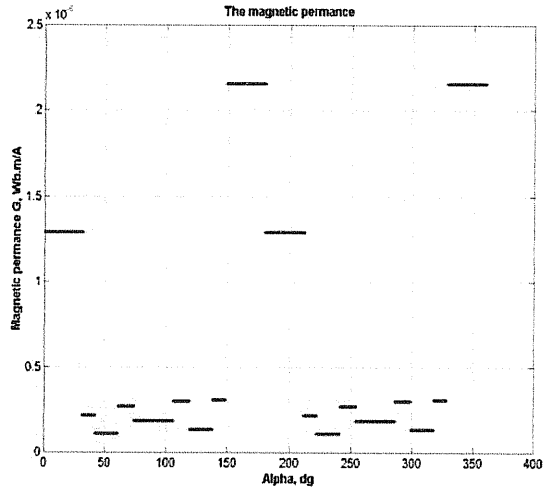
Figure(5.A5: a) Mean torque ratio; b) Torque-current ratio; c) 2nd torque harmonic ratio; and d) Torque ripples ratio- versus the signal width β .



(a)

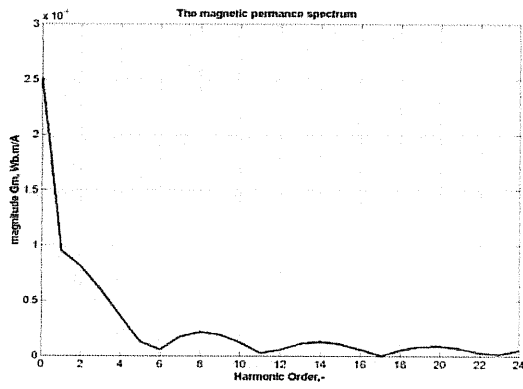


(b)

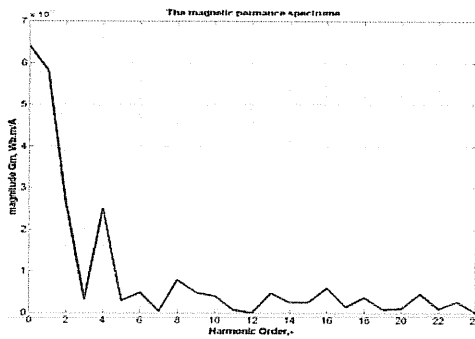


(C)

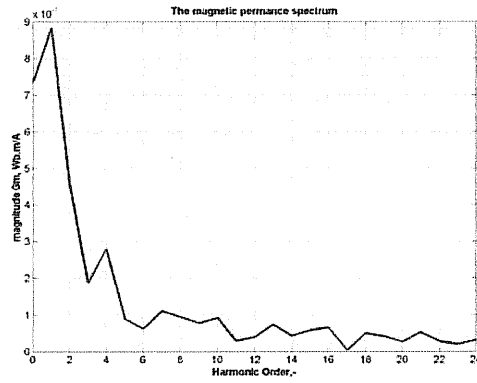
Figure (5.A1. Magnetic permanent at a) case#1;
b) Case#2, and c) case#3



(a)

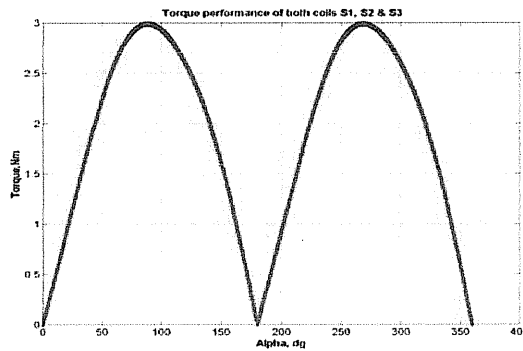


(b)

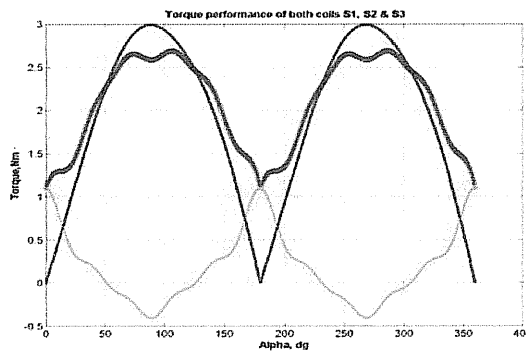


(C)

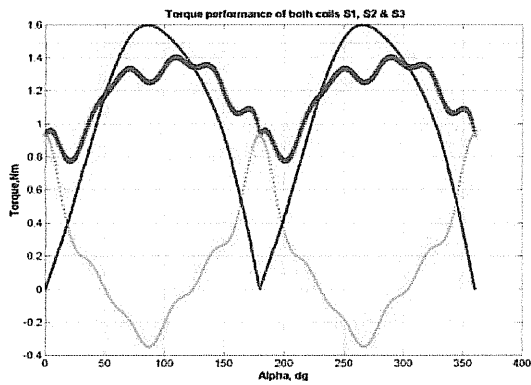
FigA2. harmonic spectrum of Magnetic permanent for the same cases at a) case#1; b) case#2, and c) case# 3



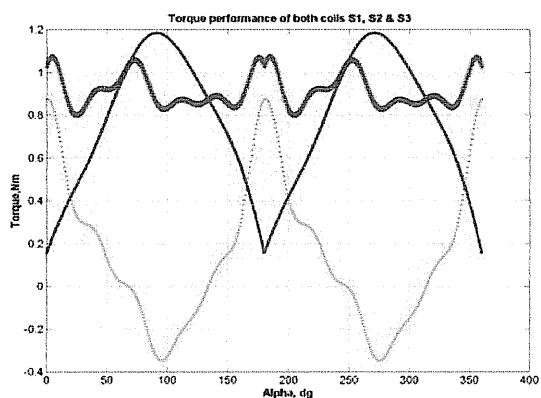
(a)



(b)

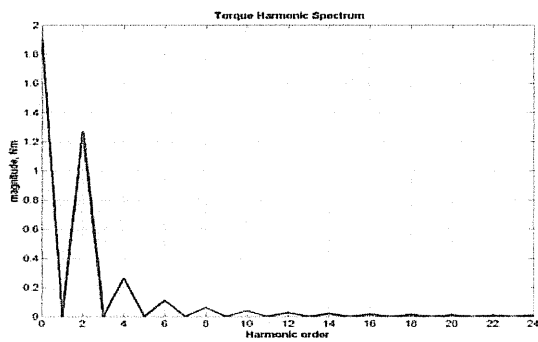


(c)

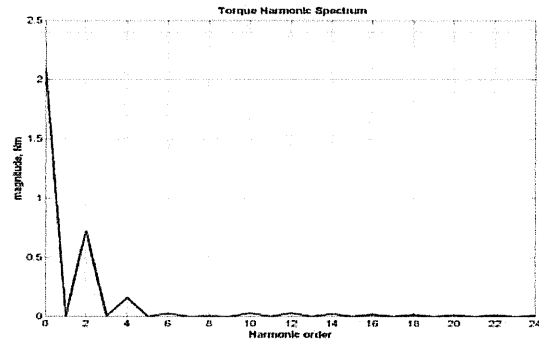


(d)

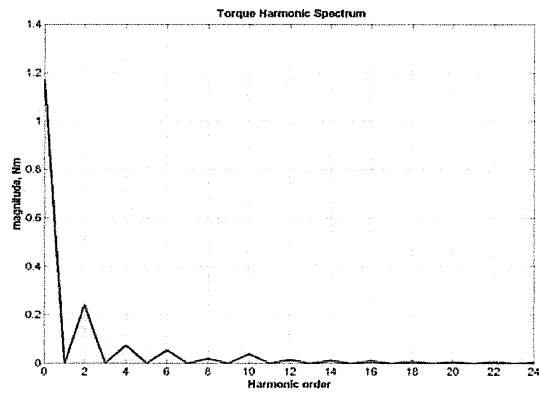
Figure (5.A3. The total electromagnetic torque at four cases:
a) case#1; b) case#2; c) case#3; and d) case#4.



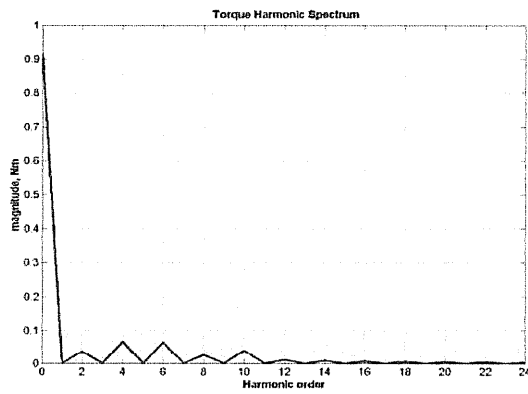
(a)



(b)



(c)



(d)

Figure (5.A4. The harmonic spectrum of produced electromagnetic torque at the same cases:

Case#1; b) case#2; c) case#3; and d) case#4

Chapter Six

Theoretical Background and constructions motor

6.1 Introduction.

6.2 Equivalent Circuit and General Equations.

6.3 Performance of Brushless DC Motor.

6.4 Calculation of construction motor

6.5 Motor Construction.

6.6 How the motor operates.

Chapter Six

Theoretical Background and constructions motor

6.1 Introduction.

Conventional DC motors are highly efficient and their characteristics make them usable in variable speed applications. However, their only drawback is that they need a commutator and brushes which are subject to wear and require maintenance. When the functions of commutator and brushes were implemented by solid-state switches, maintenance-free motors were realized. These motors are now known as brushless DC motors.

In this chapter, the basic structures drive circuits, fundamental principles, steady state characteristics, and the applications of brushless DC motors will be discussed.

6.2 Equivalent Circuit and General Equations.

The per phase equivalent circuit is shown in Figure (6.1) as follows.

$$e = \left(\frac{d\lambda_m}{dt} \right) \dots\dots\dots (E 6.1)$$

Where:

λ_m : is the per phase flux linkage of stator.

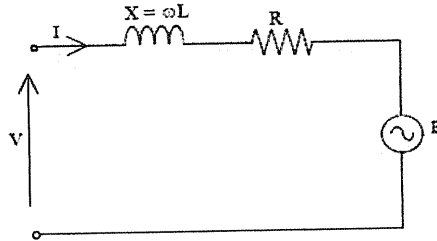


Figure (61): Steady State Equivalent Circuit per phase

For steady state condition, the equivalent circuit becomes as shown in the Figure (6.1), where,

$$X = \omega.L \dots\dots\dots (E6.2)$$

$$E = \frac{d\lambda_m}{dt} \dots\dots\dots (E 6.3)$$

The steady state circuit equation (for one phase) can be written as:

$$V = E + I(R + j\omega L) \dots\dots\dots (E 6.4)$$

Where:

E: is the e.m.f for one phase.

ω: is the angular frequency.

Before friction, windage, and iron losses, the electromagnetic output power is:

$$P_{em} = m|E||I| \dots\dots\dots (E 6.5)$$

Where m is the number of phases

And the electromagnetic torque is:

$$T_{em} = C\phi I_a \dots\dots\dots (E6.6)$$

Where:

C: is the motor constant and its unit is (V.s / Wb)

Φ: is the air gap magnetic flux (Wb).

I_a : armature current.

Also, **ω_r** = 2ω/p is the rotor speed in Rad/s, and p the number of poles.

The actual shaft output torque is:

$$T_{load} = T_{em} - T_{losses} \dots\dots\dots (E 6.7)$$

Where, **T_{losses}** is the total torque due to friction, wind age, and iron losses.

And in terms of rotor speed, the motor induced voltage is given by:

$$E_g = C\phi.\omega_r \dots\dots\dots (E6.8)$$

6.3 Performance of Brushless DC Motor.

The voltage equation can be simplified in algebraic form as:

$$V_a = E_g + R_a * I_a \dots\dots\dots (E 6.9)$$

Substituting relations (E6.9) and (E6.8), we obtain:

$$V_a = C\phi\omega + I_a R_a \dots\dots\dots (E3.10)$$

And

$$\omega_r = \frac{V_a}{(C\phi)} - \frac{R_a T_{em}}{(C\phi)^2} \dots\dots\dots (E 6.11)$$

6.3.1 Efficiency.

Efficiency is defined as the ratio of the output power and input power, i.e.

$$\eta = \left(\frac{P_{in}}{P_{out}} \right) \times 100 \% \dots\dots\dots (E 6.12)$$

Where $P_{in} = V_a * I_a$, and $P_{out} = T_{load} * \omega_r$

In term of the power flow,

$$P_{in} = P_{cu} + P_{Fe} + P_{mec} + P_{out} \dots\dots\dots (E6.13)$$

Where:

$P_{cu} = m * R_a * I_a^2$ is the copper loss due to windings resistance.

P_{Fe} : is the iron loss due to hysteresis and eddy currents.

P_{mec} : Are the mechanical losses due to wind age and friction.

6.4 Calculation of construction motor

6.4.1 Properties of Motors

Through the simulation with mat lab program we obtain the best case of motor nominal as show below:

The Properties of Motors Table (6.1)

| | | |
|---------------------------|--|--|
| V_c | 12V | Supply voltage of third coil S3 |
| E_c | 0.9V | Phase induced back emf of S3 |
| L_c | 8mH | Circuit inductance of S3 |
| R_c | 1Ω | Circuit resistance of coil S3 |
| I_{cmax} | (2.4 – 4)A | Phase current of coil S3 |
| I_{crms} | 3A | Root mean square of fundamental current harmonic |
| V | 2*V_c | Supply voltage of coils S1 & S2 |
| E_a | (N_a/N_c)*E_c | Phase induced back emf of S1 & S2 |
| L_a | N_a² *μ*G | Circuit inductance of S1 & S2 |
| R_a | 2*R_c | Circuit resistance of S1 & S2 |
| I_{a(avr)} | (5.6 - 6)A | Phase current of coil S1 |
| I_{rms} | 4A | Root mean square of fundamental current Harmonic |
| P | (30 – 40) watt | Output Power |
| G | 4 – 5 A/mm² | Magnetic permanent in the air gap |

6.4.2 Calculation of Stator Parameters

The diameter of coil per phase:

$$A_{wire} = \frac{I}{G} \dots\dots\dots (E 6.14)$$

Where:

A_{wire}: area of the wire.

G: Magnetic permanent in the air gap.

I: the current of phase A or B or coil C

$$D = \sqrt{(4 * A) / \pi} \dots\dots\dots (E 6.15)$$

Where **D**: the diameter of the wire

$$A_{coil} = N_{turn} * A_{wire} \dots\dots\dots (E 6.16)$$

Where;

A_{coil}: area of the coil.

N_{turn}: number of turn.

A_{wire}: area of the wire.

$$A_{wire} = \frac{\pi * D_{wire}^2}{4} \dots\dots\dots (E 6.17)$$

$$A_{slot} = \frac{A_{coil}}{FF} \dots\dots\dots (E 6.18)$$

Where:

A_{slot}: area of the slot

FF= 0.5 → 0.7: filing factor

Now to calculate the area and the depth of the slot we must find the X, Y, H parameter as show in figure (6.2):

:

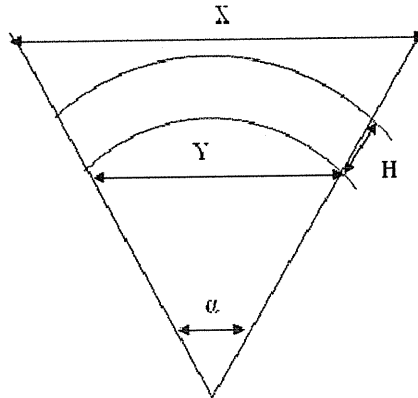


Figure (6.2): Crosse section of the stator

$$A_{slot} = H * Y \dots\dots\dots (E 6.19)$$

Where:

H: the depth of the slot

Y: area of the slot by inner diameter by degrees.

$$Y = \pi * D_T * X \Rightarrow \frac{A_{slot}}{H} \dots\dots\dots (E 6.20)$$

Where:

X: area of the slot by outer diameter by degrees.

D_T: the outer diameter of the stator

$$X = \frac{Y}{\pi D_T} \dots\dots\dots (E 6.21)$$

$$D_T = D_{in} + 2 * Y \dots\dots\dots (E 6.22)$$

Where:

D_{in}: the inner diameter of the stator

$$\alpha_{percoil} = X * 360^\circ \dots\dots\dots (E 6.23)$$

Where:

$\alpha_{percoil}$: Area of slot per one coil

6.4.3 Calculation of magnetic:

We wish to design a brushless DC motor that produces a torque of (0.1)Nm. Then we will size this motor and compute the air gap flux density. To do this we applied the design steps and the design equations of motors.

First we will estimate the rotor volume according to the equation:

$$T_{RV} = \frac{T}{V_r} \dots\dots\dots (E6.24)$$

$$\Rightarrow T_{RV} = \frac{T}{(\pi * rr^2 * L)} \dots\dots\dots (E 6.25)$$

Where:

T_{RV}: torque per unit Rotor Volume.

T: needed torque.

V_r: rotor volume.

rr: rotor radius.

L: axial rotor length.

If the average shear stress is (σ) then the torque is given by:

$$T = (2 * \pi * r^2 * L * \sigma) \dots\dots\dots (E 6.26)$$

$$T_{RV} = 2 * \sigma \dots\dots\dots (E6.27)$$

Where,

σ : Average shear stress.

Then,

$$\sigma = \frac{T_{RV}}{2} \dots\dots\dots (E 6.28)$$

Also we have a two arc permanent magnets and their remnants flux are Br = 1.39 T,

Our magnets have a width (W degree) of (128) degree and a length (Lm) of 60mm, and 7mm thickness (ℓ_m).

So the pole area of the magnet (A_m) is:

$$A_m = L_m * W_m \dots\dots\dots (E 6.29)$$

And also we need to compute the remnant flux:

$$\Phi_r = B_r * A_m \dots\dots\dots (E 6.30)$$

And the internal leakage permanent is given by:

$$P_{m0} = \frac{\mu_0 \mu_{rec} A_m}{l_m} \dots\dots\dots (E 6.31)$$

Where:

P_{m0} = is the internal leakage permanent.

μ_{rec} : Relative coil permeability and we take μ_{rec} . To be 1.

μ_0 : Air permeability.

l_m = 9mm (radial length, the magnet length in the direction of magnetization)

The stator volume follows the rotor volume, for every rough estimation of overall size; a typical value of split ratio S (rotor/stator diameter ratio) can be used.

Then,

$$V_s = \frac{V_r}{S^2} \dots\dots\dots (E 6.32)$$

Where, V_s is the stator volume.

From the stator volume, we can compute the effective stator radius r_s .

Then the air gap was calculated. And so the internal stator radius (r_{s-in}) is equal to rotor radius plus the air gap length. After that we computed the external radius of the stator (r_{s-out}) by adding the effective radius to the internal radius.

And so we can compute by as follows.

The area of the air gap (A_g) is the area above the permanent magnet and it given by:

$$A_g = (\varphi) \left[(r) - \frac{g}{2} \right] L \dots\dots\dots (E 6.33)$$

Where:

φ : The angle against or opposite to the area magnet which equals 128degrees,

r : The radius from center to air gap average ($r = 22.5\text{mm}$).

L : Axial length.

g : Equivalent air gap length.

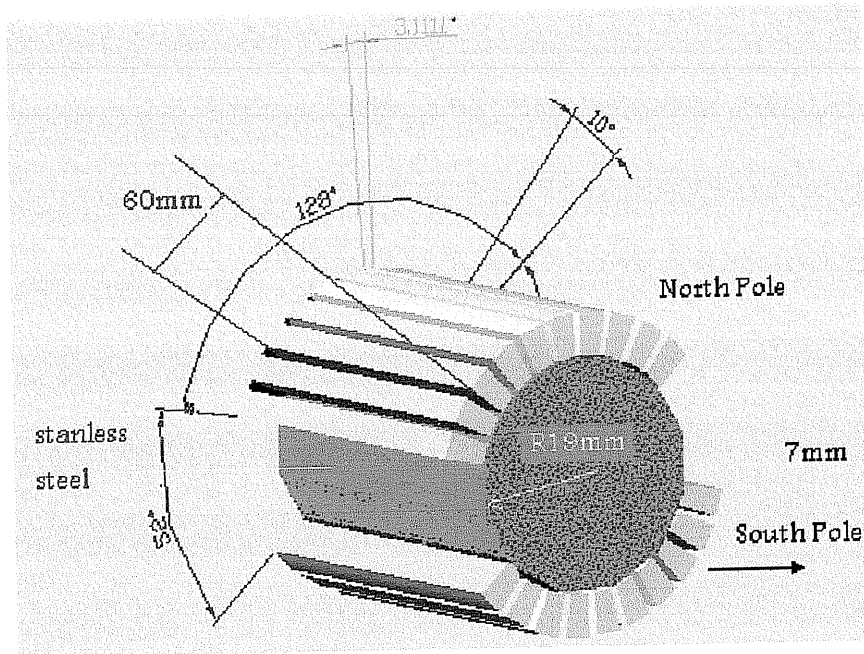


Figure (6.3): Rotor cross section

Then we need to compute the air gap reluctance as the following relation.

$$R_g = \frac{g}{\mu_0 A_g} \dots\dots\dots (E 6.34)$$

Also, we need to calculate the internal permanent, and it given by:

$$P_m = P_{m0} (1 + P_{r1}) \dots\dots\dots (E 6.35)$$

Where P_{r1} is the rotor leakage permanent, which represents the paths of magnet flux components that fail to cross the air gap

Then we computed the MMF across the magnet to the MMF across the air gap as:

$$F_m = \frac{\Phi_r}{1 + P_m R_g} \dots\dots\dots (E 6.36)$$

Then we wrote the ratio of the magnet pole area to the air gap area as C'

$$C' \Phi = \frac{A_m}{A_g} \dots\dots\dots (E 6.37)$$

And then the air gap flux density can be extracted as follows.

$$B_g = \frac{c' \Phi \cdot Br}{1 + P_m R_g} \dots\dots\dots (E 6.38)$$

And then from this equation we computed the air gap flux.

Then the magnetic flux in the air gap is

$$\Phi_g = B_g * A_g \dots\dots\dots (E 6.39)$$

After that we determined our motor constant C ,

$$C = \frac{(Z * P)}{(2 * \pi * a)} \dots\dots\dots (E 6.40)$$

Where:

P: number of poles and here =2.

a: number of parallel paths and equal.

But:

$$Z = 2 * N * C' \dots\dots\dots (E 6.41)$$

Where:

N: number of turns per one coil, which equals to .

C': number of coils and here C' =3.

After that we compensated all the previous design equation in table (6.2).

Table (6.2): Magnetic Parameter

| Equation | Answer |
|--|---------------------------|
| V_r | 127.348e3 mm ³ |
| r_r | 26mm |
| S | 0.981 |
| r_s | 26.5mm |
| g | 0.5mm |
| r_{s-in}, r_{s-out} | 26.5mm 33.5 mm |
| r (gap) | 26.5mm |
| V_s | 132.371e3mm ³ |
| A_m | 6970.6mm ² |
| Φ_r | .00968Wb |
| P_{mo} | 1.4e-4 (Wb/At) |
| A_g | 2977.05mm ² |
| R_g | 1399At/Wb |
| P_m | 1.575e-4Wb/At |
| F_m | .0094818 At |
| c'Φ | 0.427 |
| B_g | 0.48T |
| Φ_g | 1.45Wb |
| Z | 200conductors |
| C | 15.8 Vs./Wb |
| CΦ | 0.152V.s |

6.5 Motor Construction.

Our 2-phase brushless DC motor consists of:

1. Motor frame, this house in outer said contain of cylindrical aluminum and in inner said contains the iron stator laminated sheets which is surrounds the stator phases.
2. Bearing houses: and here we have two bearing houses in both motor faces.
3. Bearings: the internal diameter of these bearings is 10mm and the outside diameter is 25mm.
4. Stator.
5. Rotor.

Now, we will discuss the stator and rotor in details.

6.5.1 Stator:

It has slot construction and has two phases with Coil 3, and each phase connected to the inverter circuit which provides it with the needed sequences voltages.

Each phase consists of 3 coils, connected in series (end to star) to construct a two poles (north and south), each pole lies in 170 degree of the stator, and so the two poles lies in 180 degree of the stator.

The coil 3 consists of four coils, is connected in series of the (end of star) we distributed surrounded the stator by each two coils covered angle 180 degree and another two coils to covered the parallel angle, this distribution of coil 3 to reduce the dead point of torque by operating continues as PWM which seen in chapter four.

The wires diameter we used in phase A and phase B is 1mm and in coil3 the wire diameter is 0.9mm which calculates in this chapter.

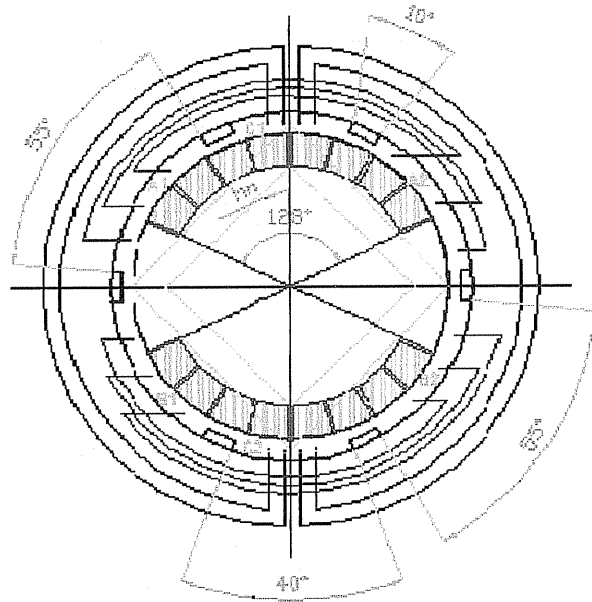


Figure (6.4): Stator windings construction

Figure (6.5) shows one of the stator coils by phase 1 and 2. It is implemented using a cylindrical core with 55 degree of each side of windings and empty in the internal 60 degree.

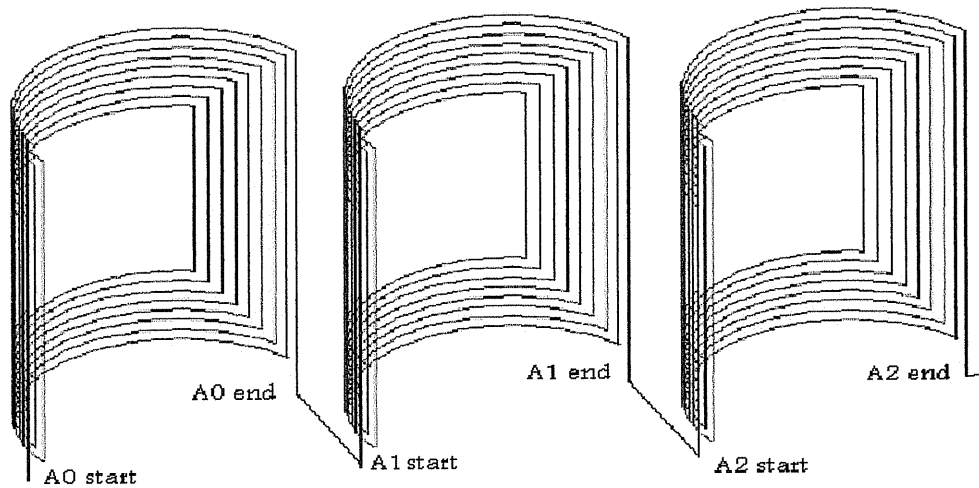


Figure (6.5): One-phase connection

Figure (6.6) shows one of the stator coils 3 by PWM. It is implemented using a cylindrical core with 20 degree of each side of two windings and empty in the internal 140 degree

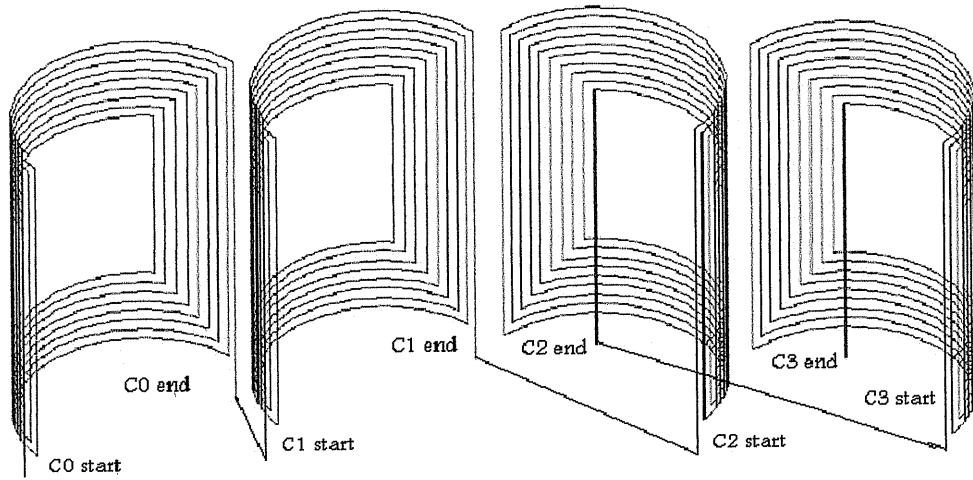


Figure (6.6): Coil 3 Connection

Figure (6.7) shows the stator construction we designed.

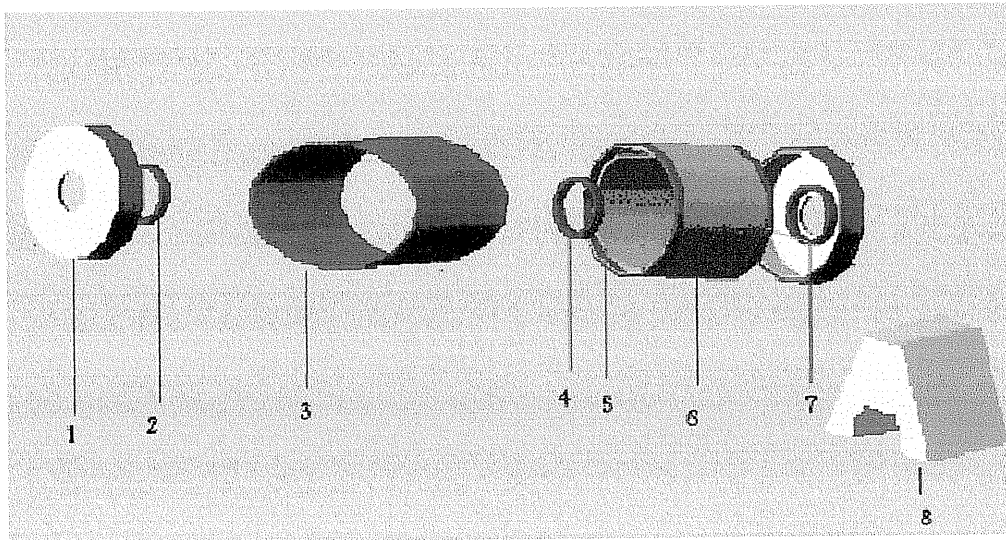


Figure (6.7): Stator construction

The figure shows the construction of the stator and the motor frame with their covers. These components are explained as follows.

1. Bearing cover (Aluminum).
2. Bearing number 1.
3. Plants core (steel).
4. Bearing number 2.
5. Slots.
6. Stator fixture (Aluminum).
7. Bearing house (Aluminum).
8. Motor base (Aluminum).

6.5.2 Permanent magnet rotor:

In our motor the exciter is the rotor which is a permanent magnet, it consists of two magnets, one of them performs a north pole and the other performs a south pole, these two magnets are arc. The magnets we used are of the type NdFeB permanent magnet. At room temperature NdFeB has the highest energy product of all commercially available magnets. The high permanence and coercivity permit marked reductions in motor frame size for the same output compared with motors using ferrite magnets. Its properties are shown in appendix B.

Figure (6.8) shows the rotor construction we designed.

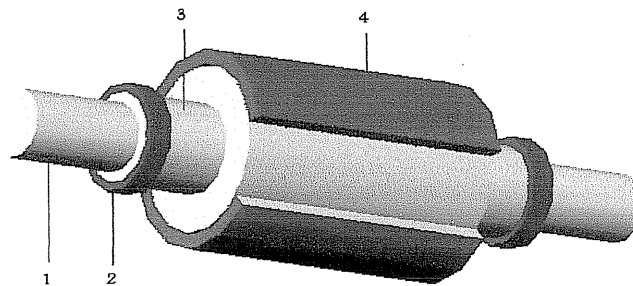


Figure (6.8): Rotor construction

The rotor numbered parts are:

1. Steel shaft outer.
2. Bearing.
3. Rotor core.
4. Permanent magnet.

The combined motor is shown in figure (6.9).

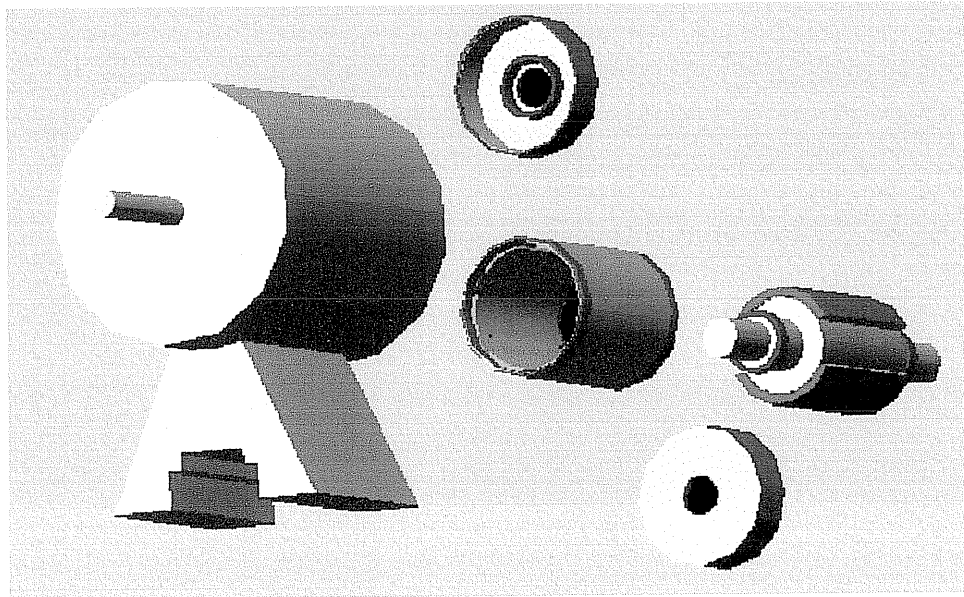


Figure (6.9): the 2-phase BDC motor

6.6 How the motor operates.

When we apply the first phase with a voltage then it flows a current in this phase, the current value is proportional to voltage applied on this phase, and this flowing current will generate a magnetic temporary flux which affects the rotor pole, at this moment the rotor will repel and it will rotate.

At the moment the rotor reaches the second phase it will be far from the first phase, here, phase two must be fed (by encoder signal) and the first phase must be idle because if it not, it will hold or attract the south pole of the rotor.

As the phase voltages increased then the current increased and so the resulting magnetic flux increased (until it reaches the saturation value), as the flux increased then the pole repelling will be greater and so the speed of rotation will be higher.

When the rotor rotate then its flux also rotates, this flux is a changing flux for the fixed position relative to stator and so there will be a changing flux applied to the idle phase, so an induced voltage will be generated in this idle phase, this induced voltage called back electromotive force (back e.m.f).

At the same time the coil 3 will operation in continue to kill or to reduce the dead point on the torque as when change operating phase 1 or phase 2 as shown in fig(6.10).

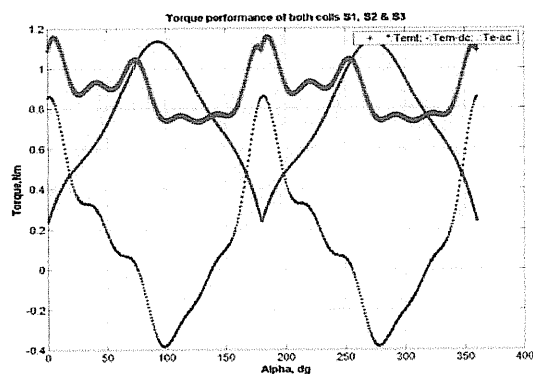


Figure (6.10): The total electromagnetic torque of both phases 1, 2, & coil 3.

As the motor speed increases, then the back e.m.f increases and this phenomenon can be used for controlling motor speed without using any sensor.

Chapter Seven

Software system design

7.1 Initializations.

7.2 Parallel Port.

7.3 Calculation of PWM by Program.

Chapter Seven

Software system design

7.1 Initializations.

Two-Phase Brushless DC Motor of our project is controlled in both directions by an inverter that feed the motor phases in clockwise and counter clockwise direction operation. This inverter receives its signals from the Computer control-based system.

The Computer control interchanges these signals from one phase to another, when it receives a changing phase signals from the sensorless circuit, which senses the rotor position. Although, when the rotor is in the first phase region then it outputs a hexadecimal code used to operate the first phase for a period of time until this signal goes high. Here, the Computer control changes its output to another code that operates the second phase until the signal goes low. The same can be done for the speed reversal mode. These signals are transferred to one of the interface ports.

The following steps must be followed in order to create the program of the PC math lab -based system.

7.1.1 Determining the mission of each MOSFET of the inverter.

Table (7.1): Inverter MOSFET's missions,

| Forward operation | | | |
|--------------------------|---------------|----------------|---------------|
| Phase 1 | C3 PWM | Phase 2 | C3 PWM |
| TR2 & TR4 | TR10,T12 | TR6 & TR8 | TR9,T11 |
| Reverse operation | | | |
| Phase 1 | C3 PWM | Phase 2 | C3 PWM |
| TR2 & TR4 | TR10,T12 | TR6 & TR8 | TR9,T11 |

7.1.2 Calculating the hex codes for each phase in both directions.

Table (7.2): bidirectional motor operation codes

| Binary | Hexa | Usage | Usage | T(9,11) | T(10,12) |
|-----------|------|-----------------|-------|---------|----------|
| 0010 0010 | 22 | Forward / phase | PWM | 1 | 0 |
| 0100 1001 | 49 | Forward / phase | PWM | 0 | 1 |
| 1001 0001 | 91 | Reverse / phase | PWM | 0 | 1 |
| 1100 0110 | B6 | Reverse / phase | PWM | 1 | 0 |

7.2 Parallel Port

7.2.1 Introduction to Parallel Port

The Parallel Port is the most commonly used port for interfacing home made projects. This port will allow the input of up to 9 bits or the output of 12 bits at any one given time, thus requiring minimal external circuitry to implement many simpler tasks. The port is composed of 4 control lines, 5 status lines and 8 data lines. It's found commonly on the back of your PC as a D-Type 25 Pin female connector. There may also be a D-Type 25 pin male connector. This will be a serial RS-232 port and thus, is a totally incompatible port.

7.2.2 Parallel Port Hardware Properties

Below is a table of the "Pin Outs" of the D-Type 25 Pin connector and the Centronics 34 Pin connector. The D-Type 25 pin connector is the most common connector found on the Parallel Port of the computer, while the Centronics Connector is commonly found on printers.

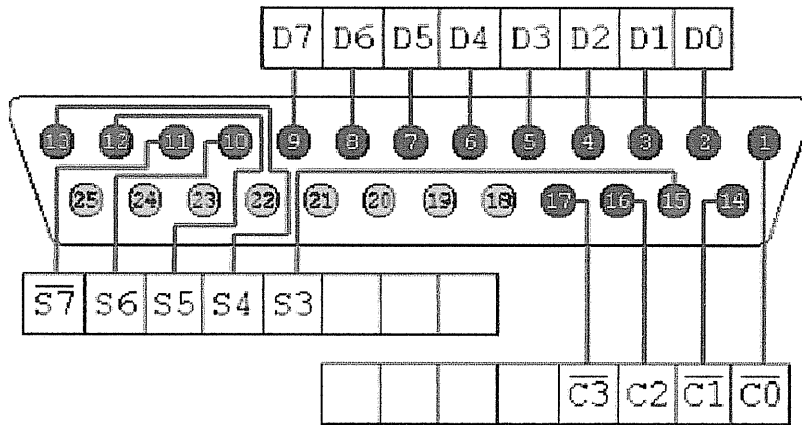


Figure (7.1): Parallel Port Pins

Table (7.3): Pin Assignments of the D-Type 25 pin Parallel Port Connector.

| Pin No (D-Type 25) | Pin No (Centronics) | SPP Signal | Direction In/out | Register | Hardware Inverted |
|--------------------|---------------------|------------------------------|------------------|----------|-------------------|
| 1 | 1 | nStrobe | In/Out | Control | Yes |
| 2 | 2 | Data 0 | Out | Data | |
| 3 | 3 | Data 1 | Out | Data | |
| 4 | 4 | Data 2 | Out | Data | |
| 5 | 5 | Data 3 | Out | Data | |
| 6 | 6 | Data 4 | Out | Data | |
| 7 | 7 | Data 5 | Out | Data | |
| 8 | 8 | Data 6 | Out | Data | |
| 9 | 9 | Data 7 | Out | Data | |
| 10 | 10 | nAck | In | Status | |
| 11 | 11 | Busy | In | Status | Yes |
| 12 | 12 | Paper-Out / Paper-End | In | Status | |
| 13 | 13 | Select | In | Status | |
| 14 | 14 | nAuto-Linefeed | In/Out | Control | Yes |
| 15 | 32 | nError / nFault | In | Status | |
| 16 | 31 | nInitialize | In/Out | Control | |
| 17 | 36 | nSelect-Printer / nSelect-In | In/Out | Control | Yes |
| 18 - 25 | 19-30 | Ground | Gnd | | |

The above table uses "n" in front of the signal name to denote that the signal is active low. e.g. n Error. If the printer has occurred an error then this line is low. This line normally is high, should the printer be functioning correctly. The "Hardware Inverted" means the signal is inverted by the Parallel card's hardware. Such an example is the busy line. If +5v (Logic 1) was applied to this pin and the status register read, it would return back a 0 in Bit 7 of the Status Register.

The output of the Parallel Port is normally TTL logic levels. The voltage levels are the easy part. The current you can sink and source varies from port to port. Most Parallel Ports implemented in ASIC, can sink and source around 12mA. However these are just some of the figures taken from Data sheets, Sink/Source 6mA, Source 12mA/Sink 20mA, Sink 16mA/Source 4mA, and Sink/Source 12mA. As you can see they vary quite a bit. The best bet is to use a buffer, so the least current is drawn from the Parallel Port.

7.2.3 Port Addresses

The Parallel Port has three commonly used base addresses. These are listed in table (7,4) below. The 3BCh base address was originally introduced used for Parallel Ports on early Video Cards. This address then disappeared for a while, when Parallel Ports were later removed from Video Cards. They have now reappeared as an option for Parallel Ports integrated onto motherboards, upon which there configuration can be changed using BIOS.

LPT1 is normally assigned base address 378h, while LPT2 is assigned 278h. However this may not always is the case as explained later. 378h & 278h have always been commonly used for Parallel Ports. The lower case h denotes that it is in hexadecimal. These addresses may change from machine to machine.

Table (7.4): Port Addresses

| Address | Notes: |
|-------------|---|
| 3BCh - 3BFh | Used for Parallel Ports which were incorporated on to Video Cards - Doesn't support ECP addresses |
| 378h - 37Fh | Usual Address For LPT 1 |
| 278h - 27Fh | Usual Address For LPT 2 |

7.2.4 How to Connect Circuits to Parallel Port

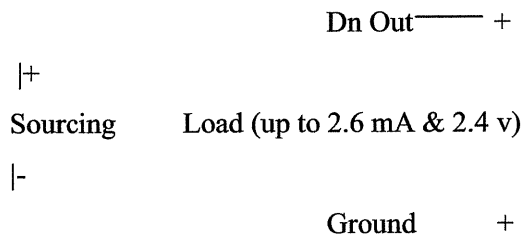
PC parallel port is 25-pin D-shaped female connector in the back of the computer. It is normally used for connecting computer to printer, but many other types of hardware for that port are available today.

Not all 25 are needed always. Usually you can easily do with only 8 output pins (data lines) and signal ground. I have presented those pins in the table below. Those output pins are adequate for many purposes.

| <u>Pin</u> | <u>function</u> |
|------------|-----------------|
| 2 | D0 |
| 3 | D1 |
| 4 | D2 |
| 5 | D3 |
| 6 | D4 |
| 7 | D5 |
| 8 | D6 |
| 9 | D7 |

Pins 18,19,20,21,22,23,24 and 25 are all ground pins.

Those data pins are TTL level output pins. This means that they put out ideally 0V when they are in low logic level (0) and +5V when they are in high logic level (1). In real world the voltages can be something different from ideal when the circuit is loaded. The output current capacity of the parallel port is limited to only few mill amperes.



7.2.5 How to Calculate Your Own Values to Send To Program

You have to think the value you give to the program as a binary number. Every bit of the binary number control one output bit. The following table describes the relation of the bits, parallel port output pins and the value of those bits.

| | | | | | | | | | | |
|-------|----|----|----|----|----|----|----|----|-----|----|
| Pin | 1 | 2 | 3 | 4 | 5 | 6 | 7 | 8 | 9 | 14 |
| Bit | C1 | D0 | D1 | D2 | D3 | D4 | D5 | D6 | D7 | C2 |
| Value | 1 | 1 | 2 | 4 | 8 | 16 | 32 | 64 | 128 | 2 |

7.2.6 Interfacing Circuit of Diode Clamped Multilevel inverter

In this project the switching devices (MOSFETs) will triggered by using the PC through parallel port, the output pins of parallel port will used to give output signal (Data lines), the parallel port has just (8) output pins and the inverter contain (6) switching devices, and the parallel port contents of (8) pin input, in this project we well needs (2) input to replace the sensorless signal.

And parallel port must be insolated from high power devices by using Opt coupler devices (OP4N25) to protect it from reversing current of inductive load and to give voltage by optocoupler more than output voltage from parallel port. And interfacing circuit must be containing resistor to limit current between optocoupler and decoder, and between optocoupler and MOSFETs.

In figure(7.2) the interfacing circuit is plotted for one phase 'A', and this circuit is similar to each phase A,B, and coil C because the phase shift will done by software.

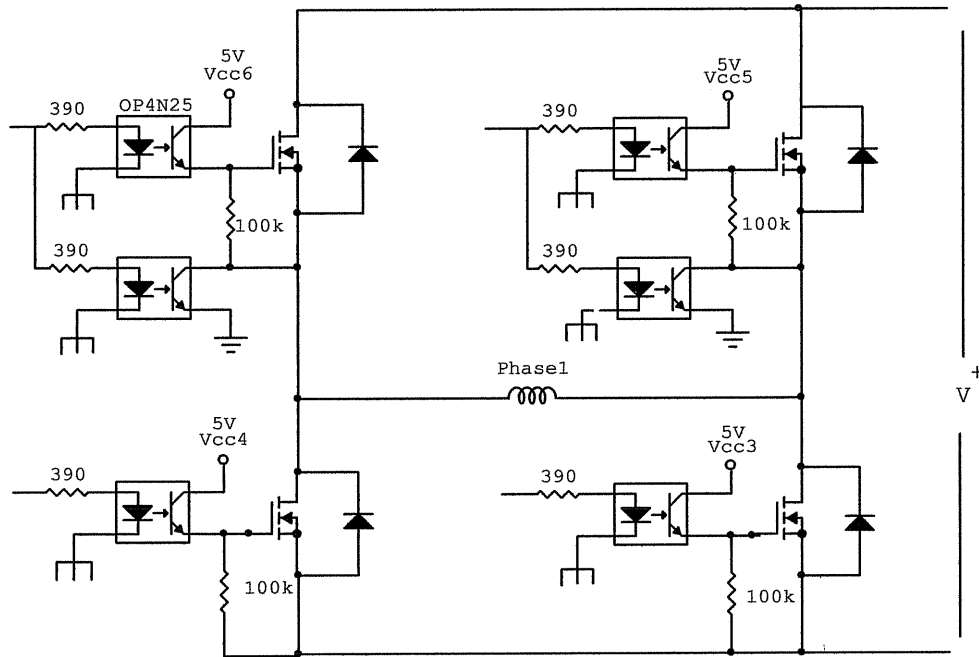


Figure (7.2): the interfacing circuit per phase

Note: show interfacing devices characteristics in appendix of Data sheet.

Table (7.5): Represent the motor work using the program

| input | | | Output | | | | | |
|---------|------------|--------|-----------------------|-----------------------|-----------------------|-----------------------|--------------------|---------------------|
| F/R | sensorless | sensor | FP ₁ (1,3) | RP ₁ (2,4) | FP ₂ (5,7) | RP ₂ (6,8) | TC _{9,11} | TC _{10,12} |
| 0 | 0 | 0 | 1 | 0 | 0 | 0 | 1 | 0 |
| 0 | 1 | 0 | 0 | 0 | 1 | 0 | 0 | 1 |
| 1 | 0 | 0 | 0 | 1 | 0 | 0 | 0 | 1 |
| 1 | 1 | 0 | 0 | 0 | 0 | 1 | 1 | 0 |
| Pin/in | 12 | 12 | - | - | - | - | - | - |
| Pin/out | - | - | 4 | 5 | 2 | 3 | 7 | 6 |

7.2.7 This table is explained as the following

F/R column represents the motor revolving toward left and right, and the column sensorless represent the process of operating phase₁ and phase₂ in both directions. And sensor column represents operating the motor in both directions without depending on sensorless. The F_{Ph1} represents revolving or operating phase₁ toward right. And R_{Ph1} column represents revolving or operating phase₁ in opposite direction to F_{Ph1}. The column F_{Ph2} represents operating phase₂ toward right, and R_{Ph2} represents operating phase₂ in counter direction to F_{Ph2}. The column T_{C9,11} represents operating coil₃ as PWM, which is controlled by the matlab program, by indicating the trigger angle, which is also indicated by the program. The column T_{C10,12} represents the work of coil₃ as PWM.

7.2.8 The program works as the following

When the number is taken (00100010), it means that phase₁ works toward right, and T_{C9, 11} works PWM with phase₁. And when it read (01001001) that mean the work of phase₂ with T_{C10}, which operates coil₃, to give coil₃ PWM.

When it reads (10010001) this means that phase₁ is worked toward left and coil₃ is worked by T_{C10, 12} to take PWM. When it reads the number (11000110) that means working of phase₂ toward left with coil₃, which is operated by T_{C9} to give PWM.

The column F/R is indicated by the program, and the program inputs and outputs data by the parallel port, which the following pins.

Pin₁₄: in parallel port represents the input of data from the sensorless circuit by the binary number (01), where the number 0 means operating phase₁, and 1 means operating phase₂.

Pin₄: in parallel port represents the output of data to the inverter circuit, which represents the number (1000) to operate phase₁ that operates the MOSFETs F_{T1} and F_{T3} toward right.

Pin₅: in parallel port represents the output of data to the inverter circuit, which represents the number (0010) to operate phase₁ that operates the MOSFETs F_{T2} and F_{T4} toward left.

Pin₂: in parallel port represents the output of data to the inverter circuit, which represents the number (0100) to operate phase₂ that operates the MOSFETs F_{T5} and F_{T7} toward right.

Pin₅: in parallel port represents the output of data to the inverter circuit, which represents the number (0001) to operate phase₂ that operates the MOSFETs F_{T6} and F_{T8} toward left.

Pin₇: in parallel port represents the output of data to the inverter circuit, which represents the number (1001) to operate coil₃ that operates the MOSFETs T_{C9} and T_{C10}.

To produce PWM in both directions with phase₁ where T_{C9} works with forward direction and T_{C10} in reverse direction to phase₁.

Pin₆: in parallel port represents the output of data to the inverter circuit, which represents the number (0110) to operate coil₃ that operates the MOSFETs T_{C9,11} and T_{C10,12}.

To produce PWM in both directions with phase₂ where T_{C10,12} works with forward direction, and T_{C9,11} in reverse direction to phase₂.

When the motor is turned on by replacing the sensor instead of the sensorless, the program will do the same work, where the sensor takes the read of the code number of the sensorless (0101).

7.3 Calculation of PWM by Program.

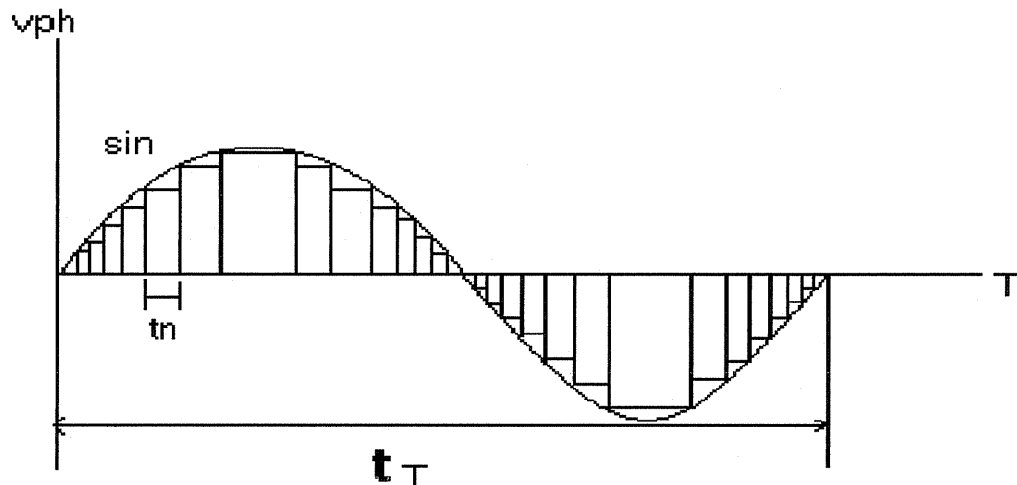


Figure (7.3): Wave of PWM as sinusoidal.

This figure shows the process of formatting the sinusoidal wave as pulse width modulation (PWM) where in the beginning the graph takes alpha value which is fire angle and it divides alpha into small pulses with different widths as following:

$(0-\alpha)$ the wave will be pulse with different width. $(\alpha-\alpha_2)$ the wave will be one continues pulse. And finally (α_2-180) represents the width of pulse that decreasing in width.

And the figure (7.4): is shape of the wave when the modules equal one

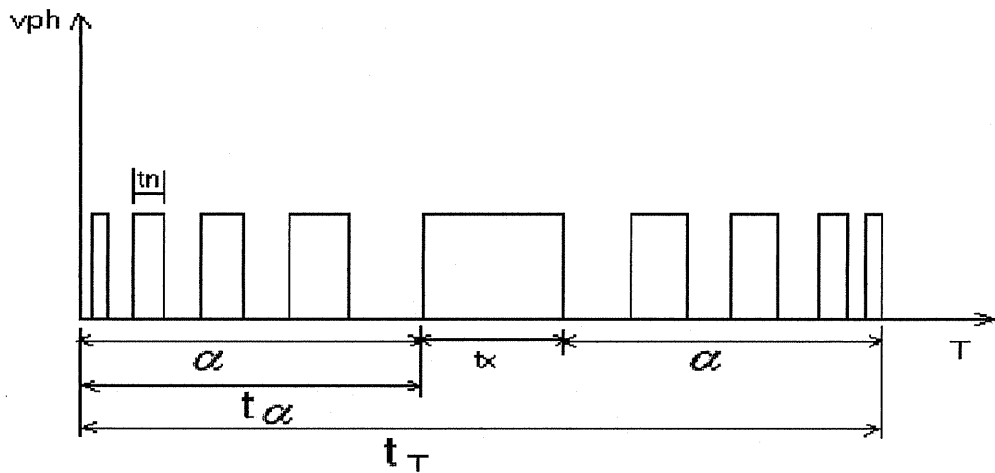


Figure (7.4): The shape of PWM.

7.3.1 The equation of PWM

$$F = \frac{(p * speed)}{120} \dots\dots\dots E (7.1)$$

$$t_T = \frac{1}{F} \dots\dots\dots E (7.2)$$

$$t = [0, \dots\dots\dots, t_T] \dots\dots\dots E (7.3)$$

$$x(t) = \sin 2\pi Ft \dots\dots\dots E (7.4)$$

$$Np = \text{Entered by user} \dots\dots\dots E (7.5)$$

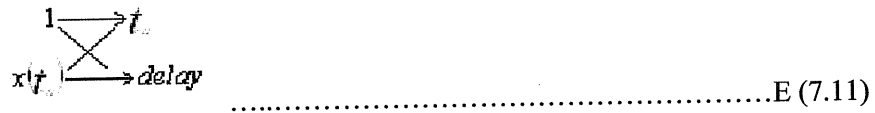
$$t_n = \frac{t_T}{N_P} \dots\dots\dots E (7.6)$$

$$T_{\alpha} = \frac{(t_T * \alpha)}{360} \dots\dots\dots E (7.7)$$

$$t_x = \frac{t_T}{2} - 2T\alpha \dots\dots\dots E (7.8)$$

$$x(t_n)_{\max} = 1 \dots\dots\dots E (7.9)$$

$$\max(\text{delay}) = t_n \dots\dots\dots E (7.10)$$



$$\text{delay} = t_n * x(t_n) \dots\dots\dots E (7.12)$$

Table (7.6): Definition Symbols

| | |
|----------------------|--|
| F | Frequency (HZ) |
| P | Number of poles |
| speed | Revolution per minute (rpm) |
| t_T | The Total Period |
| N_p | Number Of Pulses |
| t_n | The Time Of Each Pulse |
| t_x | The Time of the continuous pulse |
| t_α | from the initial time till the time when the continuous pulses start |
| α | Angle that we use to determine the number of discrete pulses |
| X(tn) | Show the Amplitude and it is constant (equal one) |

Chapter Eight

Conclusion and Recommendation

8.1 Conclusion.

8.2 Results.

8.3 Recommendation.

Chapter Eight

Conclusion and Recommendation

8.1 Conclusion

1. The applied innovative design of two phases/ three coils two-pulse brushless DC motor with combined control produced electromagnetic torque having self-starting and reduced fluctuation. This is due to the dissymmetry in the rotor construction where the reluctance torque nulls do not occur at the same angles of the electromagnetic torque.
2. By introducing the PWM control of third coil the torque ripples are further decreases, because of the generated train of pulses with variable width. Once torque ripples decreases, the additional stability in the motor torque could be achieved, dissipated power reduction and motor utility increasing. The motor electromagnetic performances are directly depends on the continuous width of the PWM signal β , where by increasing this angle the Torque-current ration keeps relatively acceptable result .
3. Discussed results related to rotor slots width, where illustrated graphically mentioned that by increasing the width of main rotor slot B5, the consumed phase current increases with purpose to cover the required MMF. At the same time the mean torque decreases because of additional reduction in the magnetic permanent. The rotor has optimized slots width B5, which will be the design value in the future application of this motor.
4. The proposed design allow two operation modes depending on the required operation conditions and discussed results in the appendix :

8.2 Results

After testing the motor we achieved the result as shown below

Table (8.1):Result of motor

| V_a | I_a | N | T | ω_n | P_{in} | P_{out} | μ |
|-------|-------|-----|------|------------|----------|-----------|-------|
| 10 | 0.6 | 500 | 0.07 | 52.3 | 6 | 3.661 | 61 |
| 10 | 0.65 | 460 | 0.08 | 48.17 | 6.5 | 3.85 | 59 |
| 10 | 0.7 | 420 | 0.09 | 43.98 | 7 | 3.95 | 56 |
| 10 | 0.73 | 390 | 0.1 | 40.84 | 7.3 | 4.089 | 56 |
| 15 | 0.63 | 530 | 0.07 | 55.5 | 9.45 | 3.885 | 41 |
| 15 | 0.67 | 490 | 0.08 | 51.3 | 10.05 | 4.104 | 40 |
| 15 | 0.69 | 455 | 0.09 | 47.84 | 10.35 | 4.28 | 41 |
| 15 | 0.77 | 410 | 0.1 | 42.93 | 11.55 | 4.29 | 37 |
| 24 | 0.67 | 700 | 0.07 | 73.3 | 16.08 | 5.131 | 32 |
| 24 | 0.7 | 673 | 0.08 | 70.47 | 16.8 | 5.63 | 33 |
| 24 | 0.74 | 610 | 0.09 | 63.88 | 17.76 | 5.75 | 32 |
| 24 | 0.79 | 580 | 0.1 | 60.75 | 18.96 | 6.073 | 32 |

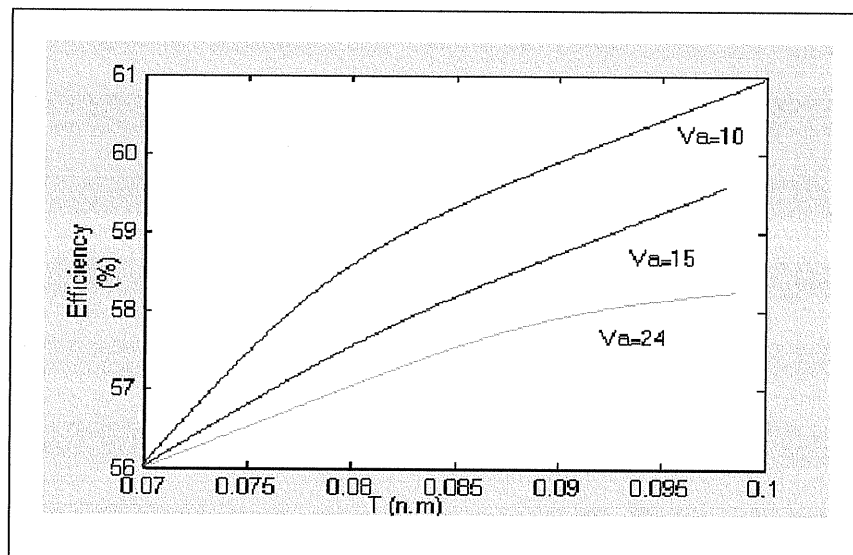


Figure (8.1): The relation of efficiency and torque

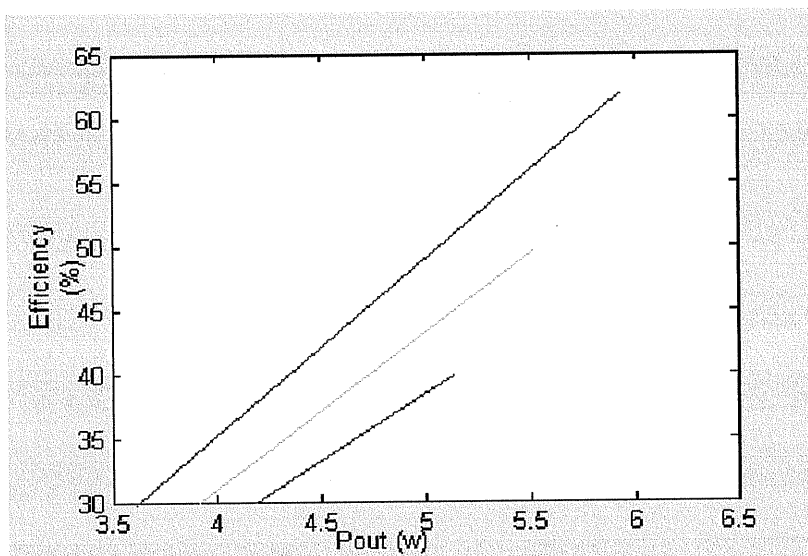


Figure (8.2): The relation of efficiency and P_{out}

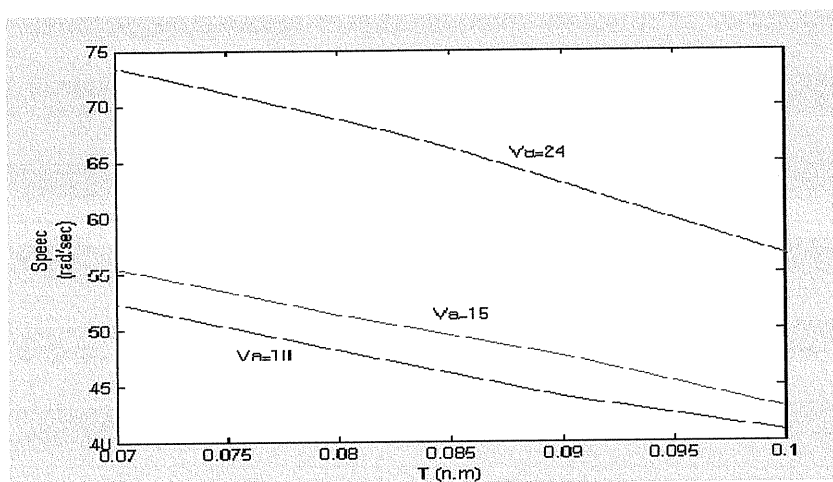


Figure (8.3): The relation of speed and torque

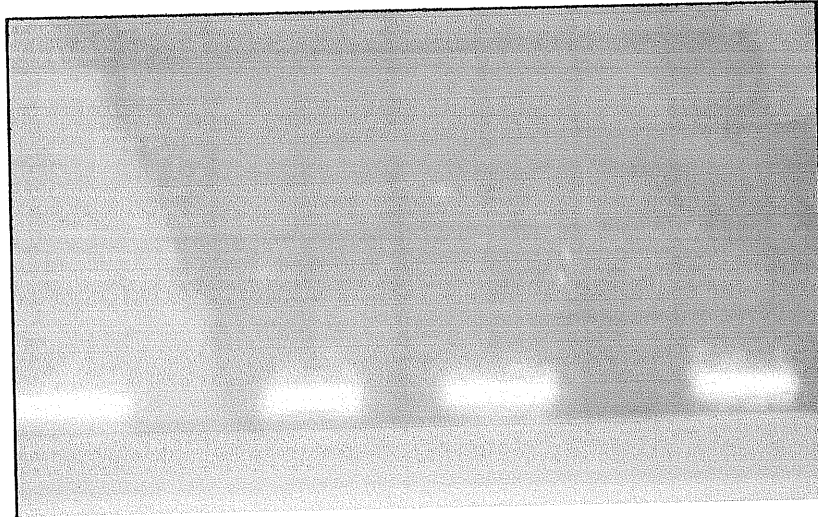


Figure (8.4): The wave of current with ohm load

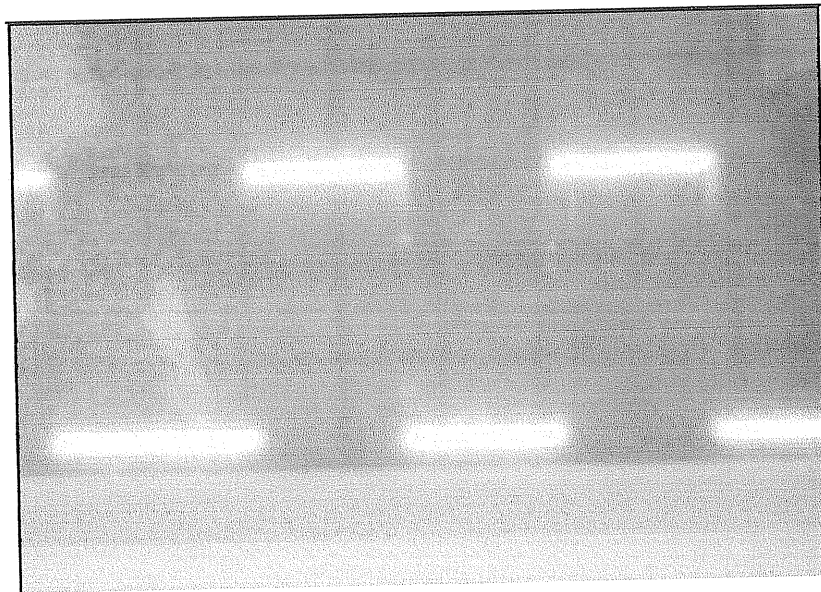


Figure (8.4): The wave of PWM

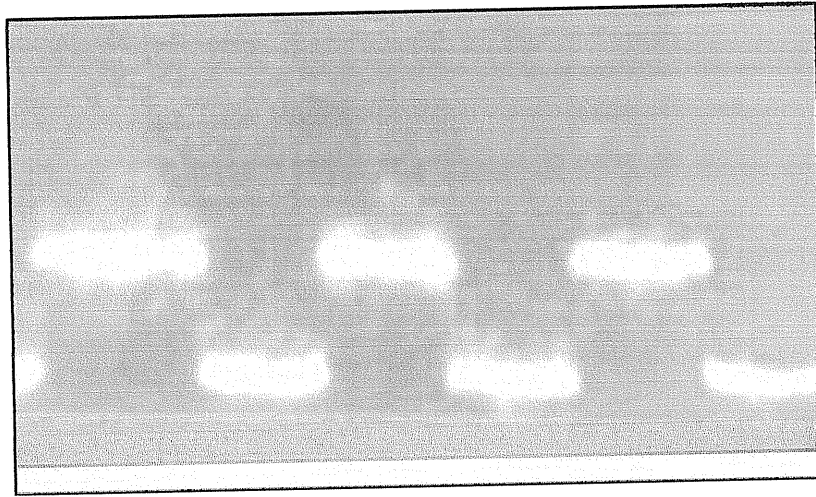


Figure (8.4): The wave of current with phase one



Figure (8.4): The wave of current

8.2 Recommendation.

Finally, we recommend the next researcher generations the following:

1. Added sense windings on motor
2. Continuing the studies of the 2-phase brushless DC motors for improving the values of the torque, speed and motor volume.
3. Design a two phase BDCM using the slottessd construction and comparing it with the slotted construction.
4. Design a single and three-phase BDCM and comparing it with the two phase BDCM performance.
5. Measure motor winding impedance changes.
 - Probing” with current pulses.
 - High-frequency sense carrier.

REFERENCES

REFERENCES

1. Alexander Kusko and Syed M. Peeran, " Brushless DC motor using usymmetrical Field magnetization " , in proc. IA Vol.23, No.2, march/april 1987, p.319 .
2. Kenjo T. and Nagamori S., "permanent – Magnet and Brushless dc motors", Oxford, England, Clarendon press 1985.
3. Bolton H. R. and Ashen R.A. , " influence of motor design and feed-current waveform on torque ripple in brushless dc motor", IEE proc. Vol.131, pt.B, No.3, may/1984, pp.82 –90.
4. Miller, T. J. E., "Switched Reluctance Motors and their Control, Oxford /UK, Magna Phys. Publication and Clarendon, press 1993.
5. Faiz, J. and Finch J.W.," Aspects of design optimization for Switched Reluctance Motors", IEEE trans. On energy conversion 8, 1993, No.4, pp.704-713.
6. Torrey D.A., Niu X.M. and Unkauf, E.J., "Analytical Modelling of Variable-Reluctance machine Mgnetization characteristics. IEEE proc.B-142/ 1995, No.1, pp.14-22.
7. Cathey J. J, and Krimm T. W., " A Theoretical Study of Reduction of Torque Pulsations in Low-Speed Self-Synchronous MotorDrives fed through a Cycloconverter Link.", Electric Machines and Power systems, No.13, 229-243, 1987, Hemisphere Publ. Corp.

REFERENCES

8. Krimm T.W, "harmonic Control to reduce torque Pulsations in brushless DC Motor Drives", MSEE Thesis, University of Kentucky, 1984.
9. Stephen Chapman, "Electric machines Fundamentals", 3rd ed. 1998, McGraw-Hill International Edition.
10. F. Piriou, A.Razek, R. Perret and H. LeHuy, "Torque characteristics of Brushless DC motor with imposed current waveform" , IEEE IAS Annual Meeting conference record, 1986 .
11. Bolton H.R., Liu Y.D. and Mallenson N.M., "Investigation into a class of Brushless DC motor with quasquare voltages and currents", IEE proc. Vol.133, Pt. B, No.2, March 1986.
12. Sameer H. Khader, "Implementation of an Accurate Mathematical Method for Modeling Electromagnetic Processes of Brushless DC Motor", MESM'2001, Amman 2-3 /Sept. Jordan, pp.31-38.

Appendix (A)

List of symbols

Appendix (A, B, C, D)

List of symbols

| | | |
|-------------|---|--|
| V_s | - | Motor supply voltage |
| V_{ds} | - | supply voltage of coils S1 & S2 |
| V_d | - | supply voltage of third coil S3 |
| e_A | - | phase induced back emf of S1 & S2 |
| e_C | - | phase induced back emf of S3 |
| L_A | - | circuit inductance of S1 & S2 |
| L_C | - | circuit inductance of S3 |
| L_{2m} | - | magnitude of highest order harmonic of the Circuit inductance |
| λ_C | - | Flux linkage of third coil S3 |
| R_A | - | circuit resistance of S1 & S2 |
| R_C | - | circuit resistance of coil S3 |
| n | - | Number of harmonic that must be eliminated |
| N_p | - | number of generated pulses in the quarter Interval (0...90°) |
| K | - | The sequence number of generated pulses |
| α_k | - | the instant of k-th pulse |
| $h(\alpha)$ | - | harmonic function |
| E_{mC} | - | magnitude of induced emf of coil S3 |
| E_{mA} | - | magnitude of induced emf of coils S1 & S2 |
| i_A, i_C | - | phase current of coil S1 and S3 |
| I_{mv} | - | magnitude of highest order current harmonics of S3 |
| Ψ_v | - | Phase shift of v-th harmonic current |
| ω | - | Electrical angular frequency |
| TRA | - | reluctance torque component of S1 |
| WRA | - | reactive component of magnetic Coenergy of S1 |
| FSA | - | MMF of coils S1 and S2 |

Appendix (A, B, C, D)

| | |
|-----------------|--|
| NphA- | number of coils conductor of S1 |
| KwA- | winding factor of S1 |
| g- | harmonic order of circuit permance |
| Nt- | number of rotor teeth per pole |
| G- | magnetic permance in the airgap |
| Go- | constant component of circuit permance |
| Gmg- | magnitude of highest order harmonic of permance |
| β g- | Phase shift of highest order harmonics |
| WEA- | Active component of magnetic coenergy |
| TEA- | Active torque component of S1 Coenergy of S1 |
| ϕ R- | Rotor magnetic flux per pole of used Permanent magnet |
| FR- | rotor MMF |
| Hm- | magnetic intensity of the permanent magnet |
| Lm- | permanent magnet length |
| TTA- | total magnetic torque produced by S1 or S2 |
| TTC - | total magnetic torque produced by S3 |
| WEC- | magnetic coenergy of third coil S3 |
| FSC- | space time MMF produced by S3 |
| NphC- | number of coils conductor of S3 |
| Im1- | fundamental current of S3 |
| KwC- | winding factor of S3 |
| Kvi- | ratio of v-th current harmonic to the Fundamental value Im1 |
| ν, γ - | time and space harmonic order respectively |
| TEM- | total electromagnetic torque produced by both coils S1, s2 and S3 . |
| TCR- | torque –current ratio |
| TAV- | means value of total electromagnetic torque |
| ITRMS- | total root mean square of the current of both |

Appendix (A, B, C, D)

Coils S1, s2 and S3

IvRMS- root mean square of highest current Harmonic

TRR- torque ripple ratio

TR- torque ripples

HFI- current harmonic factor

IRMS- root mean square of fundamental current

Harmonic

Appendix (B)

Motor

Construction

Appendix (A, B, C, D)

Graphs of Parts of BDCM:

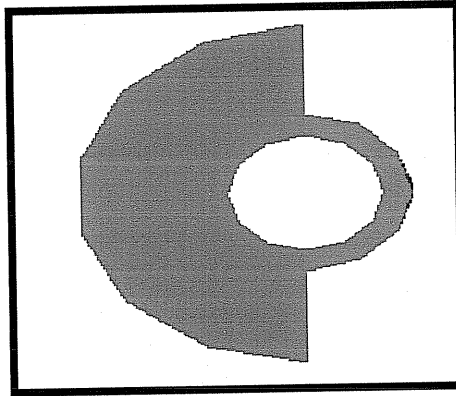


Figure (A1): Crosse section of angular of sensor

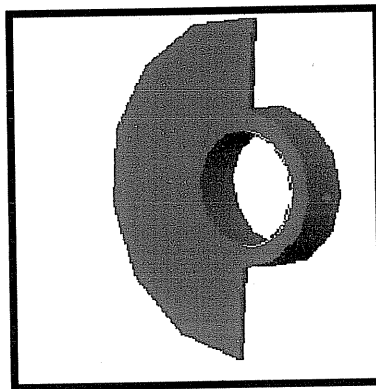


Figure (A2): Crosse section of angular of sensor

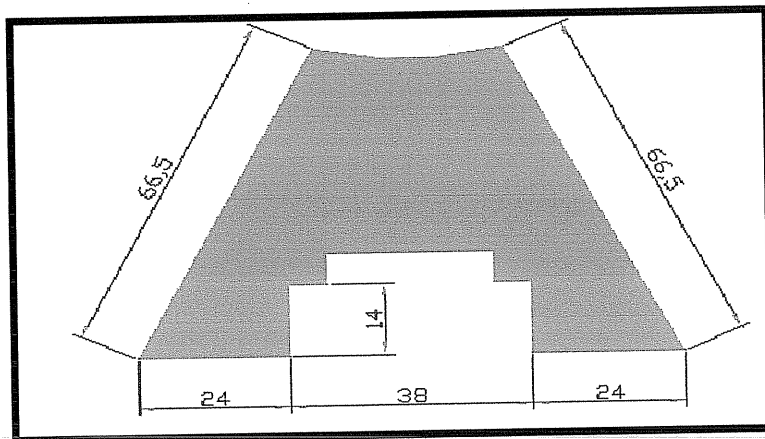


Figure (A3):Crosse section of Dimension of The Band

Appendix (A, B, C, D)

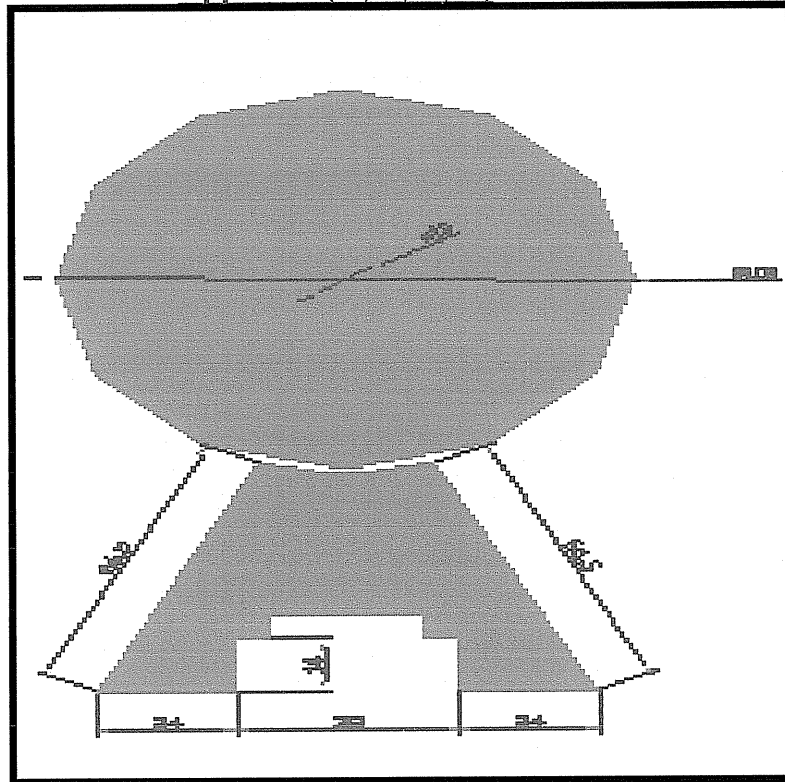


Figure (A4): Crosse section of Dimension of The Motor Body

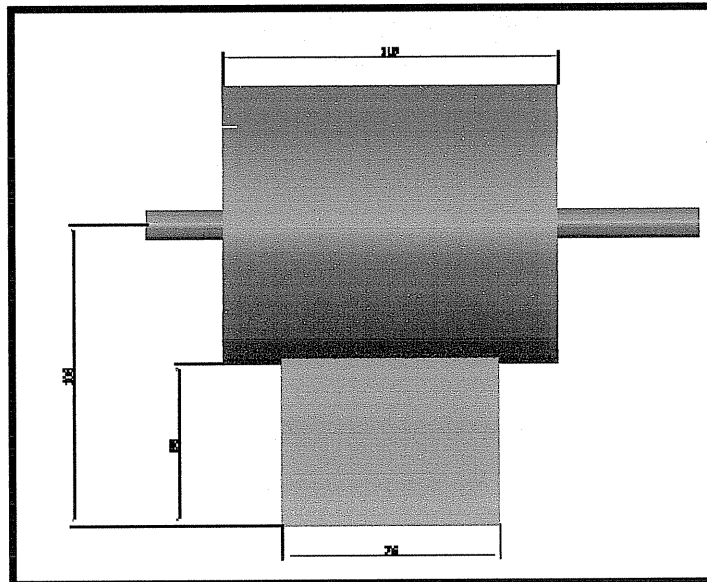


Figure (A5): Crosse section of Motor Body

Appendix (A, B, C, D)

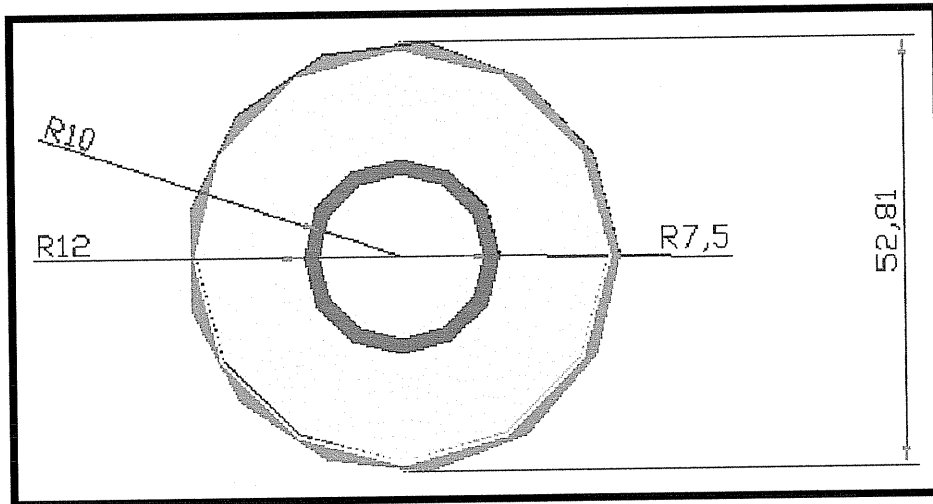


Figure (A6): Crosse section of Covers and Bering house

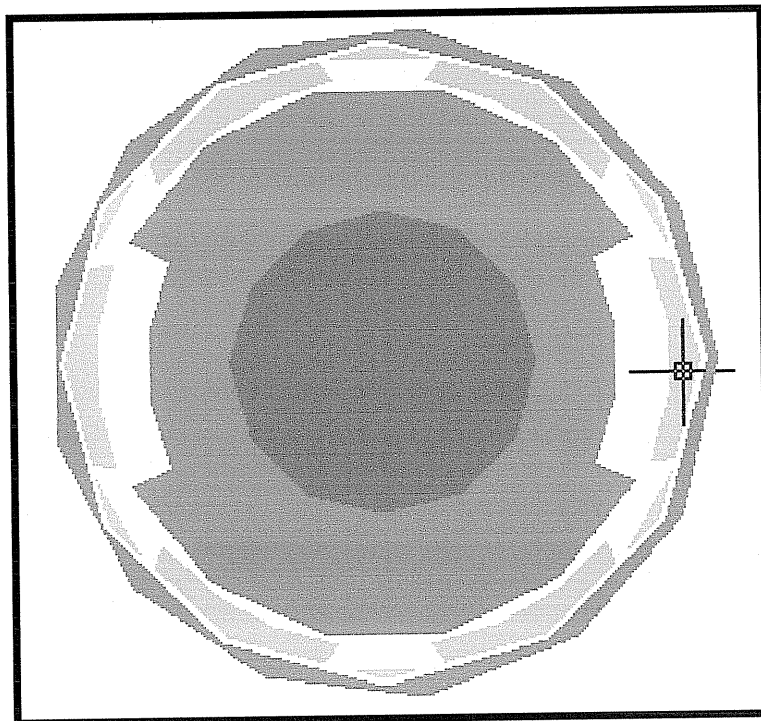


Figure (A7): Crosse section of stator and rotor

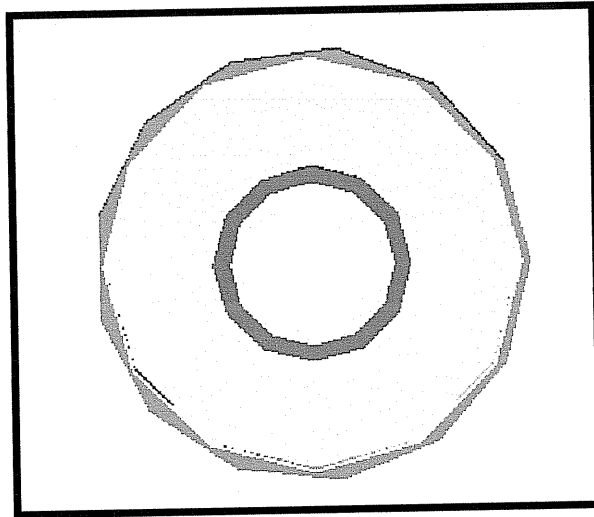


Figure (A8): Crosse section of Covers and Bering house

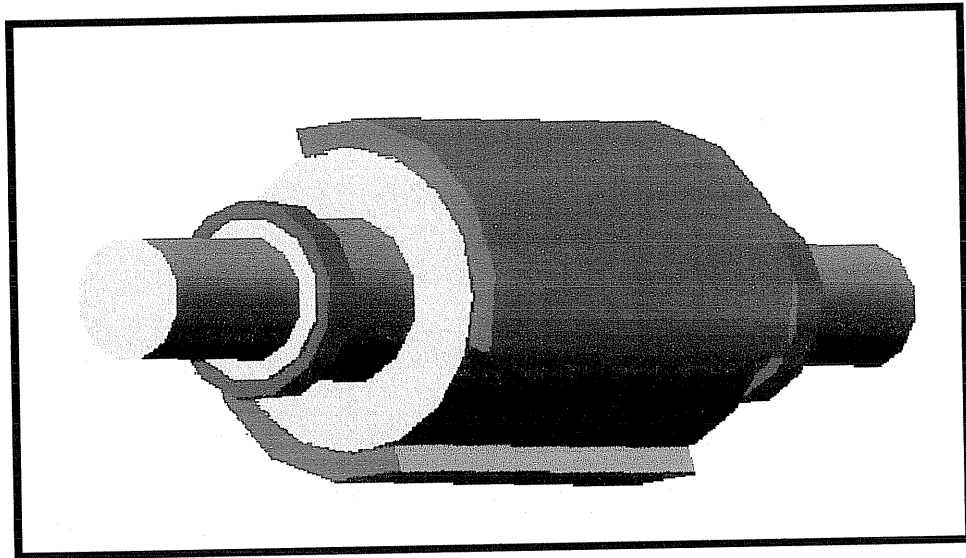


Figure (A9): Crosse section of rotor with permanent magnetic

Appendix (A, B, C, D)

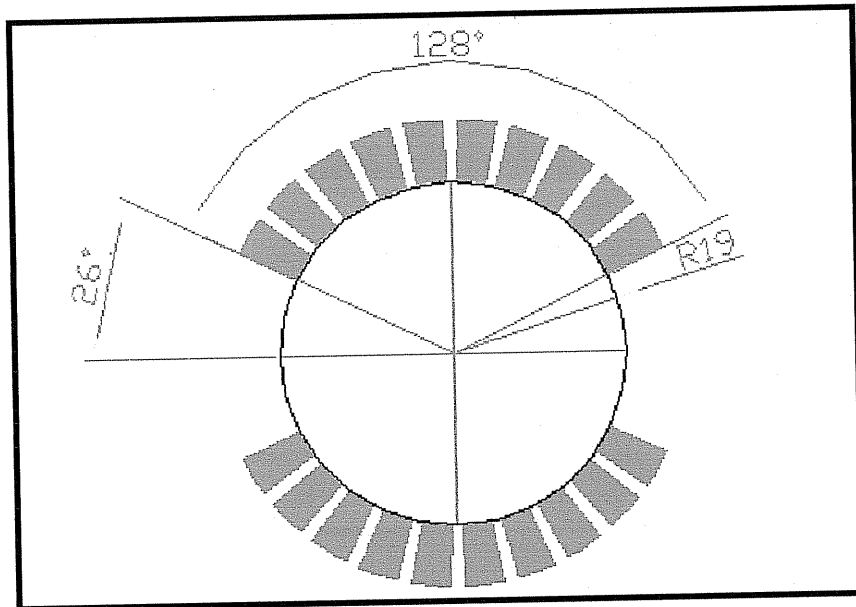


Figure (A10): Crosse section of Dimension Permanent magnet bar.

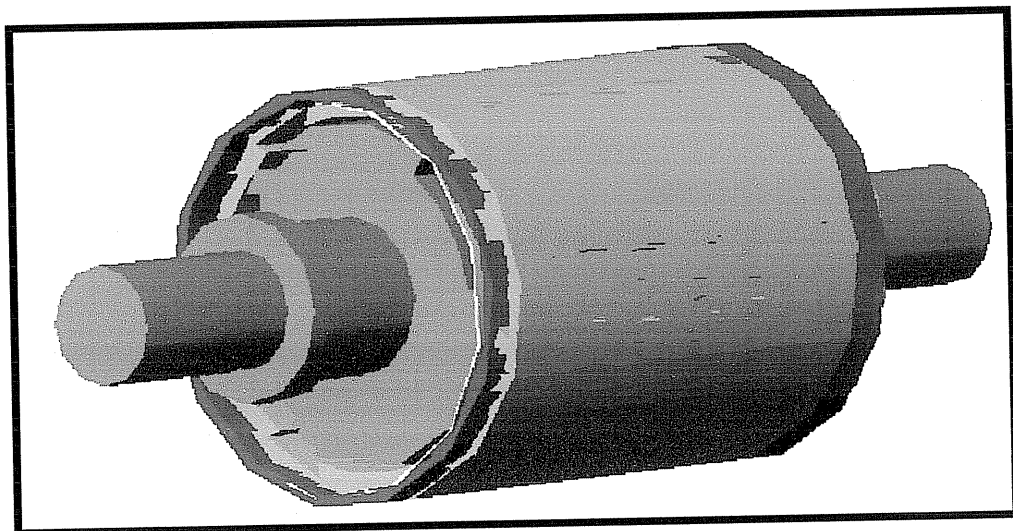


Figure (A11): Crosse section of stator and rotor

Appendix (A, B, C, D)

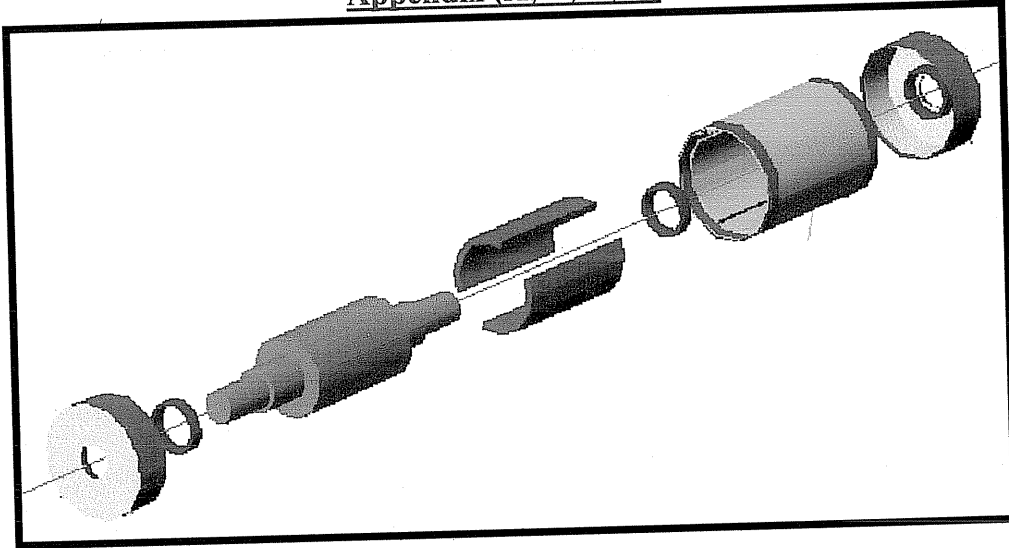


Figure (A14): Crosse section: of construction motor as designed

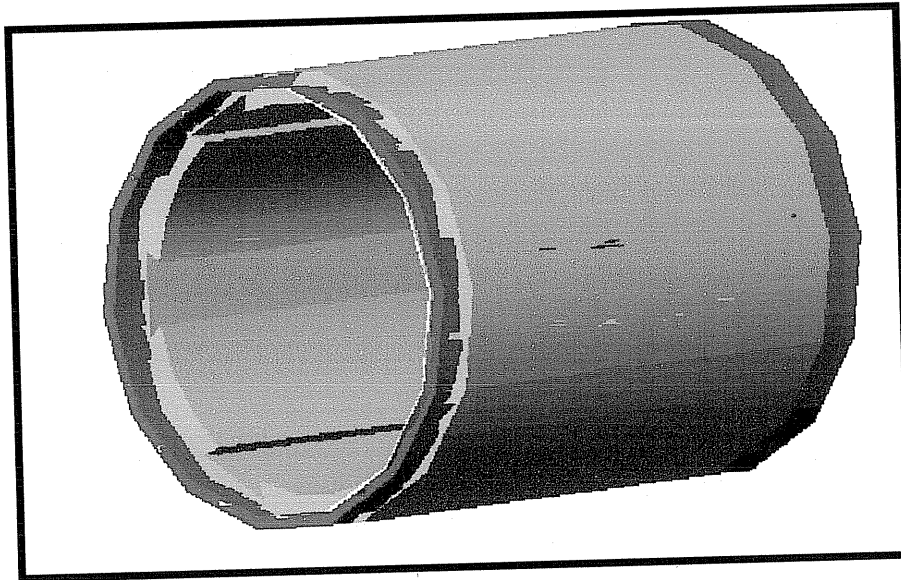


Figure (A15): Crosse section of stator

Appendix (A, B, C, D)

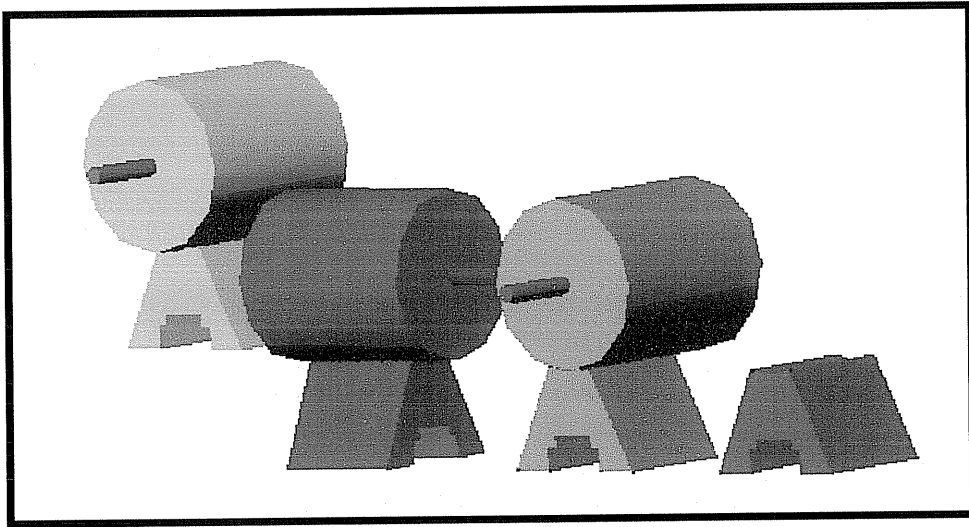


Figure (A16): Crosse section of the body motor

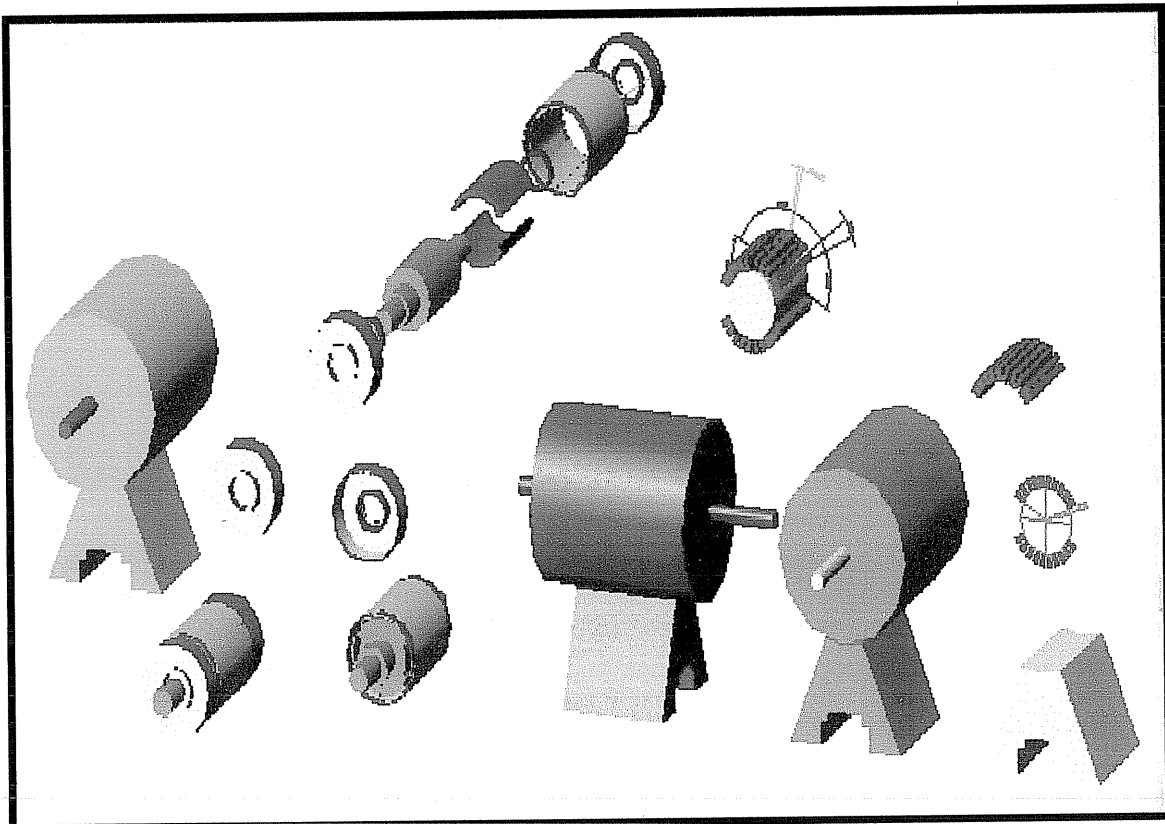


Figure (A17): Crosse section of Total Motor

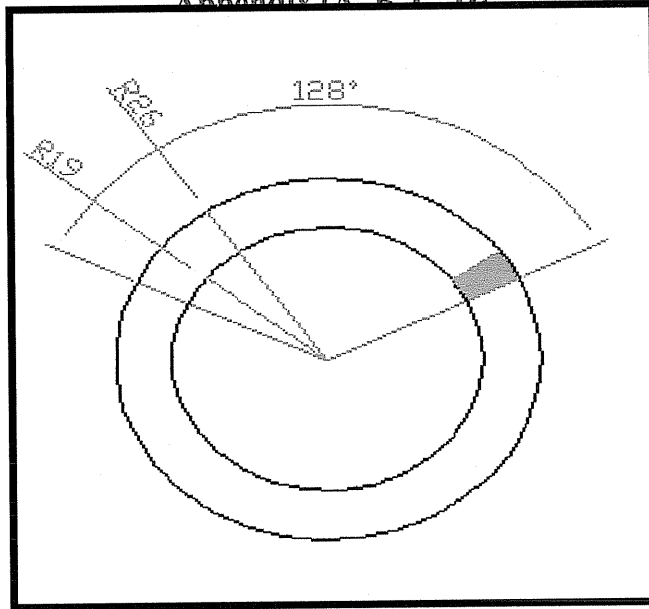


Figure (A18): Crosse section of Permanent magnet

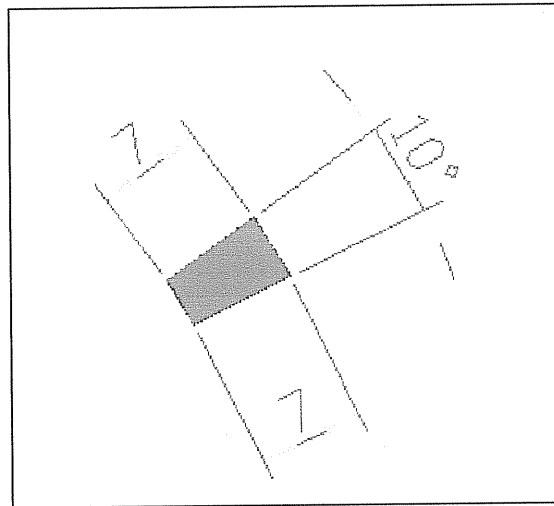


Figure (A19): Crosse section of Dimension of Permanent magnet bar.

Appendix (A, B, C, D)

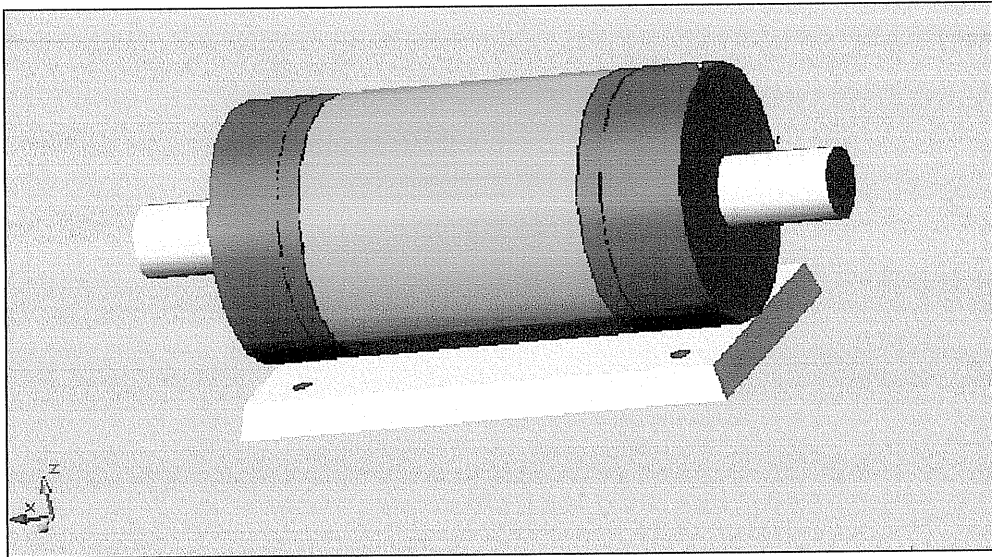


Figure (A20): Crosse section of 2-phase BDCM.

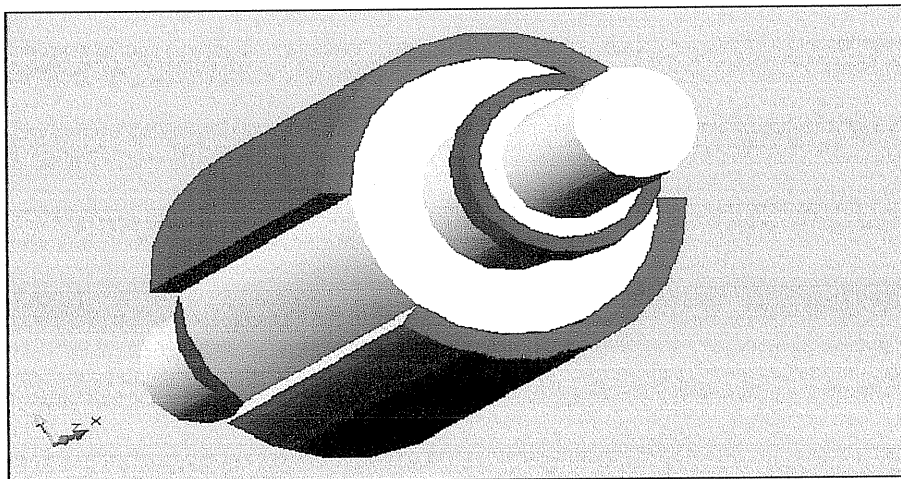


Figure (A21): Crosse section of rotor with permanent magnetic

Appendix (A, B, C, D)

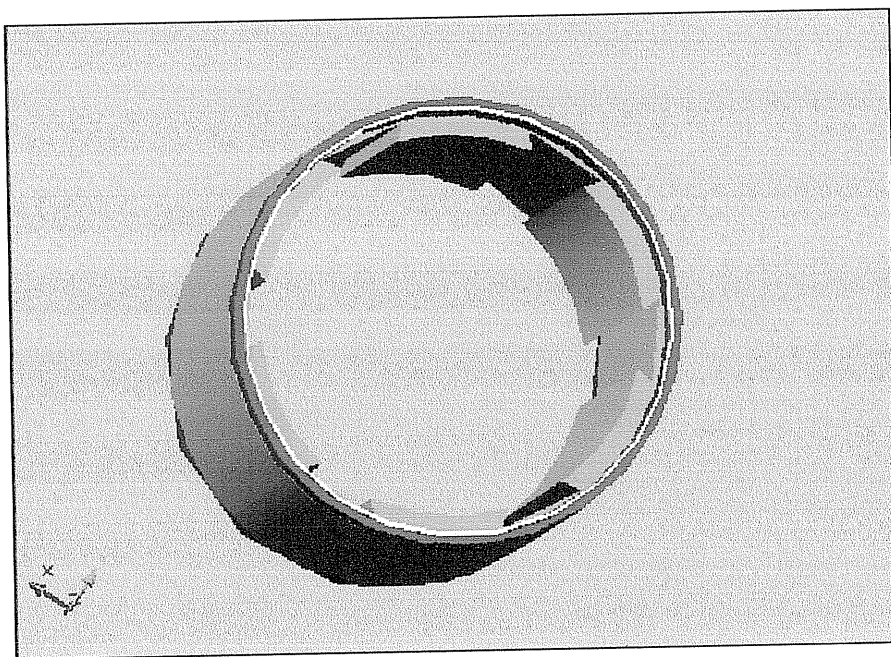


Figure (A22): Crosse section of stator with slots

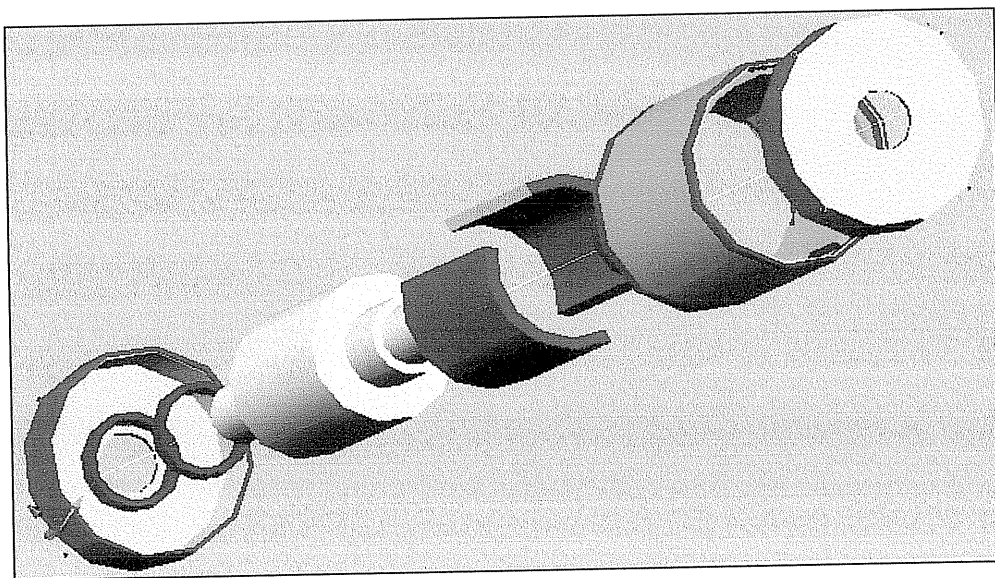


Figure (A23): Crosse section of construction motor as designed

Appendix (A, B, C, D)

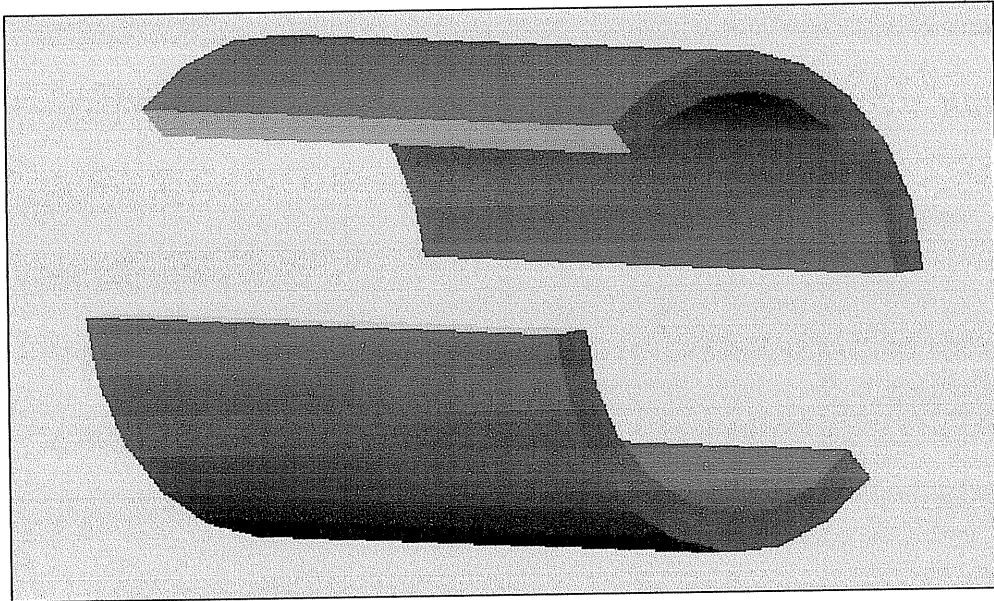


Figure (A24): Crosse section of Permanent magnet arc

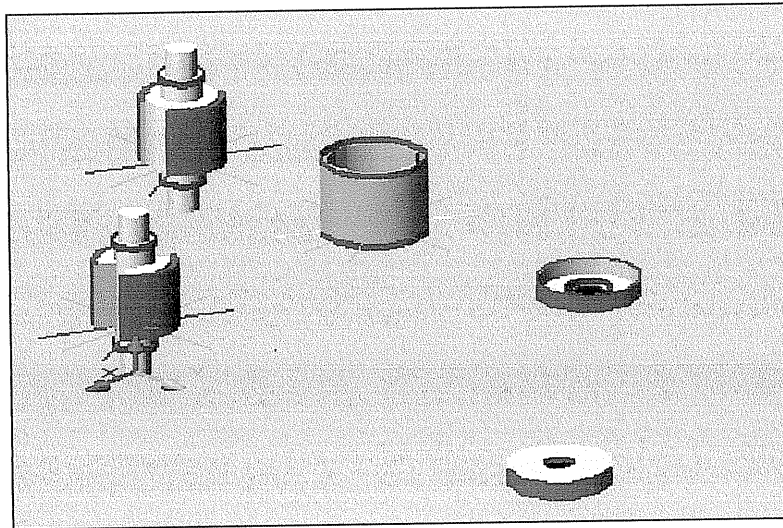


Figure (A25): Crosse section of stator with slots and rotor with permanent magnetic and Covers

Appendix (A, B, C, D)

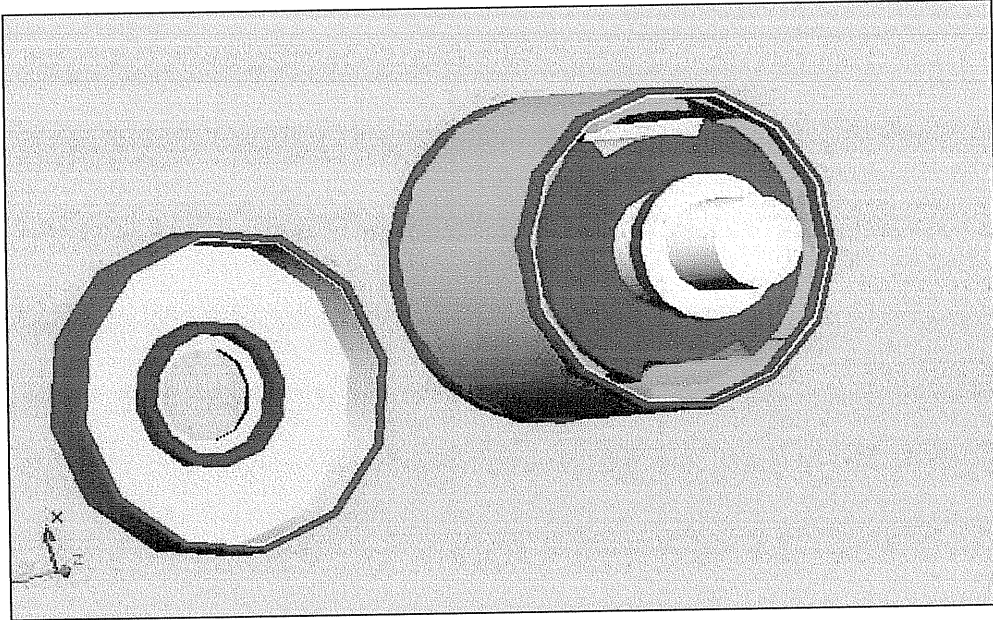


Figure (A26): Crosse section of the rotor and stator and cover and bearing house

Appendix (A, B, C, D)

| Case No | Rotor construction | | | Displayed results on figure |
|--|--------------------|---------------------------------------|----------------------------|------------------------------|
| | Slots width mm | Slots depth mm | Air gap width mm | |
| Case#1 Uniform rotor construction with 2 coils S1&S2 | B1 =14B | $h1 = \delta 0 - \delta 1$ | $\delta 1 = 2 \delta$ | A1-a A2-a A3-a A4-a |
| | B5 =6B | $h5 =hm$ | $\delta 5 =hm+ \delta 1$ | |
| | B3 =2B | -- | $\delta 3 = \delta 1+ hm$ | |
| | B2 =0 | $h2 =h8$ | $\delta 9 =2 \delta$ | |
| | B9 =14B | -- | -- | |
| | B8 =0 | $h5 =h6$ | -- | |
| | B4 =B | $h4 =h6$ | -- | |
| Case#2 Uniform rotor construction with 3 coils S1,S2&S3 | B1 =0B | $h1 = \delta 0 - \delta 1$ | $\delta 1 = 2 \delta$ | A1-a A2-b A3-b A4-b |
| | B5 =6B | -- | $\delta 5 =hm + \delta 1$ | |
| | B9 =10B | -- | $\delta 9 = \delta 1$ | |
| | | -- | -- | |
| Case#3 Uniform rotor construction with multi slots,3coils and constant width of air gap | B1 =6B | $h1 = \delta 0 - \delta 1$ | $\delta 1=2 \delta$ | A1-b A2-c A3-c A4-c |
| | B2 =2B | $h 2 =h1- \delta 1$ | $\delta 2=h1-h2+ \delta 1$ | |
| | B3 =3.5B | - | $\delta 3=h2+2 \delta 1$ | |
| | B4 =2.5B | $h 4= \delta 0 - \delta 1$ | $\delta 2=h1-h2+ \delta 1$ | |
| | B5 =6B | - | $\delta 5=hm+\delta 1$ | |
| | B6 =2.5B | $h 6=h4$ | $\delta 6=x4* \delta 4$ | |
| | B7 =3.5B | - | $\delta 7=x3*\delta 3$ | |
| | B8 =2B | $h 8=h2$ | $\delta 8=x2*\delta 2$ | |
| | B9 =6B | | $\delta 9=x1*\delta 1$ | |
| | | $X1=X2=X3=X4=1$ | | |
| Case#4 Rotor | B1 =6B | $h1 = \delta 0 - \delta 1$ | $\delta 1=2 \delta$ | A1c A2-d A3-d A4-d |
| | B2 =2B | $h 2 =h1- \delta 1$ | $\delta 2=h1-h2+ \delta 1$ | |
| | B3 =3.5B | - | $\delta 3=h2+2 \delta 1$ | |
| | B4 =2.5B | $h 4= \delta 0 - \delta 1$ | $\delta 2=h1-h2+ \delta 1$ | |
| | B5 =6B | - | $\delta 5=hm+\delta 1$ | |
| | B6 =2.5B | $h 6=h4$ | $\delta 6=x4* \delta 4$ | |
| | B7 =3.5B | - | $\delta 7=x3*\delta 3$ | |
| | B8 =2B | $h 8=h2$ | $\delta 8=x2*\delta 2$ | |
| | B9 =6B | - | $\delta 9=x1*\delta 1$ | |
| | | $X1=0.6 ; X2=0.7 ; X3=0.8 ; X4=0.9 ;$ | | |

Appendix (C)

Data Sheets

The B-H hysteresis loop of a hard permanent magnet material:

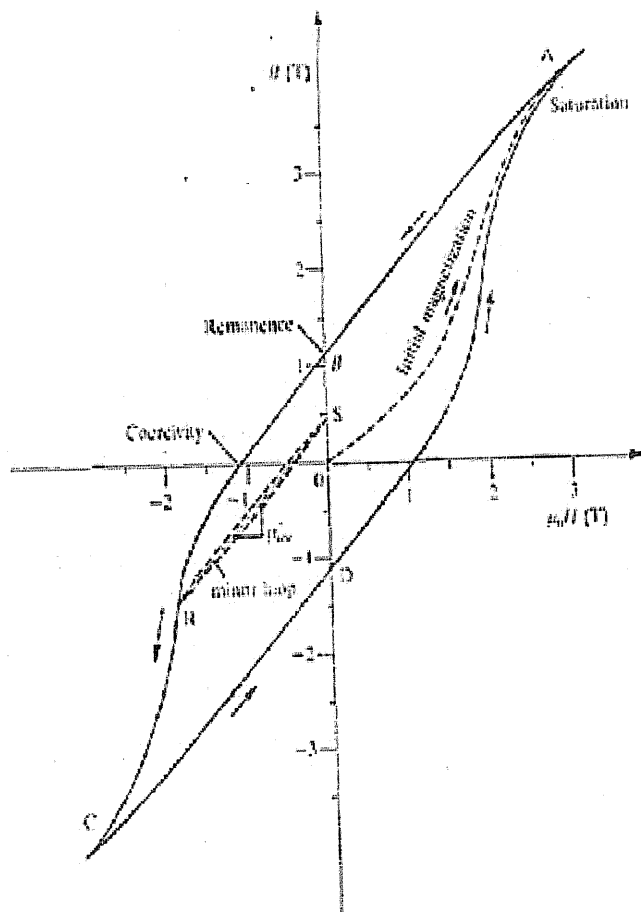


Table 3.1. Magnet properties

| Property | Units | Alnico 5-7 | Ceramic | Sm ₂ Co ₁₇ | NdFeB |
|-------------------------------|--------------------------|---------------|----------|----------------------------------|--------|
| B_r | T | 1.35 | 0.405 | 1.06 | 1.12 |
| $\mu_0 H_c$ | T | 0.074 | 0.37 | 0.94 | 1.06 |
| $(BH)_{max}$ | MGOe | 7.5 | 3.84 | 26.0 | 30.0 |
| B_{rec} | | 1.9 | 1.1 | 1.03 | 1.1 |
| Specific gravity | | 7.31 | 4.8 | 8.2 | 7.4 |
| Resistivity | $\mu\Omega$ cm | 47 | $> 10^4$ | 86 | 150 |
| Thermal expansion | $10^{-6}/^\circ\text{C}$ | 11.3 | 13 | 9 | 3.4 |
| B_r temperature coefficient | %/°C | -0.02 | -0.2 | -0.025 | -0.1 |
| Saturation H | kOe | 3.5 | 14.0 | > 40 | > 30 |

ADC0801, ADC0802, ADC0803, ADC0804, ADC0805 8-Bit μ P Compatible A/D Converters

General Description

The ADC0801, ADC0802, ADC0803, ADC0804 and ADC0805 are CMOS 8-bit successive approximation A/D converters that use a differential potentiometric ladder—similar to the 256R products. These converters are designed to allow operation with the NSC800 and INS800CA derivative control bus with TRI-STATE[®] output latches directly driving the data bus. These A/Ds appear like memory locations or I/O ports to the microprocessor and no interfacing logic is needed.

Differential analog voltage inputs allow increasing the common-mode rejection and offsetting the analog zero input voltage value. In addition, the voltage reference input can be adjusted to allow encoding any smaller analog voltage span to the full 8 bits of resolution.

Features

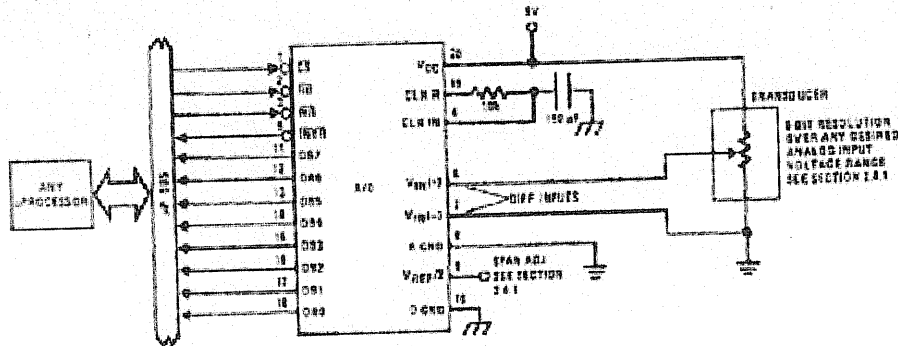
- Compatible with 8080 μ P derivatives—no interfacing logic needed - access time - 135 ns
- Easy interface to all microprocessors, or operates "stand alone"

- Differential analog voltage inputs
- Logic inputs and outputs meet both MOS and TTL voltage level specifications
- Works with 2.5V (LM335) voltage reference
- On-chip clock generator
- 0V to 5V analog input voltage range with single 5V supply
- No zero adjust required
- 0.3" standard width 20-pin DIP package
- 20-pin molded chip carrier or small outline package
- Operates ratiometrically or with 5 V_{CC}, 2.5 V_{CC}, or analog span adjusted voltage reference

Key Specifications

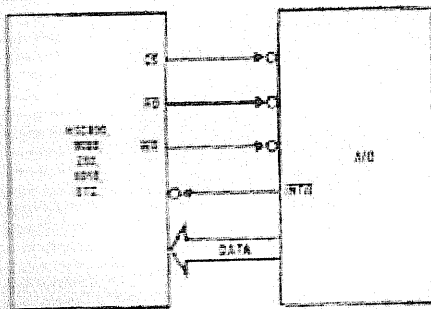
- Resolution 8 bits
- Total error $\pm 1/4$ LSB, $\pm 1/2$ LSB and ± 1 LSB
- Conversion time 100 μ s

Typical Applications



TLUW5671-1

8080 Interface



TLUW5671-2

Error Specification (Includes Full-Scale, Zero Error, and Non-Linearity)

| Part Number | Full-Scale Adjusted | V _{REF} /2 = 2.500 V _{CC} (No Adjustments) | V _{REF} /2 = No Connection (No Adjustments) |
|-------------|---------------------|--|--|
| ADC0801 | $\pm 1/4$ LSB | | |
| ADC0802 | | $\pm 1/2$ LSB | |
| ADC0803 | $\pm 1/2$ LSB | | |
| ADC0804 | | ± 1 LSB | |
| ADC0805 | | | ± 1 LSB |

ADC0801/ADC0802/ADC0803/ADC0804/ADC0805

AC Electrical Characteristics (Continued)

The following specifications apply for $V_{CC} = 5V_{DC}$ and $T_{MIN} \leq T_A \leq T_{MAX}$, unless otherwise specified.

| Symbol | Parameter | Conditions | Min | Typ | Max | Units |
|--|---|---|-----|--------|------------|------------------------------|
| CONTROL INPUTS [Note: CLK IN (Pin 4) is the input of a Schmitt trigger circuit and is therefore specified separately] | | | | | | |
| $V_{IN(0)}$ | Logical "0" Input Voltage (Except Pin 4 CLK IN) | $V_{CC} = 4.75 V_{DC}$ | | | 0.8 | V_{DC} |
| $I_{IN(1)}$ | Logical "1" Input Current (All Inputs) | $V_{IN} = 5 V_{DC}$ | | 0.005 | 1 | μA_{DC} |
| $I_{IN(0)}$ | Logical "0" Input Current (All Inputs) | $V_{IN} = 0 V_{DC}$ | -1 | -0.005 | | μA_{DC} |
| CLOCK IN AND CLOCK II | | | | | | |
| V_{T+} | CLK IN (Pin 4) Positive Going Threshold Voltage | | 2.7 | 3.1 | 3.5 | V_{DC} |
| V_{T-} | CLK IN (Pin 4) Negative Going Threshold Voltage | | 1.5 | 1.8 | 2.1 | V_{DC} |
| V_H | CLK IN (Pin 4) Hysteresis ($V_{T+} - V_{T-}$) | | 0.6 | 1.3 | 2.0 | V_{DC} |
| $V_{OUT(0)}$ | Logical "0" CLK R Output Voltage | $I_O = 360 \mu A$ $V_{CC} = 4.75 V_{DC}$ | | | 0.4 | V_{DC} |
| $V_{OUT(1)}$ | Logical "1" CLK R Output Voltage | $I_O = -360 \mu A$ $V_{CC} = 4.75 V_{DC}$ | 2.4 | | | V_{DC} |
| DATA OUTPUTS AND INTR | | | | | | |
| $V_{OUT(0)}$ | Logical "0" Output Voltage Data Outputs INTR Output | $I_{OUT} = 1.6 mA, V_{CC} = 4.75 V_{DC}$ $I_{OUT} = 1.0 mA, V_{CC} = 4.75 V_{DC}$ | | | 0.4 0.4 | V_{DC} V_{DC} |
| $V_{OUT(1)}$ | Logical "1" Output Voltage | $I_O = -360 \mu A, V_{CC} = 4.75 V_{DC}$ | 2.4 | | | V_{DC} |
| $V_{OUT(1)}$ | Logical "1" Output Voltage | $I_O = -10 \mu A, V_{CC} = 4.75 V_{DC}$ | 4.5 | | | V_{DC} |
| I_{OUT} | TRI-STATE Disabled Output Leakage (All Data Buffers) | $V_{OUT} = 0 V_{DC}$ $V_{OUT} = 5 V_{DC}$ | -3 | | 3 | μA_{DC} μA_{DC} |
| I_{SOURCE} | | V_{OUT} Short to Gnd, $T_A = 25^\circ C$ | 4.5 | 6 | | mA_{DC} |
| I_{SINK} | | V_{OUT} Short to V_{CC} , $T_A = 25^\circ C$ | 9.0 | 16 | | mA_{DC} |
| POWER SUPPLY | | | | | | |
| I_{CC} | Supply Current (Includes Ladder Current) ADC0801/02/03/04/LCJ/05 ADC0804/LCN/LCV/LCWM | $f_{CLK} = 640 kHz$, $V_{REF/2} = NC, T_A = 25^\circ C$ and $\overline{CS} = 5V$ | | | 1.1 1.9 | 1.8 2.5 mA mA |

- Note 1:** Absolute Maximum Ratings indicate limits beyond which damage to the device may occur. DC and AC electrical specifications do not apply when operating the device beyond its specified operating conditions.
- Note 2:** All voltages are measured with respect to Gnd, unless otherwise specified. The separate A Gnd point should always be wired to the D Gnd.
- Note 3:** A zener diode exists, internally, from V_{CC} to Gnd and has a typical breakdown voltage of 7 Vdc.
- Note 4:** For $V_{IN}(-)$: $V_{IN}(+)$ the digital output code will be 0000 0000. Two on-chip diodes are tied to each analog input (see block diagram) which will forward conduct for analog input voltages one diode drop below ground or one diode drop greater than the V_{CC} supply. Be careful, during testing at low V_{CC} levels (4.5V), as high level analog inputs (5V) can cause this input diode to conduct—especially at elevated temperatures, and cause errors for analog inputs near full-scale. The spec allows 50 mV forward bias of either diode. This means that as long as the analog V_{IN} does not exceed the supply voltage by more than 50 mV, the output code will be correct. To achieve an absolute 0 Vdc to 5 Vdc input voltage range will therefore require a minimum supply voltage of 4.950 Vdc over temperature variations, initial tolerance and loading.
- Note 5:** Accuracy is guaranteed at $f_{CLK} = 640 kHz$. At higher clock frequencies accuracy can degrade. For lower clock frequencies, the duty cycle limits can be extended so long as the minimum clock high time interval or minimum clock low time interval is no less than 275 ns.
- Note 6:** With an asynchronous start pulse, up to 8 clock periods may be required before the internal clock phases are proper to start the conversion process. The start request is internally latched, see Figure 2 and section 2.0.
- Note 7:** The \overline{CS} input is assumed to bracket the \overline{WR} strobe input and therefore timing is dependent on the \overline{WR} pulse width. An arbitrarily wide pulse width will hold the converter in a reset mode and the start of conversion is initiated by the low to high transition of the \overline{WR} pulse (see timing diagrams).
- Note 8:** None of these A/Ds requires a zero adjust (see section 2.5.1). To obtain zero code at other analog input voltages see section 2.5 and Figure 5.
- Note 9:** The $V_{REF/2}$ pin is the center point of a two resistor divider connected from V_{CC} to ground. Each resistor is 2.2k, except for the ADC0804/LCJ where each resistor is 18k. Total ladder input resistance is the sum of the two equal resistors.
- Note 10:** Human body model, 100 pF discharged through a 1.5 k Ω resistor.

Absolute Maximum Ratings (Notes 1 & 2)

If Military/Aerospace specified devices are required, contact the National Semiconductor Sales Office/Distributors for availability and specifications.

| | |
|--|-----------------------------------|
| Supply Voltage (V _{CC}) (Note 3) | 6.5V |
| Voltage | |
| Logic Control Inputs | -0.3V to +18V |
| All Other Input and Outputs | -0.3V to (V _{CC} + 0.3V) |
| Lead Temp. (Soldering, 10 seconds) | |
| Dual In-Line Package (plastic) | 260°C |
| Dual In-Line Package (ceramic) | 300°C |
| Surface Mount Package | |
| Vapor Phase (50 seconds) | 215°C |
| Infrared (15 seconds) | 220°C |

| | |
|--|-----------------|
| Storage Temperature Range | -66°C to +150°C |
| Package Dissipation at T _A = 25°C | 875 mW |
| ESD Susceptibility (Note 10) | 800V |

Operating Ratings (Notes 1 & 2)

| | |
|--------------------------|--|
| Temperature Range | T _{MIN} ≤ T _A ≤ T _{MAX} |
| ADC0801/02LJ | -55°C ≤ T _A ≤ +125°C |
| ADC0801/02/03/04LCJ | -40°C ≤ T _A ≤ +85°C |
| ADC0801/02/03/05LCN | -40°C ≤ T _A ≤ +85°C |
| ADC0804LCN | 0°C ≤ T _A ≤ +70°C |
| ADC0802/03/04LCV | 0°C ≤ T _A ≤ +70°C |
| ADC0802/03/04LCWM | 0°C ≤ T _A ≤ +70°C |
| Range of V _{CC} | 4.5 V _{CC} to 6.3 V _{CC} |

Electrical Characteristics

The following specifications apply for V_{CC} = 5 V_{CC}, T_{MIN} ≤ T_A ≤ T_{MAX} and f_{CLK} = 640 kHz unless otherwise specified.

| Parameter | Conditions | Min | Typ | Max | Units |
|--|---|-------------|------------|------------------------|-----------------|
| ADC0801: Total Adjusted Error (Note 8) | With Full-Scale Adj. (See Section 2.5.2) | | | ± 1/4 | LSB |
| ADC0802: Total Unadjusted Error (Note 8) | V _{REF} /2 = 2.500 V _{CC} | | | ± 1/2 | LSB |
| ADC0803: Total Adjusted Error (Note 8) | With Full-Scale Adj. (See Section 2.5.2) | | | ± 1/2 | LSB |
| ADC0804: Total Unadjusted Error (Note 8) | V _{REF} /2 = 2.500 V _{CC} | | | ± 1 | LSB |
| ADC0805: Total Unadjusted Error (Note 8) | V _{REF} /2 - No Connection | | | ± 1 | LSB |
| V _{REF} /2 Input Resistance (Pin 8) | ADC0801/02/03/05 ADC0804 (Note 9) | 2.5 0.75 | 6.0 1.1 | | kΩ kΩ |
| Analog Input Voltage Range | (Note 4) V ₍₊₎ or V ₍₋₎ | Grid - 0.05 | | V _{CC} + 0.05 | V _{CC} |
| DC Common-Mode Error | Over Analog Input Voltage Range | | ± 1/16 | ± 1/8 | LSB |
| Power Supply Sensitivity | V _{CC} = 5 V _{CC} ± 10% Over Allowed V _{IN} (+) and V _{IN} (-) Voltage Range (Note 4) | | ± 1/16 | ± 1/8 | LSB |

AC Electrical Characteristics

The following specifications apply for V_{CC} = 5 V_{CC} and T_A = 25°C unless otherwise specified.

| Symbol | Parameter | Conditions | Min | Typ | Max | Units |
|--|--|--|-----------|-----|------|--------------------|
| T _C | Conversion Time | f _{CLK} = 640 kHz (Note 6) | 103 | | 114 | μs |
| T _C | Conversion Time | (Note 5, 6) | 66 | | 73 | 1/f _{CLK} |
| f _{CLK} | Clock Frequency Clock Duty Cycle | V _{CC} = 5V, (Note 5) (Note 5) | 100 40 | 640 | 1460 | kHz % |
| CR | Conversion Rate in Free-Running Mode | INT _H tied to \overline{WR} with CS = 0 V _{CC} , f _{CLK} = 640 kHz | 8770 | | 9708 | conv/s |
| t _{W_{WR}} | Width of \overline{WR} Input (Start Pulse Width) | CS = 0 V _{CC} (Note 7) | 100 | | | ns |
| t _{ACC} | Access Time (Delay from Falling Edge of \overline{RD} to Output Data Valid) | C _L = 100 pF | | 135 | 200 | ns |
| t _{TR_{STATE}} | TRI-STATE Control (Delay from Rising Edge of \overline{RD} to Hi-Z State) | C _L = 10 pF, R _L = 10k (See TRI-STATE Test Circuits) | | 125 | 200 | ns |
| t _{W_{INT_H}} | Delay from Falling Edge of \overline{WR} or \overline{RD} to Reset of INT _H | | | 300 | 450 | ns |
| C _{IN} | Input Capacitance of Logic Control Inputs | | | 5 | 7.5 | pF |
| C _{OUT} | TRI-STATE Output Capacitance (Data Buffers) | | | 5 | 7.5 | pF |

CONTROL INPUTS (Note: CLK IN (Pin 4) is the input of a Schmitt trigger circuit and is therefore specified separately)

| | | | | | | |
|---------------------|---|--|-----|--|----|-----------------|
| V _{IN} (1) | Logical "1" Input Voltage (Except Pin 4 CLK IN) | V _{CC} - 5.25 V _{CC} | 2.0 | | 15 | V _{CC} |
|---------------------|---|--|-----|--|----|-----------------|

ADC0801/ADC0802/ADC0803/ADC0804/ADC0805

Power MOSFETS (cont'd)

| ECG Type | Description and Application | Transconductance g_{fs} $\mu mhos$ | Drain to Source Breakdown Voltage V_{DSS} | Gate to Source Breakdown Voltage V_{GGS} | Continuous Drain Current I_D Amps | Gate to Source Threshold Voltage $V_{GS(th)}$ | Drain to Source Resistance (DS(on)) Ohms | Input Cap. C_{iss} pF | Source Inductance L_s nH | Package |
|--|---|--------------------------------------|---|--|-------------------------------------|---|--|-------------------------|----------------------------|--|
| ECG2388 Δ | MOSFET, N-Ch, Enhancement Hi Speed Switch | 5 Min | 200 Min | ± 20 Max* | 12.5 | 4 Max | 2 Max | 1000 Typ | 25 Max | TO-18 |
| | | | | | | | | | | $t_d(off) = 120$ ns, $t_d(on) = 20$ ns, $t_f = 60$ ns, $t_r = 60$ ns |
| ECG2374 Δ | MOSFET, N-Ch, Enhancement Hi Speed Switch | 6 Min | 200 Min | ± 20 Max* | 10 | 4 Max | 18 Max | 1300 Typ | 125 Max | TO-18 |
| | | | | | | | | | | $t_d(off) = 50$ ns, $t_d(on) = 20$ ns, $t_f = 40$ ns, $t_r = 60$ ns |
| ECG2900 Δ | MOSFET, N-Ch, Enhancement Hi Speed Switch | 6 Min | 250 Min | ± 20 Max | 14 | 4 Max | 28 Max | 1300 Typ | 125 Max | TO-18 |
| | | | | | | | | | | $t_d(off) = 60$ ns, $t_d(on) = 20$ ns, $t_f = 50$ ns, $t_r = 30$ ns |
| ECG67 Δ | MOSFET, N-Ch, Enhancement Hi Speed Switch | 2 Min | 400 Min | ± 20 Max* | 5 | 4.5 Max | 1.5 Max | 1200 Max | 75 Max | TO-18 |
| | | | | | | | | | | $t_d(off) = 200$ ns, $t_d(on) = 50$ ns, $t_f = 100$ ns, $t_r = 100$ ns |
| ECG2391 Δ | MOSFET, N-Ch, Enhancement Hi Speed Switch | 2.1 Min | 400 Min | ± 30 Max* | 4 | 4 Max | 1.8 Max | 500 Max | 75 Max | TO-18 |
| | | | | | | | | | | $t_d(off) = 65$ ns, $t_d(on) = 20$ ns, $t_f = 40$ ns, $t_r = 60$ ns |
| ECG2397 Δ | MOSFET, N-Ch, Enhancement Hi Speed Switch | 5 Min | 400 Min | ± 30 Max* | 10 | 4 Max | 5 Max | 1800 Max | 150 Max | TO-18 |
| | | | | | | | | | | $t_d(off) = 200$ ns, $t_d(on) = 20$ ns, $t_f = 75$ ns, $t_r = 50$ ns |
| ECG2380 Δ (Compl to ECG2381) | MOSFET, N-Ch, Enhancement Hi Speed Switch | 1 Min | 500 Min | ± 20 Max* | 2 | 4.5 Max | 4 Max | 500 Max | 75 Max | TO-18 |
| | | | | | | | | | | $t_d(off) = 60$ ns, $t_d(on) = 40$ ns, $t_f = 30$ ns, $t_r = 60$ ns |
| ECG2381 Δ (Compl to ECG2380) | MOSFET, P-Ch, Enhancement Hi Speed Switch | 5 Min | 500 Min | ± 20 Max* | 2 | 4.5 Max | 6 Max | 1000 Max | 75 Max | TO-18 |
| | | | | | | | | | | $t_d(off) = 150$ ns, $t_d(on) = 150$ ns, $t_f = 50$ ns, $t_r = 100$ ns |
| ECG2398 Δ | MOSFET, N-Ch, Enhancement Hi Speed Switch | 3.5 Min | 500 Min | ± 30 Max* | 5 | 4 Max | 1.5 Max | 1000 Max | 100 Max | TO-18 |
| | | | | | | | | | | $t_d(off) = 100$ ns, $t_d(on) = 10$ ns, $t_f = 40$ ns, $t_r = 45$ ns |
| ECG2385 Δ | MOSFET, N-Ch, Enhancement Hi Speed Switch | 5 Min | 500 Min | ± 30 max* | 8 | 4 Max | 8 Max | 1800 Max | 125 Max | TO-18 |
| | | | | | | | | | | $t_d(off) = 250$ ns, $t_d(on) = 40$ ns, $t_f = 90$ ns, $t_r = 90$ ns |
| ECG2901 Δ | MOSFET, N-Ch, Enhancement Hi Speed Switch | 1 Min | 600 Min | ± 20 Max* | 2.5 | 4 Max | 4 Max | 500 Max | 80 Max | TO-18 |
| | | | | | | | | | | $t_d(off) = 20$ ns, $t_d(on) = 30$ ns, $t_f = 30$ ns, $t_r = 40$ ns |
| ECG2379 Δ | MOSFET, N-Ch, Enhancement Hi Speed Switch | 3 Min | 600 Min | ± 20 Max* | 5 | 4 Max | 1.25 Max | 1400 Typ | 100 Max | TO-18 |
| | | | | | | | | | | $t_d(off) = 85$ ns, $t_d(on) = 40$ ns, $t_f = 20$ ns, $t_r = 25$ ns |

Package Outlines - See Page 1-91

* Warning - Exceeding V_{GGS} maximum will result in permanent damage to the gate region oxide layer.
 Δ Refer to MOSFET Handling Precautions - Page 1-34

Power MOSFETS (cont'd)

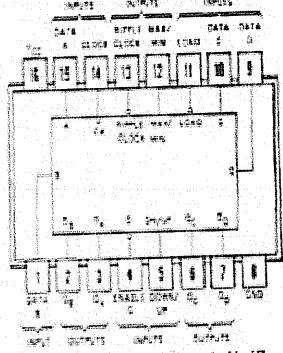
| ECG Type | Description and Application | Transconductance g_{fs} $\mu mhos$ | Drain to Source Breakdown Voltage V_{DS} | Gate to Source Breakdown Voltage V_{GS} | Continuous Drain Current I_D Amps | Gate to Source Threshold Voltage $V_{GS(th)}$ | Drain to Source Resistance (OSon) Ohms | Input Cap. C_{iss} pf | Output Capacitance C_{oss} pf | Package | |
|---|---|--------------------------------------|--|---|-------------------------------------|---|--|-------------------------|---------------------------------|--|--|
| ECG2368 ▲ | MOSFET, N-Ch, Enhancement Hi Speed Switch | 5 Min | 200 Min | ± 20 Max* | 12.5 | 4 Max | 2 Max | 1000 Typ | 25 Max | | |
| <td>$t_d(off) = 120$ ns, $t_d(on) = 20$ ns, $t_f = 60$ ns, $t_r = 60$ ns</td> | | | | | | | | | | | $t_d(off) = 120$ ns, $t_d(on) = 20$ ns, $t_f = 60$ ns, $t_r = 60$ ns |
| ECG2374 ▲ | MOSFET, N-Ch, Enhancement Hi Speed Switch | 6 Min | 200 Min | ± 20 Max* | 10 | 4 Max | .10 Max | 1200 Typ | 125 Max | | |
| <td>$t_d(off) = 50$ ns, $t_d(on) = 20$ ns, $t_f = 40$ ns, $t_r = 60$ ns</td> | | | | | | | | | | | $t_d(off) = 50$ ns, $t_d(on) = 20$ ns, $t_f = 40$ ns, $t_r = 60$ ns |
| ECG2390 ▲ | MOSFET, N-Ch, Enhancement Hi Speed Switch | 6 Min | 250 Min | ± 20 Max | 14 | 4 Max | .20 Max | 1300 Typ | 125 Max | | |
| <td>$t_d(off) = 60$ ns, $t_d(on) = 20$ ns, $t_f = 60$ ns, $t_r = 30$ ns</td> | | | | | | | | | | | $t_d(off) = 60$ ns, $t_d(on) = 20$ ns, $t_f = 60$ ns, $t_r = 30$ ns |
| ECG67 ▲ | MOSFET, N-Ch, Enhancement Hi Speed Switch | 2 Min | 400 Min | ± 20 Max* | 5 | 4.5 Max | 1.5 Max | 1200 Max | 75 Max | | |
| <td>$t_d(off) = 200$ ns, $t_d(on) = 50$ ns, $t_f = 100$ ns, $t_r = 100$ ns</td> | | | | | | | | | | | $t_d(off) = 200$ ns, $t_d(on) = 50$ ns, $t_f = 100$ ns, $t_r = 100$ ns |
| ECG2391 ▲ | MOSFET, N-Ch, Enhancement Hi Speed Switch | 2.1 Min | 400 Min | ± 30 Max* | 4 | 4 Max | 1.8 Max | 500 Max | 75 Max | | |
| <td>$t_d(off) = 65$ ns, $t_d(on) = 20$ ns, $t_f = 40$ ns, $t_r = 60$ ns</td> | | | | | | | | | | | $t_d(off) = 65$ ns, $t_d(on) = 20$ ns, $t_f = 40$ ns, $t_r = 60$ ns |
| ECG2397 ▲ | MOSFET, N-Ch, Enhancement Hi Speed Switch | 5 Min | 400 Min | ± 30 Max* | 10 | 4 Max | .5 Max | 1800 Max | 150 Max | | |
| <td>$t_d(off) = 200$ ns, $t_d(on) = 20$ ns, $t_f = 75$ ns, $t_r = 90$ ns</td> | | | | | | | | | | | $t_d(off) = 200$ ns, $t_d(on) = 20$ ns, $t_f = 75$ ns, $t_r = 90$ ns |
| ECG2380 ▲ (Compl to ECG2381) | MOSFET, N-Ch, Enhancement Hi Speed Switch | 1 Min | 500 Min | ± 20 Max* | 2 | 4.5 Max | 4 Max | 500 Max | 75 Max | | |
| <td>$t_d(off) = 60$ ns, $t_d(on) = 40$ ns, $t_f = 30$ ns, $t_r = 60$ ns</td> | | | | | | | | | | $t_d(off) = 60$ ns, $t_d(on) = 40$ ns, $t_f = 30$ ns, $t_r = 60$ ns | |
| ECG2391 ▲ (Compl to ECG2390) | MOSFET, P-Ch, Enhancement Hi Speed Switch | 5 Min | 500 Min | ± 20 Max* | 2 | 4.5 Max | 6 Max | 1000 Max | 70 Max | | |
| <td>$t_d(off) = 150$ ns, $t_d(on) = 150$ ns, $t_f = 50$ ns, $t_r = 100$ ns</td> | | | | | | | | | | $t_d(off) = 150$ ns, $t_d(on) = 150$ ns, $t_f = 50$ ns, $t_r = 100$ ns | |
| ECG2399 ▲ | MOSFET, N-Ch, Enhancement Hi Speed Switch | 3.5 Min | 500 Min | ± 30 Max* | 5 | 4 Max | 1.5 Max | 1000 Max | 100 Max | | |
| <td>$t_d(off) = 100$ ns, $t_d(on) = 10$ ns, $t_f = 40$ ns, $t_r = 45$ ns</td> | | | | | | | | | | $t_d(off) = 100$ ns, $t_d(on) = 10$ ns, $t_f = 40$ ns, $t_r = 45$ ns | |
| ECG2385 ▲ | MOSFET, N-Ch, Enhancement Hi Speed Switch | 5 Min | 500 Min | ± 30 max* | 8 | 4 Max | .8 Max | 1800 Max | 125 Max | | |
| <td>$t_d(off) = 250$ ns, $t_d(on) = 40$ ns, $t_f = 90$ ns, $t_r = 90$ ns</td> | | | | | | | | | | $t_d(off) = 250$ ns, $t_d(on) = 40$ ns, $t_f = 90$ ns, $t_r = 90$ ns | |
| ECG2901 ▲ | MOSFET, N-Ch, Enhancement Hi Speed Switch | 1 Min | 600 Min | ± 20 Max* | 2.5 | 4 Max | 4 Max | 500 Max | 60 Max | | |
| <td>$t_d(off) = 20$ ns, $t_d(on) = 30$ ns, $t_f = 30$ ns, $t_r = 40$ ns</td> | | | | | | | | | | $t_d(off) = 20$ ns, $t_d(on) = 30$ ns, $t_f = 30$ ns, $t_r = 40$ ns | |
| ECG2379 ▲ | MOSFET, N-Ch, Enhancement Hi Speed Switch | 3 Min | 600 Min | ± 20 Max* | 5 | 4 Max | 1.25 Max | 1400 Typ | 100 Max | | |
| <td>$t_d(off) = 85$ ns, $t_d(on) = 40$ ns, $t_f = 20$ ns, $t_r = 25$ ns</td> | | | | | | | | | | $t_d(off) = 85$ ns, $t_d(on) = 40$ ns, $t_f = 20$ ns, $t_r = 25$ ns | |

* Warning - Exceeding V_{GS} maximum will result in permanent damage to the gate region oxide layer.
 ▲ Refer to MOSFET Handling Precautions - Page 1-34

Package Outlines - See Page 1-91

Diag. 155 16-Pin DIP See Fig. D8

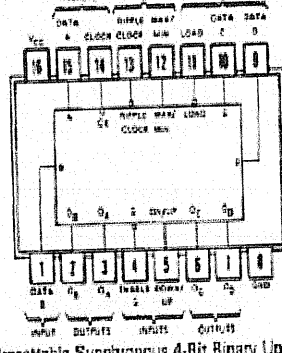
ECG74190, ECG74LS190



Presettable Synchronous Decade Up/Down Counter

Diag. 156 16-Pin DIP See Fig. D8

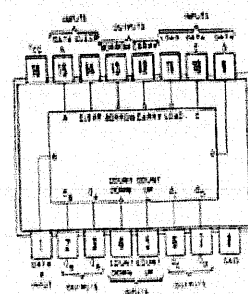
ECG74191, ECG74LS191



Presettable Synchronous 4-Bit Binary Up/Down Counter

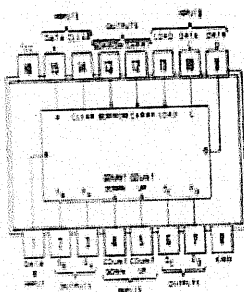
Diag. 157 16-Pin DIP See Fig. D8

ECG74192, ECG74C192, ECG74LS192



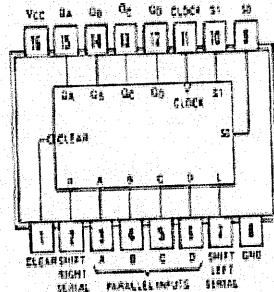
Presettable Synchronous Decade Up/Down Counter with Dual Clocks

Diag. 158 16-Pin DIP See Fig. D8
ECG74193, ECG74C193, ECG74LS193



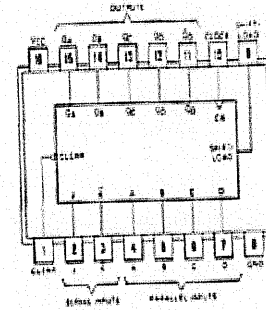
Presettable Synchronous 4-Bit Binary Up/Down Counter with Dual Clocks

Diag. 159 16-Pin DIP See Fig. D8
ECG74LS194A, ECG74S194



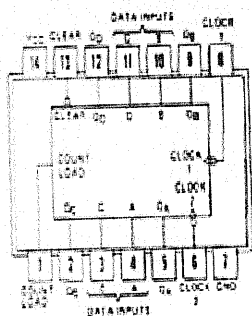
4-Bit Bidirectional Parallel Shift Register

Diag. 160 16-Pin DIP See Fig. D8
ECG74195, ECG74LS195A



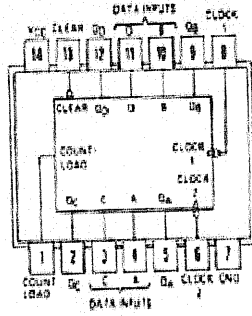
4-Bit Parallel Shift Register with Complementary Final Stage

Diag. 161 14-Pin DIP See Fig. D6
ECG74196, ECG74LS196



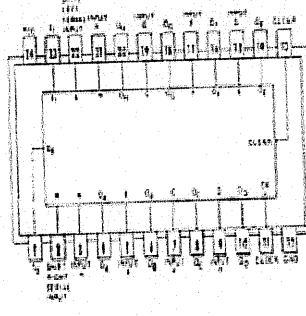
Presettable Decade Counter/Latch

Diag. 162 14-Pin DIP See Fig. D6
ECG74197, ECG74LS197



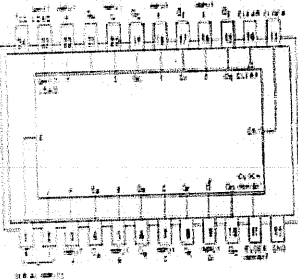
Presettable 4-Bit Binary Counter/Latch

Diag. 163 24-Pin DIP See Fig. D15
ECG74198



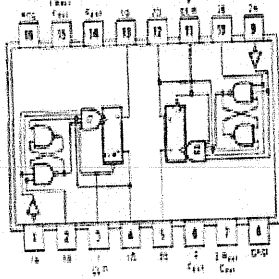
8-Bit Bidirectional Parallel Shift Register

Diag. 164 24-Pin DIP See Fig. D15
ECG74199

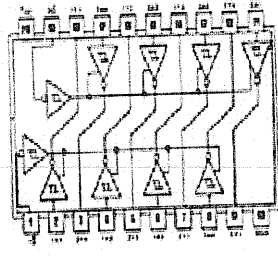


4-Bit Serial or Parallel-In/Parallel-Out Shift Register

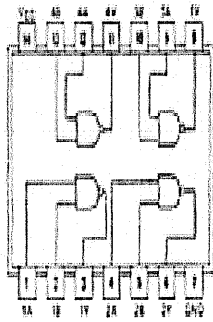
Diag. 165 16-Pin DIP See Fig. D8
ECG74C221, ECG74C221, ECG74LS221



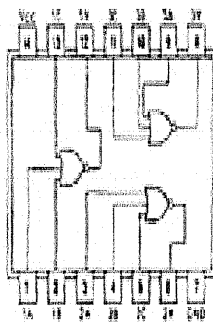
Diag. 166 20-Pin DIP See Fig. D12
ECG74C240, ECG74HC240, ECG74HC240, ECG74LS240



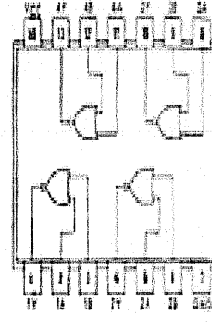
Octal Buffer/Line Driver/Line Receiver with Tri-State Outputs



Quad 2-Input Hi-Volt Interface NAND Gate with Open Collector Output



Triple 3-Input NOR Gate

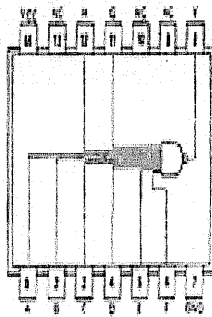


Quad 2-Input NOR Buffer

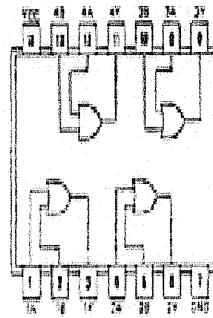
Diag. 28 14-Pin DIP See Fig. D6
**ECG7430, ECG74C30, ECG74H30,
 ECG74LS30, ECG74S30**

Diag. 29 14-Pin DIP See Fig. D6
**ECG7432, ECG74C32, ECG74HC32,
 ECG74HCT32, ECG74LS32**

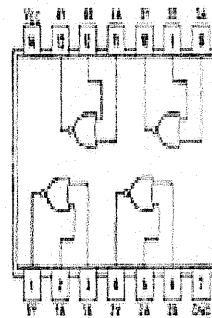
Diag. 30 14-Pin DIP See Fig. D6
ECG7433, ECG74LS33



8-Input NAND Gate



Quad 2-Input OR Gate

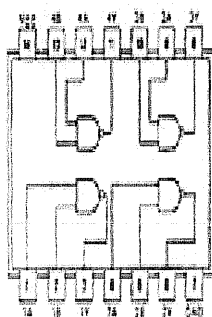


Quad 2-Input NOR Buffer with Open Collector Output

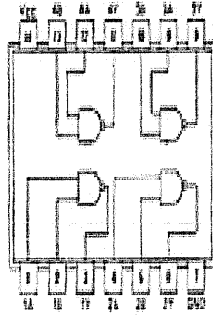
Diag. 31 14-Pin DIP See Fig. D6
ECG7437, ECG74LS37

Diag. 32 14-Pin DIP See Fig. D6
ECG7438, ECG74LS38

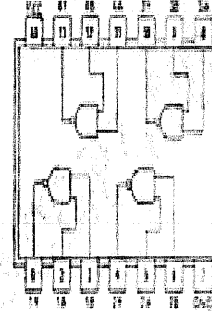
Diag. 33 14-Pin DIP See Fig. D6
ECG7439



Quad 2-Input NAND Buffer



Quad 2-Input NAND Buffer with Open Collector Output

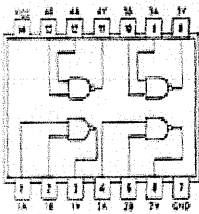
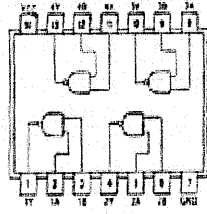
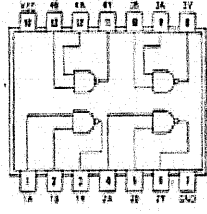
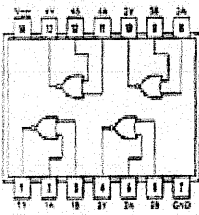
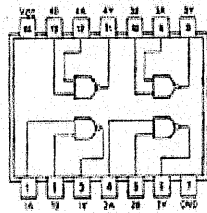
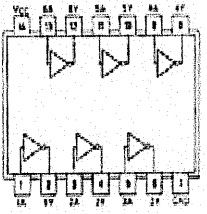
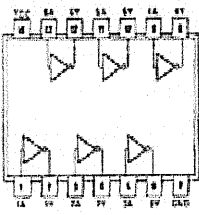
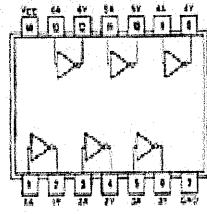
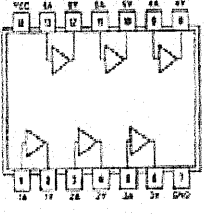
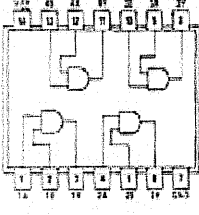
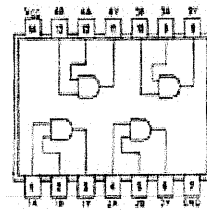
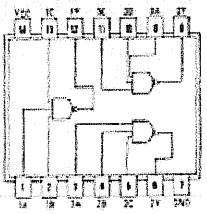


Quad 2-Input NAND Buffer with Open Collector Output

Diag. 34 14-Pin DIP See Fig. D6

Diag. 35 16-Pin DIP See Fig. D8

Diag. 36 16-Pin DIP See Fig. D8

| | | |
|---|---|---|
|  <p>Quad 2-Input NAND Gate</p> |  <p>Quad 2-Input NAND Gate with Open Collector Output</p> |  <p>Quad 2-Input NAND Gate with Open Collector Output</p> |
| <p>Diag. 4 14-Pin DIP See Fig. D5 ECG7402, ECG74C02, ECG74HC02, ECG74LS02, ECG74S02</p>  <p>Quad 2-Input NOR Gate</p> | <p>Diag. 5 14-Pin DIP See Fig. D6 ECG7403, ECG74LS03, ECG74S03</p>  <p>Quad 2-Input NAND Gate with Open Collector Output</p> | <p>Diag. 6 14-Pin DIP See Fig. I ECG7404, ECG74C04, ECG74H04, ECG74HC04, ECG74HCT04, ECG74LS04, ECG74S04</p>  <p>Hex Inverter</p> |
| <p>Diag. 7 14-Pin DIP See Fig. D6 ECG7405, ECG74H05, ECG74LS05, ECG74S05</p>  <p>Hex Inverter with Open Collector Output</p> | <p>Diag. 8 14-Pin DIP See Fig. D6 ECG7406</p>  <p>Hex Inverter/Buffer with Hi-Volt (30 V) Open Collector Output</p> | <p>Diag. 9 14-Pin DIP See Fig. I ECG7407</p>  <p>Hex Buffer with Hi-Volt (30 V) Open Collector Output</p> |
| <p>Diag. 10 14-Pin DIP See Fig. D5 ECG7408, ECG74C08, ECG74H08, ECG74HC08, ECG74HCT08, ECG74LS08, ECG74S08</p>  <p>Quad 2-Input AND Gate</p> | <p>Diag. 11 14-Pin DIP See Fig. D5 ECG7409, ECG74LS09, ECG74S09</p>  <p>Quad 2-Input AND Gate with Open Collector Output</p> | <p>Diag. 12 14-Pin DIP See Fig. C ECG7410, ECG74C10, ECG74H10, ECG74HC10, ECG74LS10, ECG74S10</p>  <p>Triple 3-Input NAND Gate</p> |

Linear IC and Module Circuits (cont'd)

ECG847 14-Pin DIP See Fig. L103
Low Level Audio Amp. Replaces PA230 and PA238, $V_{CC} = 12\text{ V Typ}$

ECG849 14-Pin DIP See Fig. L104
TV Horiz/Vert Countdown

ECG851 14-Pin DIP See Fig. L104
TV VHF-UHF Pre-scaler

ECG852 14-Pin DIP See Fig. L104
No Hold Control, Vert/ Horiz Circuit

ECG853 16-Pin DIP See Fig. L111
Narrow Band FM, IF, Squelch, Scan Control

ECG855 14-Pin DIP See Fig. L104
Color TV Video Modulator

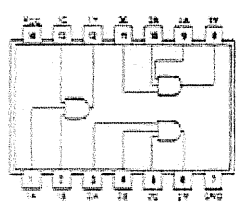
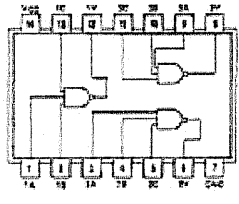
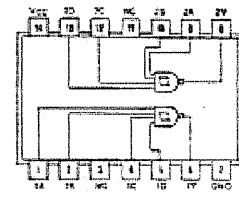
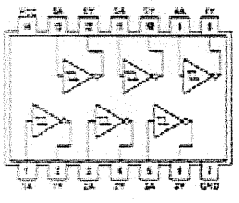
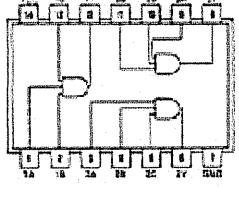
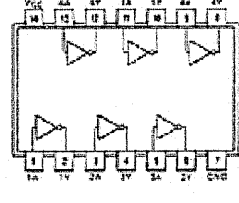
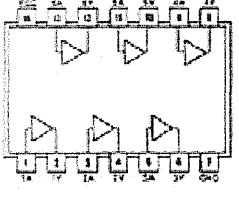
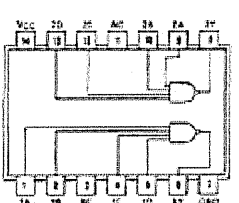
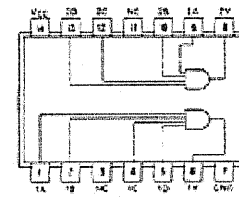
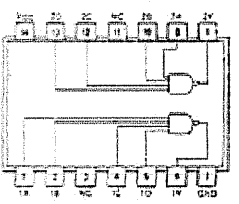
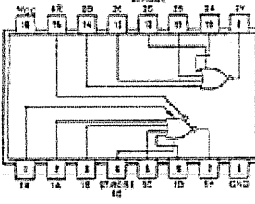
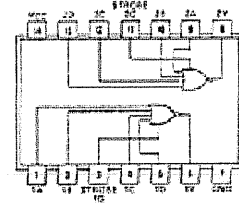
ECG856 8-Pin DIP See Fig. L97
TV Video Modulator

ECG857M 8-Pin DIP See Fig. L98
ECG857SM 8-Pin SOIC See Fig. L159
Lo Noise JFET Input Op Amp

ECG858M 8-Pin DIP See Fig. L98
ECG858SM 8-Pin SOIC See Fig. L159
Dual Lo Noise JFET Input Op Amp

ECG859 14-Pin DIP See Fig. L104
ECG859SM 14-Pin SOIC See Fig. L160
Quad Lo Noise JFET Input Op Amp

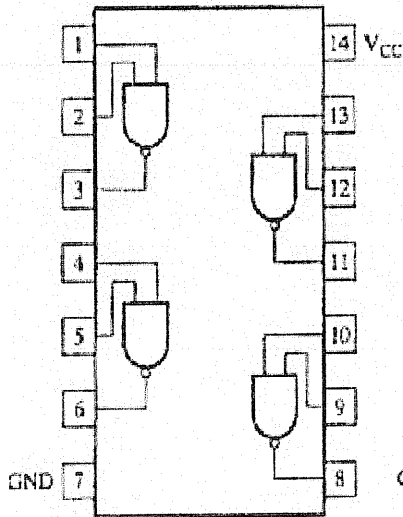
ECG860 18-Pin DIP See Fig. L115
Narrow Band FM, IF Amp Scan Control Squelch Osc, Mixer, DET and AFC

| | | |
|---|---|--|
| <p>Diag. 13 14-Pin DIP See Fig. D6 ECG7411, ECG74H11, ECG74HC11, ECG74LS11, ECG74S11</p>  <p>Triples 3-Input AND Gate</p> | <p>Diag. 14 14-Pin DIP See Fig. D6 ECG7412, ECG74LS12</p>  <p>Triples 3-Input NAND Gate with Open Collector Output</p> | <p>Diag. 15 14-Pin DIP See Fig. D6 ECG7413, ECG74LS13</p>  <p>Dual 4-Input NAND Schmitt Trigger</p> |
| <p>Diag. 16 14-Pin DIP See Fig. D6 ECG7414, ECG74C14, ECG74HC14, ECG74HCT14, ECG74LS14</p>  <p>Hex Schmitt Trigger Inverter</p> | <p>Diag. 17 14-Pin DIP See Fig. D6 ECG7415, ECG74S15</p>  <p>Triples 3-Input AND Gate with Open Collector Output</p> | <p>Diag. 18 14-Pin DIP See Fig. D6 ECG7418</p>  <p>Hex Inverter/Buffer with Hi-Volt (15 V) Open Collector Output</p> |
| <p>Diag. 19 14-Pin DIP See Fig. D6 ECG7417</p>  <p>Hex Buffer with Hi-Volt (15 V) Open Collector Output</p> | <p>Diag. 20 14-Pin DIP See Fig. D6 ECG7420, ECG74C20, ECG74H20, ECG74LS20, ECG74S20</p>  <p>Dual 4-Input NAND Gate</p> | <p>Diag. 21 14-Pin DIP See Fig. D6 ECG7421, ECG74H21, ECG74LS21</p>  <p>Dual 4-Input AND Gate</p> |
| <p>Diag. 22 14-Pin DIP See Fig. D6 ECG7422, ECG74H22, ECG74LS22, ECG74S22</p>  <p>Dual 4-Input NAND Gate with Open Collector</p> | <p>Diag. 23 18-Pin DIP See Fig. D8 ECG7423</p>  <p>Expandable Dual 4-Input NOR Gate with Open Collector Output</p> | <p>Diag. 24 14-Pin DIP See Fig. D6 ECG7425</p>  <p>Dual 4-Input NOR Gate with Open Collector Output</p> |

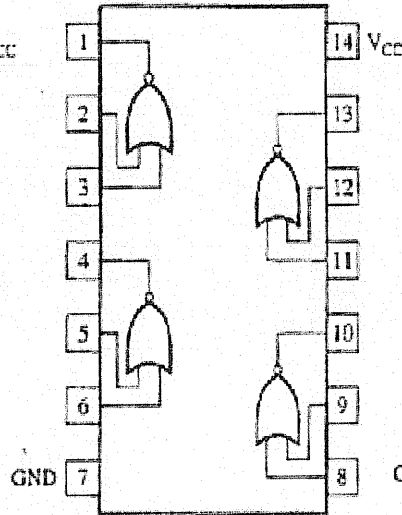
C.1

SELECTED LOGIC AND DISPLAY DEVICES: PIN CONFIGURATION AND LOGIC SYMBOLS

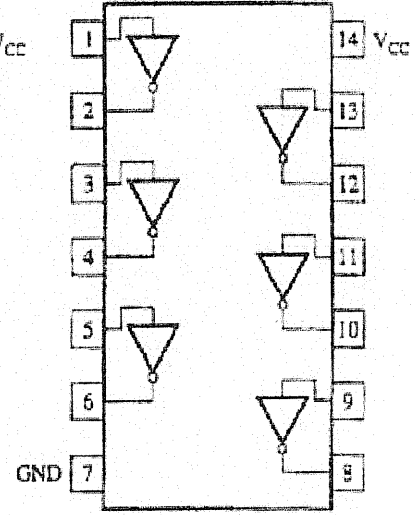
00: Quad Two-Input NAND Gate



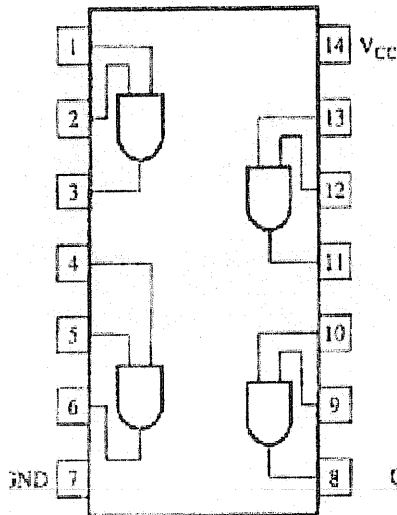
02: Quad Two-Input NOR Gate



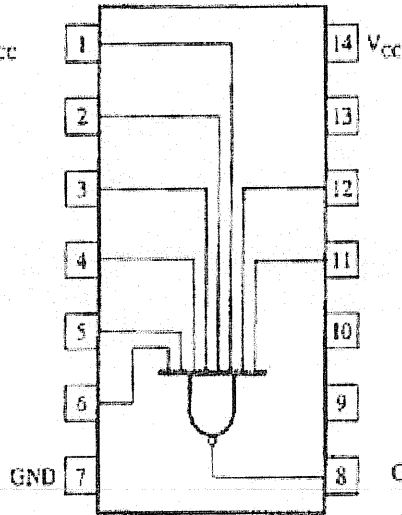
04: Hex Inverter



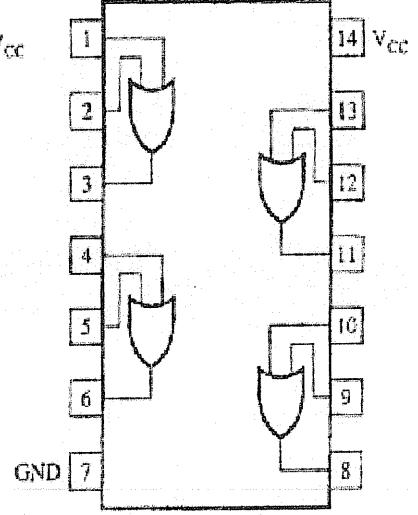
08: Quad Two-Input AND Gate



30: Eight Input NAND Gate



32: Quad Two-Input OR Gate



| TYPE | DEVICE | DESCRIPTION | PIN | CASE |
|--------------|-----------|---|-------|------|
| 2SK 684 | MOS-N-FET | V-MOS, 800V, 7A, 100W, <1,5 (4A) | G D S | |
| 2SK 727 | MOS-N-FET | V-MOS, S-L, 900V, 5A, 125W | G D S | |
| 2SK 792 | MOS-N-FET | V-MOS, 900V, 3A, 100W, <4,5 (1,5A) | G D S | |
| 2SK 812 | MOS-N-FET | V-MOS, S-L, 900V, 5A, 125W, <2,5 (2,5A) | G D S | |
| 2SK 903* | MOS-N-FET | V-MOS, S-L, 800V, 3A, 40W, <4 (1,5A) | G D S | |
| 2SK 1082 | MOS-N-FET | V-MOS, S-Reg, 800V, 6A, 125W, <2,2 (3A) | G D S | |
| 2SK 1083* | MOS-N-FET | V-MOS, LogL, 60V, 8A, 20W, <0,35 (4A) | G D S | |
| 2SK 1117 | MOS-N-FET | V-MOS, S-Reg, 600V, 6A, 100W | G D S | |
| 2SK 1118* | MOS-N-FET | V-MOS, S-Reg, 600V, 6A, 45W | G D S | |
| 2SK 1191* | MOS-N-FET | MOS, 60V, 30A, 40W, <28m (15A) | G D S | |
| 2SK 1398* | MOS-N-FET | V-MOS, 50V, 0,1A, 0,25W, <20 (10mA) | G D S | |
| 2SK 1419 | MOS-N-FET | V-MOS, S-L, 60V, 15A, 25W, <0,08 (10A) | G D S | |
| 2SK 1460* | MOS-N-FET | V-MOS, S-L, 900V, 3,5A, 40W, <3,6 (2A) | G D S | |
| 2SK 1611* | MOS-N-FET | V-MOS, S-L, 800V, 3A, 50W, <4 (2A) | G D S | |
| 2SK 1833* | MOS-N-FET | V-MOS, 500V, 2,5A, 40W, <4 (1,5A) | G D S | |
| 2SK 1940 | MOS-N-FET | V-MOS, 600V, 12A, 125W, <0,75 (6A) | G D S | |
| 2SK 2038 | MOS-N-FET | V-MOS, 800V, 5A, 125W, <2,2 (3A) | G D S | |
| 2SK 2043* | MOS-N-FET | V-MOS, 600V, 2A, 25W, <4,3 (1A) | G D S | |
| 2SK 2129* | MOS-N-FET | V-MOS, 800, 3A, 40W, <4 (2A), 40/140ns | G D S | |
| 2SK 2180 | MOS-N-FET | V-MOS, 500V, 3A, 40W, <2,3 (1,5A) | G D S | |
| 2SK 2183 | MOS-N-FET | V-MOS, 500V, 5A, 50W, <1,5, 55/100ns | G D S | |
| 2SK 2381* | MOS-N-FET | V-MOS, 200V, 5A, 25W, <0,8 (2,5A) | G D S | |
| 2SK 2545 | MOS-N-FET | V-MOS, 600V, 6A, 40W, <1,25 (3A) | G D S | |
| 2SK 2632* | MOS-N-FET | V-MOS, 800V, 2,5A, 25W, <4,8 (1,3A) | G D S | |
| 2SK 2645* | MOS-N-FET | V-MOS, 600V, 9A, 50W, <1,2 (4,5A) | G D S | |
| 2SK 2651* | MOS-N-FET | V-MOS, 900V, 6A, 50W, <2,5 (3A) | G D S | |
| 2SK 2723* | MOS-N-FET | V-MOS, LogL, 60V, 25A, 25W, <60m (13A) | G D S | |
| 2SK 2761* | MOS-N-FET | V-MOS, 600V, 10A, 50W, <1 (4,5A) | G D S | |
| BUK 444-800* | MOS-N-FET | V-MOS, 800V, 1,2, 4A, 25W, <8 | G D S | |
| BUZ 11 | MOS-N-FET | V-MOS, 50V, 30A, 75W, <0,04 (19A) | G D S | |
| BUZ 77 | MOS-N-FET | V-MOS, 600V, 2,7A, 75W, <4 (1,7A) | G D S | |
| BUZ 80A | MOS-N-FET | V-MOS, 800V, 6,1A, 100W, <4 (2A) | G D S | |
| BUZ 80AF | MOS-N-FET | V-MOS, 800V, 2,1A, 40W, <4 (2A) | G D S | |
| BUZ 90A | MOS-N-FET | V-MOS, 600V, 4,5A, 75W, <2 (2,8A) | G D S | |
| BUZ 90AF | MOS-N-FET | V-MOS, 600V, 4,5A, 75W, <1,6 (2,8A) | G D S | |
| BUZ 91AF | MOS-N-FET | V-MOS, 600V, 8,5A, 150W, <0,8 (5A) | G D S | |
| IRF 3205 | MOS-N-FET | V-MOS, 55V, 110A, 200W, <8m (59A) | G D S | |
| IRF 530 | MOS-N-FET | V-MOS, 100V, 14A, 88W, <0,16 (8,4A) | G D S | |
| IRF 540 | MOS-N-FET | V-MOS, 100V, 28A, 150W, <77m (17A) | G D S | |
| IRF 630 | MOS-N-FET | V-MOS, 200V, 9A, 74W, <0,4 (5,4A) | G D S | |
| IRF 634 | MOS-N-FET | V-MOS, 250V, 8,1A, 74W, <0,45 (5,1A) | G D S | |
| IRF 640 | MOS-N-FET | V-MOS, 200V, 18A, 125W, <0,18 (11A) | G D S | |
| IRF 644 | MOS-N-FET | V-MOS, 250V, 14A, 125W, <0,28 (8,4A) | G D S | |
| IRF 650 | MOS-N-FET | V-MOS, 200V, 28A, 156W, <85m (14A) | G D S | |
| IRF 740 | MOS-N-FET | V-MOS, 400V, 10A, 125W, <0,55 (6A) | G D S | |
| IRF 830 | MOS-N-FET | V-MOS, 500V, 4,5A, 74W, <1,5 (2,7A) | G D S | |
| IRF 840 | MOS-N-FET | V-MOS, 500V, 8A, 125W, <0,85 (4,8A) | G D S | |
| IRF 9540 | MOS-P-FET | V-MOS, 100V, 19A, 150W, <0,2 (11A) | G D S | |
| IRF 9620* | MOS-P-FET | V-MOS, 200V, 3,5A, 40W, <1,5 (1,5A) | G D S | |
| RFP50N06 | MOS-N-FET | V-MOS, 50V, 50A, 110W, <22m (50) | G D S | |
| IRFPC 50 | MOS-N-FET | V-MOS, 600V, 11A, 180W, <0,6 (6A) | G D S | |

NEODYMIUM-IRON-BORON

Abbreviated Product Information Sheet

Typical Magnetic and Physical Characteristics

| Material | Residual Induction | | | | Coercivity | | | | Intrinsic Coercivity | | Maximum Energy Product | | | | Temperature Coefficients | | Curie Temp. T _c | Max. Working Temp. °C |
|----------|--------------------|------|------|------|----------------|-------|-----------------|-----|----------------------|-----|------------------------|-----|-------|--------|--------------------------|-------|----------------------------|-----------------------|
| | B _r | | T | | H _c | | H _{ci} | | H _{ci} | | BH _{max} | | α (H) | β (Br) | | | | |
| | Min | Max | Min | Max | Min | Max | Min | Max | Min | Max | Min | Max | %/°C | %/°C | | | | |
| N25 | 11.7 | 12.5 | 1.17 | 1.21 | 10.50 | 11.50 | 100 | 90 | 12 | 95 | 24 | 24 | 36 | 36 | -0.12 | -0.60 | 320 | 100 |
| N28 | 12.2 | 12.6 | 1.21 | 1.26 | 10.00 | 11.50 | 100 | 90 | 12 | 90 | 25 | 26 | 35 | 36 | -0.12 | -0.60 | 320 | 100 |
| N40 | 12.6 | 12.9 | 1.26 | 1.29 | 10.50 | 11.00 | 100 | 90 | 12 | 90 | 26 | 27 | 36 | 36 | -0.12 | -0.60 | 320 | 100 |
| N42 | 12.9 | 13.0 | 1.29 | 1.30 | 11.00 | 12.00 | 90 | 80 | 12 | 95 | 26 | 27 | 36 | 36 | -0.12 | -0.60 | 320 | 100 |
| N45 | 12.5 | 13.1 | 1.25 | 1.31 | 11.00 | 11.00 | 90 | 80 | 12 | 90 | 25 | 26 | 36 | 36 | -0.12 | -0.60 | 320 | 100 |
| N45 M | 11.7 | 12.1 | 1.17 | 1.21 | 10.00 | 11.50 | 100 | 90 | 11 | 115 | 24 | 24 | 35 | 36 | -0.12 | -0.60 | 320 | 100 |
| N46 | 12.2 | 12.6 | 1.22 | 1.26 | 10.00 | 11.50 | 100 | 90 | 11 | 115 | 24 | 24 | 35 | 36 | -0.12 | -0.60 | 320 | 100 |
| N49 | 12.6 | 12.9 | 1.26 | 1.29 | 10.00 | 11.50 | 100 | 90 | 11 | 115 | 24 | 24 | 35 | 36 | -0.12 | -0.60 | 320 | 100 |
| N42 H | 12.8 | 13.3 | 1.28 | 1.33 | 10.00 | 11.00 | 100 | 90 | 11 | 115 | 26 | 26 | 36 | 36 | -0.12 | -0.60 | 320 | 100 |
| N47 H | 13.2 | 13.6 | 1.32 | 1.36 | 10.00 | 10.00 | 100 | 90 | 12 | 105 | 25 | 25 | 36 | 36 | -0.11 | -0.58 | 320-360 | 120 |
| N49 H | 13.6 | 14.2 | 1.36 | 1.42 | 10.00 | 10.00 | 100 | 90 | 12 | 105 | 26 | 26 | 36 | 36 | -0.11 | -0.58 | 320-360 | 120 |
| N43 H | 11.4 | 11.7 | 1.14 | 1.17 | 10.00 | 11.00 | 100 | 90 | 12 | 105 | 24 | 24 | 35 | 36 | -0.11 | -0.58 | 320-360 | 120 |
| N45 H | 11.7 | 12.1 | 1.17 | 1.21 | 10.00 | 11.50 | 100 | 90 | 12 | 105 | 24 | 24 | 35 | 36 | -0.11 | -0.58 | 320-360 | 120 |
| N48 H | 12.2 | 12.6 | 1.22 | 1.26 | 11.50 | 12.00 | 90 | 80 | 12 | 105 | 25 | 25 | 36 | 36 | -0.11 | -0.58 | 320-360 | 120 |
| N49 H | 12.6 | 12.9 | 1.26 | 1.29 | 11.50 | 12.00 | 90 | 80 | 12 | 105 | 25 | 25 | 36 | 36 | -0.11 | -0.58 | 320-360 | 120 |
| N42 H | 12.9 | 13.0 | 1.29 | 1.30 | 11.50 | 12.00 | 90 | 80 | 12 | 105 | 26 | 26 | 36 | 36 | -0.11 | -0.58 | 320-360 | 120 |
| N43 SH | 11.4 | 11.7 | 1.14 | 1.17 | 10.50 | 11.00 | 100 | 90 | 21 | 100 | 24 | 24 | 35 | 36 | -0.11 | -0.55 | 340-360 | 150 |
| N45 SH | 11.7 | 12.1 | 1.17 | 1.21 | 10.50 | 11.50 | 100 | 90 | 20 | 100 | 24 | 24 | 35 | 36 | -0.11 | -0.55 | 340-360 | 150 |
| N46 SH | 12.2 | 12.6 | 1.22 | 1.26 | 11.50 | 12.00 | 90 | 80 | 20 | 100 | 25 | 25 | 36 | 36 | -0.11 | -0.55 | 340-360 | 150 |
| N47 SH | 13.0 | 13.2 | 1.30 | 1.32 | 10.00 | 10.00 | 100 | 90 | 21 | 100 | 25 | 25 | 36 | 36 | -0.11 | -0.51 | 360 | 160 |
| N49 SH | 13.0 | 13.2 | 1.30 | 1.32 | 10.00 | 10.00 | 100 | 90 | 21 | 100 | 25 | 25 | 36 | 36 | -0.11 | -0.51 | 360 | 160 |
| N42 SH | 11.4 | 11.7 | 1.14 | 1.17 | 10.50 | 11.00 | 100 | 90 | 20 | 100 | 24 | 24 | 35 | 36 | -0.11 | -0.51 | 360 | 160 |

LH
PB

Coatings and Corrosion Resistance

| Coating | ISO 9001 Part 2 | ISO 9001 Part 1 |
|----------------------|-----------------|-----------------|
| Corrosion Resistance | Ex | Ex-1 |
| Color | Black | |
| Thickness, microns | 20-30 | |

ISO 9001 Part 2
ISO 9001 Part 1

Coatings listed here are typical and will vary depending upon size and shape of the magnet. For more information, please contact Arnold at the location below or your local Arnold Salesperson.

Physical Characteristics

| Characteristic | Symbol | Unit | Value |
|----------------------------------|----------------|----------------------|-------|
| Density | ρ | g/cm ³ | 7.5 |
| Rockwell Hardness | H _R | H _R | 50H |
| Compressive Strength | σ _c | N/mm ² | 200 |
| Coefficient of Thermal Expansion | α _p | 10 ⁻⁶ /°C | 11 |
| Electrical Resistance | R | Ω-cm | 100 |

Max. Working Temperature

| | |
|--------------------|---------------|
| Temperature (°C) | 100 |
| Max. Working Temp. | 100°C - 160°C |
| | 100°C - 160°C |
| | 100°C - 160°C |
| | 100°C - 160°C |



MAGNETIC TECHNOLOGIES CORPORATION

770 Linden Avenue, Rochester, NY 14625-2764 USA

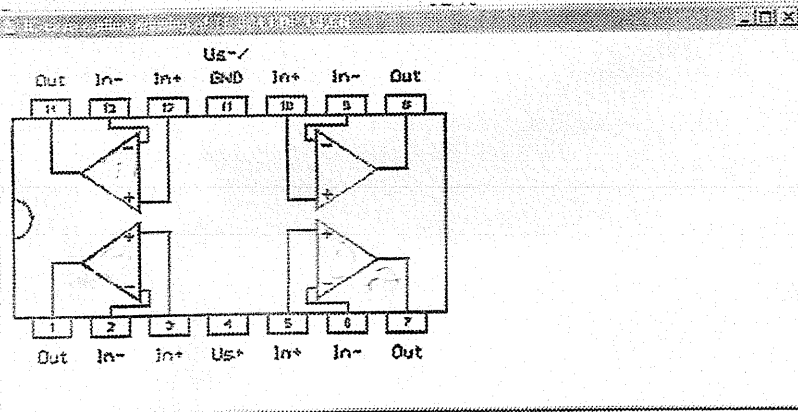
Phone: (1-813) 535-5010 • Toll free: 800-533-9127

Fax: (1-813) 535-3017

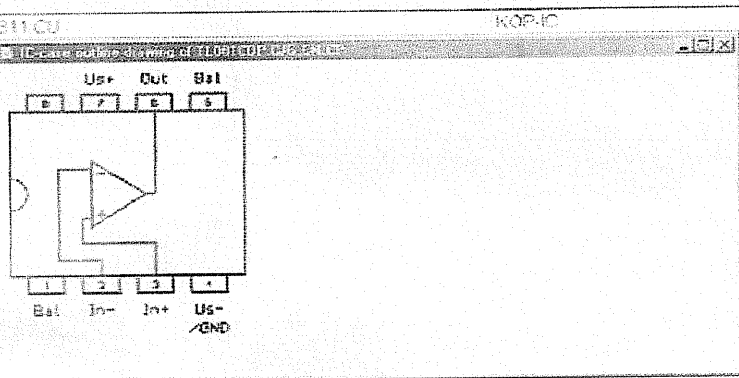
www.arnoldmagnetics.com

© 2004 Magneta Technologies Corporation

| | |
|---------------|---------|
| TL 081 084 DJ | |
| TL 081 084 ME | |
| TL 081 084 MF | |
| TL 081 084 CF | |
| TL 082 C | |
| TL 083 CJ, CN | |
| TL 083 CN | |
| TL 087 | |
| TL 088 CD | |
| TL 088 CJ, CF | |
| TL 088 I | |
| TL 088 M | |
| TL 088 MU | |
| TL 094 CDP | |
| TL 094 CFP | |
| TL 136 CD | OP-IC |
| TL 136 CJ, CN | OP-IC |
| TL 1525 A. | LINE-IC |
| TL 1527 A. | LINE-IC |
| TL 1555 P | LINE-IC |



| | |
|---------------|---------|
| TL 911 CU | KOP-IC |
| TL 994 ORP | OP-IC |
| TL 136 CD | OP-IC |
| TL 136 CJ, CN | OP-IC |
| TL 1525 A. | LINE-IC |



Appendix (D)

Software Program

control

Speed

Number of pulses

Alpha

```
function ba(a,b,c,sp,d,alpha)
global cont ln1 ln2 ln3 ln4;
dio12 = digitalio('parallel','LPT1');
addline(dio12,0:3,0,'out');
fr=a;
s=b;
c=0;
speed=sp;
%-----
if(fr==0&s==0&c==0)
bvdata = logical([1 0 0 0]);
putvalue(dio12,bvdata);
ln1=1;
ln2=0;
ln3=0;
ln4=0;
hline(1,speed,d,alpha);
end
%-----
if(fr==0&s==1&c==0)
bvdata = logical([0 0 1 0]);
putvalue(dio12,bvdata);
ln1=0;
ln2=0;
ln3=1;
ln4=0;
hline(2,speed,d,alpha);

end
%-----
if(fr==1&s==0&c==0)
bvdata = logical([0 1 0 0]);
putvalue(dio12,bvdata);

ln1=0;
ln2=1;
ln3=0;
ln4=0;
hline(2,speed,d,alpha);
end
%-----
if(fr==1&s==1&c==0)
bvdata = logical([0 0 0 1]);
putvalue(dio12,bvdata);
ln1=0;
ln2=0;
ln3=0;
ln4=1;
hline(1,speed,d,alpha);
end
%-----
```

```
dio = digitalio('parallel','LPT1');  
addline(dio,2,1,'in');  
b = getvalue(dio.Line(1))  
dio = digitalio('parallel','LPT1');  
addline(dio,4:5,0,'out');  
putvalue(dio,[0 0]);  
if b==1  
dio = digitalio('parallel','LPT1');  
addline(dio,4,0,'out');  
putvalue(dio,1);  
else  
dio = digitalio('parallel','LPT1');  
addline(dio,5,0,'out');  
putvalue(dio,1);  
end
```

b=1

```
dio2 = digitalio('parallel','LPT1');  
addline(dio2,{0,1,2,3,8},0,'out');  
bvdata = logical([b]);  
putvalue(dio2.line(2),bvdata);  
%putvalue(dio2.line(),bvdata);
```

b=1

```
dio2 = digitalio('parallel','LPT1');  
addline(dio2,{0,1,2,3,8},0,'out');  
bvdata = logical([b]);  
putvalue(dio2.line(2),bvdata);  
%putvalue(dio2.line(),bvdata);
```

```
function varargout = control(varargin)
global cont;
cont=1;
% CONTROL M-file for control.fig
%     CONTROL, by itself, creates a new CONTROL or raises the existing
%     singleton*.
%
%     H = CONTROL returns the handle to a new CONTROL or the handle to
%     the existing singleton*.
%
%     CONTROL('CALLBACK',hObject,eventData,handles,...) calls the local
%     function named CALLBACK in CONTROL.M with the given input arguments.
%
%     CONTROL('Property','Value',...) creates a new CONTROL or raises the
%     existing singleton*. Starting from the left, property value pairs are
%     applied to the GUI before control_OpeningFunction gets called. An
%     unrecognized property name or invalid value makes property application
%     stop. All inputs are passed to control_OpeningFcn via varargin.
%
%     *See GUI Options on GUIDE's Tools menu. Choose "GUI allows only one
%     instance to run (singleton)".
%
% See also: GUIDE, GUIDATA, GUIHANDLES

% Edit the above text to modify the response to help control

% Last Modified by GUIDE v2.5 08-Mar-1999 12:28:48

% Begin initialization code - DO NOT EDIT
gui_Singleton = 1;
gui_State = struct('gui_Name',       mfilename, ...
                  'gui_Singleton',  gui_Singleton, ...
                  'gui_OpeningFcn', @control_OpeningFcn, ...
                  'gui_OutputFcn',  @control_OutputFcn, ...
                  'gui_LayoutFcn',  [], ...
                  'gui_Callback',   []);
if nargin & isstr(varargin{1})
    gui_State.gui_Callback = str2func(varargin{1});
end

if nargout
    [varargout{1:nargout}] = gui_mainfcn(gui_State, varargin{:});
else
    gui_mainfcn(gui_State, varargin{:});
end
% End initialization code - DO NOT EDIT

% --- Executes just before control is made visible.
function control_OpeningFcn(hObject, eventdata, handles, varargin)
% This function has no output args, see OutputFcn.
% hObject    handle to figure
% eventdata  reserved - to be defined in a future version of MATLAB
% handles    structure with handles and user data (see GUIDATA)
% varargin   command line arguments to control (see VARARGIN)

% Choose default command line output for control
handles.output = hObject;

% Update handles structure
guidata(hObject, handles);
```

```
% UIWAIT makes control wait for user response (see UIRESUME)
% uiwait(handles.figure1);
```

```
% --- Outputs from this function are returned to the command line.
function varargout = control_OutputFcn(hObject, eventdata, handles)
% varargout cell array for returning output args (see VARARGOUT);
% hObject handle to figure
% eventdata reserved - to be defined in a future version of MATLAB
% handles structure with handles and user data (see GUIDATA)
```

```
% Get default command line output from handles structure
varargout{1} = handles.output;
```

```
% --- Executes on button press in pushbutton1.
function pushbutton1_Callback(hObject, eventdata, handles)
% hObject handle to pushbutton1 (see GCBO)
% eventdata reserved - to be defined in a future version of MATLAB
% handles structure with handles and user data (see GUIDATA)
global cont;
cont=1;
```

```
% --- Executes on button press in pushbutton2.
function pushbutton2_Callback(hObject, eventdata, handles)
% hObject handle to pushbutton2 (see GCBO)
% eventdata reserved - to be defined in a future version of MATLAB
% handles structure with handles and user data (see GUIDATA)
global cont;
```

```
cont=0;
```

```
% --- Executes during object creation, after setting all properties.
function figure1_CreateFcn(hObject, eventdata, handles)
% hObject handle to figure1 (see GCBO)
% eventdata reserved - to be defined in a future version of MATLAB
% handles empty - handles not created until after all CreateFcns called
```

```
% --- Executes on mouse press over figure background.
function figure1_ButtonDownFcn(hObject, eventdata, handles)
% hObject handle to figure1 (see GCBO)
% eventdata reserved - to be defined in a future version of MATLAB
% handles structure with handles and user data (see GUIDATA)
```

```
% --- Executes on button press in pushbutton3.
function pushbutton3_Callback(hObject, eventdata, handles)
% hObject handle to pushbutton3 (see GCBO)
% eventdata reserved - to be defined in a future version of MATLAB
% handles structure with handles and user data (see GUIDATA)
```

```
global user_string user_string1 user_string2;
a=str2num(user_string);
b=str2num(user_string1);
c=str2num(user_string2);
set(0,'RecursionLimit',2.1478e+009);
motor(a,b,c);
```

% --- Executes during object creation, after setting all properties.

```
function edit2_CreateFcn(hObject, eventdata, handles)
% hObject    handle to edit2 (see GCBO)
% eventdata  reserved - to be defined in a future version of MATLAB
% handles    empty - handles not created until after all CreateFcns called

% Hint: edit controls usually have a white background on Windows.
% See ISPC and COMPUTER.
if ispc
    set(hObject,'BackgroundColor','white');
else
    set(hObject,'BackgroundColor',get(0,'defaultUicontrolBackgroundColor'));
end
```

```
function edit2_Callback(hObject, eventdata, handles)
% hObject    handle to edit2 (see GCBO)
% eventdata  reserved - to be defined in a future version of MATLAB
% handles    structure with handles and user data (see GUIDATA)

% Hints: get(hObject,'String') returns contents of edit2 as text
% str2double(get(hObject,'String')) returns contents of edit2 as a double
```

```
global user_string;
user_string = get(hObject,'string');
```

% --- Executes during object creation, after setting all properties.

```
function edit3_CreateFcn(hObject, eventdata, handles)
% hObject    handle to edit3 (see GCBO)
% eventdata  reserved - to be defined in a future version of MATLAB
% handles    empty - handles not created until after all CreateFcns called

% Hint: edit controls usually have a white background on Windows.
% See ISPC and COMPUTER.
if ispc
    set(hObject,'BackgroundColor','white');
else
    set(hObject,'BackgroundColor',get(0,'defaultUicontrolBackgroundColor'));
end
```

```
function edit3_Callback(hObject, eventdata, handles)
% hObject    handle to edit3 (see GCBO)
% eventdata  reserved - to be defined in a future version of MATLAB
% handles    structure with handles and user data (see GUIDATA)

% Hints: get(hObject,'String') returns contents of edit3 as text
% str2double(get(hObject,'String')) returns contents of edit3 as a double
```

```
global user_string1;
user_string1 = get(hObject,'string');
```

% --- Executes during object creation, after setting all properties.

```
function edit4_CreateFcn(hObject, eventdata, handles)
% hObject    handle to edit4 (see GCBO)
% eventdata  reserved - to be defined in a future version of MATLAB
% handles    empty - handles not created until after all CreateFcns called
```

% Hint: edit controls usually have a white background on Windows.

```
% See ISPC and COMPUTER.
if ispc
    set(hObject,'BackgroundColor','white');
else
    set(hObject,'BackgroundColor',get(0,'defaultUicontrolBackgroundColor'));
end

function edit4_Callback(hObject, eventdata, handles)
% hObject handle to edit4 (see GCBO)
% eventdata reserved - to be defined in a future version of MATLAB
% handles structure with handles and user data (see GUIDATA)
global user_string2;
user_string2 = get(hObject,'string');
% Hints: get(hObject,'String') returns contents of edit4 as text
% str2double(get(hObject,'String')) returns contents of edit4 as a double

% --- Executes on button press in pushbutton4.
function pushbutton4_Callback(hObject, eventdata, handles)
% hObject handle to pushbutton4 (see GCBO)
% eventdata reserved - to be defined in a future version of MATLAB
% handles structure with handles and user data (see GUIDATA)
global right ;

right=0;

% --- Executes on button press in pushbutton5.
function pushbutton5_Callback(hObject, eventdata, handles)
% hObject handle to pushbutton5 (see GCBO)
% eventdata reserved - to be defined in a future version of MATLAB
% handles structure with handles and user data (see GUIDATA)
global right;
right=1;

% --- If Enable == 'on', executes on mouse press in 5 pixel border.
% --- Otherwise, executes on mouse press in 5 pixel border or over pushbutton2.
function pushbutton2_ButtonDownFcn(hObject, eventdata, handles)
% hObject handle to pushbutton2 (see GCBO)
% eventdata reserved - to be defined in a future version of MATLAB
% handles structure with handles and user data (see GUIDATA)
```

```
dio = digitalio('parallel', 'LPT1');  
addline(dio, 0:3, 0, 'out');  
s=2  
a=dec2bin(s);  
%bvdata = logical(a);  
putvalue(dio, a)
```

```
function hline1(ch,speed,d,alpha)
global cont user_string user_string1 user_string2 ln1 ln2 ln3 ln4;
%-----
if ch==1
dio = digitalio('parallel','LPT1');
addline(dio,0:4,0,'out');
putvalue(dio.line(2),ln2);
putvalue(dio.line(1),ln1);
putvalue(dio.line(3),ln3);
putvalue(dio.line(4),ln4);
f=speed*2/120;
Tt=1/f;
t=0:0.001:Tt;
tn=Tt/d;
%-----
%x=sin(2*pi*f*t);
%-----
ti=0;
talpha=Tt*alpha/360;
n=0;
b=0;
while (ti<talpha & (n<length(t)))
n=n+1;
x=sin(2*pi*f*t(n)*n);
del=tn*x/1000;
putvalue(dio.line(5),b);
pause(del);
b=bitcmp(b,1);

putvalue(dio.line(5),b);
pause(del);
b=bitcmp(b,1);
ti=ti+(2*del);
end
n=n+1;
tx=Tt/2-2*talpha;
b=1;
putvalue(dio.line(5),b);

pause(tx);
b=0;

while (ti<talpha & (n<length(t)))
n=n+1;
x=sin(2*pi*f*t(n)*n);
del=tn*x/1000;
putvalue(dio.line(5),b);

pause(del);
b=bitcmp(b,1);
putvalue(dio.line(5),b);

pause(del);
b=bitcmp(b,1);
ti=ti+(2*del);
end
%td=t*d/180;
%tt=t-2*td;
%talpha=(t * alpha )/180;
%n=talpha/td;
```

```
%for s=1:n
%putvalue(dio,b);
%pause(td);
%b=bitcmp(b,1);
%putvalue(dio,b);
%pause(td);
%b=bitcmp(b,1);
%end
```

```
%for s=1:n
%putvalue(dio,b);
%pause(td);
%b=bitcmp(b,1);
%putvalue(dio,b);
%pause(td);
%b=bitcmp(b,1);
%end
end
```

```
%-----
```

```
if ch==2
dio = digitalio('parallel','LPT1');
addline(dio,0:5,0,'out');
putvalue(dio.line(2),ln2);
putvalue(dio.line(1),ln1);
putvalue(dio.line(3),ln3);
putvalue(dio.line(4),ln4);
hj=0;
putvalue(dio.line(5),hj);
f=speed*2/120;
Tt=1/f;
t=0:0.001:Tt;
tn=Tt/d;
%plo(length(t))=0;
%-----
%x=sin(2*pi*f*t);
%-----
ti=0;
talpha=Tt*alpha/360;
n=0;
b=0;
while (ti<talpha & (n<length(t)))

n=n+1;

x=sin(2*pi*f*t(n)*n);
del=tn*x;
putvalue(dio.line(6),b);

pause(del);
b=bitcmp(b,1);
putvalue(dio.line(6),b);

pause(del);
b=bitcmp(b,1);
ti=ti+(2*del);
end
tx=Tt/2-2*talpha;
b=1;
putvalue(dio.line(6),b);
```

```
pause(tx);  
b=0;  
n=n+1;  
while (ti<talpha & (n<length(t)))  
n=n+1;
```

```
x=sin(2*pi*f*t(n)*n);  
del=tn*x;  
putvalue(dio.line(6),b);
```

```
pause(del);  
b=bitcmp(b,1);  
putvalue(dio.line(6),b);
```

```
pause(del);  
b=bitcmp(b,1);  
ti=ti+(2*del);  
end  
%td=t*d/180;  
%tt=t-2*td;  
%talpha=(t * alpha )/180;  
%n=talpa/td;
```

```
%for s=1:n  
%putvalue(dio,b);  
%pause(td);  
%b=bitcmp(b,1);  
%putvalue(dio,b);  
%pause(td);  
%b=bitcmp(b,1);  
%end
```

```
%for s=1:n  
%putvalue(dio,b);  
%pause(td);  
%b=bitcmp(b,1);  
%putvalue(dio,b);  
%pause(td);  
%b=bitcmp(b,1);  
%end  
end  
a=str2num(user_string);  
b=str2num(user_string1);  
c=str2num(user_string2);  
motor(a,b,c);
```

```
function motor(speed,d,alpha)
global right cont rl sen1 ln1 ln2 ln3 ln4;
if(cont==1)
dio = digitalio('parallel','LPT1');
addline(dio,2,1,'in');
if right==1
a =1;
else
a=0;
end
rl=a;
c=0;

b = getvalue(dio.Line(1));
sen1=b;
%c = getvalue(dio.Line(3));
ba(a,b,c,speed,d,alpha);

end
dio = digitalio('parallel','LPT1');
addline(dio,0:5,0,'out');
bvdata = logical([0 0 0 0 0 0]);
putvalue(dio,bvdata);
```

C++ Program

```

#include<dos.h#
#include<stdio.h#
#include<conio.h#
#include <math.h#
define b 0x378#
define in 0x379#
define PI 3.142857#
define dela 1000#

()void main
}
;int i=0x00,e
;float angle,fs,Tt,xt,tp,delt,dell
;int speed,puls
;char dr
:begin
;outport(b,0x00
;clrscr
;(:printf("Enter the speed
;scanf("%d",&speed
;(:printf("Enter the No of pulses
;scanf("%d",&puls
;(:printf("Enter angle
;scanf("%f",&angle
;(:[printf("Enter direction [L,R
;dr=getchar
;scanf("%c",&dr

;fs=speed*2.0/120
;Tt=1.0/fs
;tp=Tt/puls
;(xt=sin(2*PI*fs*Tt

} (;)for
;(i=inport(in
;if(((i&0x10)>>4)==0)goto begin
(switch(dr
}
:'case 'r
:'case 'R

(if(((i&0x20)>>5)==0
}
(++for(e=1;e<=puls;e
}
;outport(b,0x18
;delt=1.0*tp*xt
;(delay(dela*delt/2
;outport(b,0x08
;(delay(dela*delt/2
{
;outport(b,0x18
;(delay(dela*(Tt/2-2*Tt*angle/360
(--for(e=puls-1;e>=1;e
}
;outport(b,0x08
;delt=1.0*tp*xt
;(delay(dela*delt/2
;outport(b,0x18
;(delay(dela*delt/2
{
{
else
}
}
(++for(e=1;e<=puls;e
}

```

Eynass

```
        ;(outport(b,0x22
        ;delt=1.0*tp*xt
        ;(delay(de1a*delt/2
        ;(outport(b,0x02
        ;(delay(de1a*delt/2
        {
        ;(outport(b,0x22
;((delay(de1a*(Tt/2-2*Tt*angle/360
(--for(e=puls-1;e>=1;e
        }
        ;(outport(b,0x02
        ;delt=1.0*tp*xt
        ;(delay(de1a*delt/2
        ;(outport(b,0x22
        ;(delay(de1a*delt/2
        {
        {
        ;break
        :'case '1
        :'case 'L
        (if(((i&0x20)>>5)==0
        }
        (++for(e=1;e<=puls;e
        }
        ;(outport(b,0x24
        ;delt=1.0*tp*xt
        ;(delay(de1a*delt/2
        ;(outport(b,0x04
        ;(delay(de1a*delt/2
        {
        ;(outport(b,0x24
;((delay(de1a*(Tt/2-2*Tt*angle/360
(--for(e=puls-1;e>=1;e
        }
        ;(outport(b,0x04
        ;delt=1.0*tp*xt
        ;(delay(de1a*delt/2
        ;(outport(b,0x24
        ;(delay(de1a*delt/2
        {
        {
        else
        }
        }
        (++for(e=1;e<=puls;e
        }
        }
        ;(outport(b,0x11
        ;delt=1.0*tp*xt
        ;(delay(de1a*delt/2
        ;(outport(b,0x01
        ;(delay(de1a*delt/2
        {
        ;(outport(b,0x11
;((delay(de1a*(Tt/2-2*Tt*angle/360
(--for(e=puls-1;e>=1;e
        }
        ;(outport(b,0x01
        ;delt=1.0*tp*xt
        ;(delay(de1a*delt/2
        ;(outport(b,0x11
        ;(delay(de1a*delt/2
        {
        {
        ;break
        }
```

Simulation Program

```
% SPMTOT
%-----
clc ;
% Np=Fc-F1/2F1 OR Np=Fc/2F1
% F1=50 HZ
% Np number of pulses per half cycle
N_rt=2; % number of rotor teeth
N_LT=2; % number of harmonics

NP=1;nx=0;
N_ffti=1024;

speed=1500 ; p=4;
f1=p.*speed/120;
Fc=25000; % 5 kHz
% Fc=input(' The commutating frequency=' );
NP=Fc/(2*f1);
NC=60;
N_wd=4;

% N_wd=input(' The pulse step width=' );
N_wd_dg=input('The PWM duration at end sides, dg=' );
N_wd=180/N_wd_dg;

%S=input('Press a key....');

NM=1;
AMF=1.0*NM;
NS=2*NP;
TOL=0.001;
w=2*pi*f1;
t_f=1000/f1; % in ms
for M=1:1:NS
SL(M) = ((-1)^M) * (N_wd*(NS+1)/pi);
end

for M=1:2:NS
C(M) =M+1;
end

for M=2:2:NS
C(M) =-M;
end

NAT=2*NS+2;
NPT=NAT/2;
Y(1)=AMF;
X(1)=pi/2;

for M=1:1:NS
for I=1:NC
K=I+1;
X(K)=(Y(I)-C(M))/SL(M);
Y(K)=AMF*sin(X(K));
XX=abs(X(K)-Y(K-1));
if XX <=TOL I=NC; end

end% while
ALFA(M)=X(I);
end%M
```

```
ALFA(NS+1)=pi/N_wd;
ALFA(NS+2)=pi-pi/N_wd;

NAS=NS+1;
for M=NAS:1:NAT
    J=NAT-M+1 ;
    ALFA(M)=pi-ALFA(J);
end
Nq=1;
for M=1:1:NPT
    d=ALFA(M)*180/pi;
    d=d;
    % S=input('Press a key ');
end
%==9999=====
for M=1:1:2*NPT
    % clc;
    if M < NPT
        ALFAM(M)=ALFA(2*M-1);
        DELTAM(M)=ALFA(2*M)-ALFA(2*M-1);
        ALFAD(M)=ALFAM(M)*180/pi;
        DELTAD(M)=DELTAM(M)*180/pi;

    elseif M==NPT
        ALFAM(M)=pi;
        DELTAM(M)=pi-ALFA(2*M-1);
        ALFAD(M)=ALFAM(M)*180/pi;
        DELTAD(M)=DELTAM(M)*180/pi;
        % NPT=NPT+1;
    else
        ALFAM(M)=pi+ALFAM(M-NPT);
        DELTAM(M)=DELTAM(M-NPT);
        ALFAD(M)=ALFAM(M)*180/pi;
        DELTAD(M)=DELTAM(M)*180/pi;
    end %if
    ALFAD(M);
    Nq=Nq+1;
    % S=input('Press a key A');
end

%====9999=====
NQT=Nq-1;
Q=[ALFAD;DELTAD];
fid =fopen('PWM2_DG.M','w');
fprintf(fid,'%12.8f %10.5f\n',Q);
fclose(fid);

% S=input('Press a key....');

%===== Fourrier coefficients and rms voltage
Vs=1; Xh=0; Bh=0;
N_h=10 ;
for N=1:2:N_h
    Ah=0; Bh=0;sum_N=0;X_t=0;

    for M=1:1:NPT/2-1
        Xh=sin(N*(ALFAM(M)+DELTAM(M)/2))-sin(N*(pi+ALFAM(M)+DELTAM(M)/2));
        Bh=Xh*sin(N*DELTAM(M)/2)+Bh;
        Yh=cos(N*(ALFAM(M)+DELTAM(M)/2))-cos(N*(pi+ALFAM(M)+DELTAM(M)/2));
```

```

        Ah=Yh*cos(N*DELTAM(M)/2)+Ah;
        X_t= (-1)^(M+1)*cos(N*ALFAM(M));
        sum_N=sum_N+X_t;
    end% M
        An(N)=(2*Vs/(N*pi))*Ah;
        Bn(N)=(2*Vs/(N*pi))*Bh;
        Vo(N)=sqrt(An(N)^2+Bn(N)^2)/sqrt(2);
        Ho(N)=N;
        A_n(N)=4*sum_N/(N*pi);
    end%N
%=====Harmonic files
Q1=[Ho;A_n;Vo];
fid =fopen('PWM2_VL.M','w');
fprintf(fid,' %7.3f          %12.8f          %10.5f\n',Q1);
fclose(fid);

%=====Modulation files h(wt)
clc;
NT=100 ;sum_N=0;
t=0.0:(t_f/(1000*NT)):t_f/1000;
    for i=1:1:NT
        wt=w*t; sum_N=0;
    for N=1:2:N_h
        X_t=A_n(N)*sin(N*wt);
        sum_N=sum_N+X_t;
    end%N
        H =sum_N;
        XX=wt*180/pi;
    end%wt
%=====H(wt) file
% S=input('Press a key....');
Q2=[XX;H];
fid =fopen('H_wt.M','w');
fprintf(fid,'%12.8f          %10.5f\n',Q2);
fclose(fid);

%=====Harmonic spectrume=====
% Plot the Vo(n) curves

% for i=1:1:N_h
% bar(Ho,Vo);%,'color','B','linewidth',0.3,'linestyle','-');
% end
% xlabel('Harmonic ,-', 'fontweight','Bold');
% ylabel('RMS Voltage,%', 'fontweight','Bold');
% title(' Output Voltage ', 'Fontweight','Bold');
% legend('with curent -harmonic spectrum');
% grid on;
% hold on

%=====Integrating the phase current =====
N_st=30;
%Vd=50; Em=40; L1=0.007; R=2;
Vd=12; Em=0.90*Vd; L1=0.0080; R=0.5;
epsi=0.005;
del_i=0.02;
L=w*L1;
Ia2=0; Io=0; Ia1=0;
ps_s1=atan(L/R);
Lo=L;
L2m=L/3; %Lo/2;
ps_s1=atan(Lo/R);
    
```

```
Lh1(1)=2; Lt(1)=L2m;  
Lh1(2)=4; Lt(2)=L2m/4;  
Lh1(3)=6; Lt(3)=L2m/6;  
Lh1(4)=8; Lt(4)=L2m/8;  
Lh1(5)=10; Lt(5)=L2m/10;  
Lh1(6)=12; Lt(6)=L2m/12;
```

```
while del_i>=epsi  
    ju=1;  
    for M=1:1:NQT-1  
        M=M;  
        da=(ALFAM(M+1)-ALFAM(M))/N_st;  
        dal=ALFAM(M)+DELTAM(M);  
        for j=1:1:N_st  
            all=ALFAM(M)+(j-1)*da;  
            al2=all+da;  
            if al2<=pi Vsx=Vd; else Vsx=-Vd; end  
            if all <=dal Vs=Vsx;else Vs=0; end  
  
            U1(ju)=Vs;  
            ALFU(ju)=all*180/pi;  
            E1=Em*sin(all);  
            E2=Em*sin(al2);  
            Vx_A1=Vs-E1;  
            Vx_A2=Vs-E2;  
            %==L(a)=====  
            sum_A1=0;sum_A2=0;sum_Ad1=0;sum_Ad2=0;  
            L_A1=0; L_A2=0; L_Ad1=0;L_Ad2=0;  
  
            for il=1:1:N_LT  
                X_A1=Lt(il)*cos(N_rt*all);  
                X_A2=Lt(il)*cos(N_rt*al2);  
                X_Ad1=Lt(il)*N_rt*sin(N_rt*all);  
                X_Ad2=Lt(il)*N_rt*sin(N_rt*al2);  
  
                sum_A1=sum_A1+X_A1;  
                sum_A2=sum_A2+X_A2;  
                sum_Ad1=sum_Ad1+X_Ad1;  
                sum_Ad2=sum_Ad2+X_Ad2;  
  
            end  
            L_A1=Lo+sum_A1;  
            L_A2=Lo+sum_A2;  
            L_Ad1=sum_Ad1;  
            L_Ad2=sum_Ad2;  
            %=====  
            X1=(L_Ad1-R)/L_A1;  
            X2=(L_Ad2-R)/L_A2;  
            X3=Vx_A1/L_A1+Vx_A2/L_A2;  
            Y1=1+X1.*da/2;  
            Y2=X3.*da/2;  
            Y3=1-X2.*da/2;  
            Ia2=Ia1*(Y1/Y3)+Y2/Y3;  
            Ia1=Ia2;  
            IU(ju)=Ia2;  
  
        ju=ju+1;  
    end %J
```

```

        ALFX(M)=al2*180/pi;
        I1X(M)=Ia2;
    end% M
    del_i=abs(Ia1-Io);
    Io=Ia1;
    del_i=del_i;
end % while
N_pu=ju-2;
% [ ALFU,U1];
N_pu=N_pu;
S=input('Press a key... ');
clc;
%=====
% Q3=[ALFX;I1X];
% fid =fopen('Current.M','w');
% fprintf(fid,'%12.8f          %10.5f\n',Q3);
% fclose(fid);
%=====
% Q6=[ALFU;U1];
% fid =fopen('Pulses.M','w');
% fprintf(fid,'%12.8f          %10.5f\n',Q6);
% fclose(fid);
%=====
% Q7=[ALFU;IU];
% fid =fopen('Cur_ext.M','w');
% fprintf(fid,'%12.8f          %10.5f\n',Q7);
% fclose(fid);

%=====Time_harmonic domain h(wt)=====
% Plot the Vo(n) curves

    if ALFU == 360 quit; else
        plot(ALFU ,IU , 'color','B','linewidth',1.5,'linestyle','- ');
    end

    xlabel('Alfa ,dg','fontweight','Bold');
    ylabel('Current,A','fontweight','Bold') ;
    title(' Phase current ', 'Fontweight','Bold');
% legend('with curent -harmonic spectrum');
grid on;
hold on;
pause;
hold off;
S=input('Press a key.... ');

%=====
% Plot the Vo(n) curves

for i=1:1:NT-nx
plot(XX,H , 'color','B','linewidth',1.0,'linestyle','- ');
end
    xlabel('Harmonic ,-', 'fontweight','Bold');
    ylabel('RMS Voltage,%','fontweight','Bold') ;
    title(' Output Voltage ', 'Fontweight','Bold');
% legend('with curent -harmonic spectrum');
grid on;
hold on;
pause;
hold off;
%=====
% Plot the Vs(n) curves
    
```

```

if ALFU == 360 quit; else
    plot(ALFU,U1 , 'color','R', 'linewidth',0.5, 'linestyle','-' );
end
    xlabel('Alfa,dg','fontweight','Bold');
    ylabel('Pulse Voltage,V','fontweight','Bold') ;
    title(' P W M ', 'Fontweight','Bold');
% legend('with curent -harmonic spectrum');
grid on;
hold on;
pause;
hold off;

%=====START F F T - Current=====
clc;
    t=ALFX.*pi/(w*180);
    x_i=I1X;

% plot(Alf,y);
    Y_i=fft(x_i,N_ffti);

    for ji=1:1:(N_ffti/2);
        Ha=real(Y_i(ji));
        Hr=imag(Y_i(ji));
        Hq=sqrt(Ha^2+Hr^2);
        % psi=ANGLE(Y_i(ji));
        % psi=psi*180/pi;
        psi=atan(Hr/Ha);

%   psi=psi'
%   S=input('Press a key....');

        N_hi(ji)=ji-1 ;
        if ji==1 Hi(ji)=Hq*1/N_ffti; else
            Hi(ji)=Hq*2/N_ffti;
        end
        % N_hi(ji)=ji-1 ;
        psi_i(ji)=psi;
        if Hi(ji)<0.0 Hi(ji)=0.0; end
    end
    [N_hi, Hi, psi_i]'

    ppyl=0;
    ppyl=Hi.*conj(Hi)/N_ffti;
    % ppyl=ppy1,
    % f=((1000*(0:(N/2)-1))/N)*2 ;
    % f=((1000*(0:(N/2)-1))/N)*2 ;

%   plot(f,ppy1(1:N/2));
    plot(N_hi(1:N_ffti/2),Hi(1:N_ffti/2));
    %   plot(f,Hi(1:N/2));

hold on;
hold off;

Q4=[N_hi;Hi;psi_i];
fid =fopen('Cur_har.M','w');
fprintf(fid,'%12.8f          %10.4f          %10.5f\n',Q4);
fclose(fid);

%===== END F F T =====

```

```
clc;
hold off;
N_I=4;
Im1=Hi(2); Im11=Hi(1); Im12=Hi(3); Im13=Hi(4);
Im1=Im1'
Im11=Im11'
Im12=Im12'
Im13=Im13'
Im1=input('Current magnitude=');
% N_I=input('Number of current harmonics=');
N_g=N_I;
% N_g=1;
S=input('Press a key....');
Nph=50; % c1-C2
Kb1=0.87
Db=0.05;
Ld=0.07;
Bm=0.6;
Kw1=0.94;
m=1;
slot=24;
Nzt=256;
n=2*Nzt; % alpha=0.0:(2*pi/n):2*pi;

t=0.0:(t_f/(1000*n)):t_f/1000;
% wt=w*t ;
wt=w*t+pi/2;

Fmo=Db*Ld*Nph*Im1*Bm;
q=slot/(p*m);
% Fmo=0.0;
N_l=N_LT;
Lo=L1;
L2m=L1/3;
Fmr=2*Im1*Nph/pi;
%Fmr=0;
Fmor=Lo*Fmr.^2/(8*Nph^2);
Fm2r=L2m*Fmr.^2/(8*Nph^2);

ONi(1)=1; ONi(11)=21;
ONi(2)=3; ONi(12)=23;
ONi(3)=5; ONi(13)=25;
ONi(4)=7; ONi(14)=27;
ONi(5)=9; ONi(15)=29;
ONi(6)=11; ONi(16)=31;
ONi(7)=13; ONi(17)=33;
ONi(8)=15; ONi(18)=35;
ONi(9)=17; ONi(19)=39;
ONi(10)=19;

% harmonic data
Kb(1)=Kb1;
Kb(2)=Kb1/3;
Kb(3)=Kb1/5;
Kb(4)=Kb1/7;
Kb(5)=Kb1/9;
Kb(6)=0.2;
Kb(7)=0.12;
Kb(8)=0.09;
Kb(9)=0.07;
Kb(10)=0.05;
```

Kb(11)=0.07

Gama(1)=1; Gama(6)=11;
 Gama(2)=3; Gama(7)=13;
 Gama(3)=5; Gama(8)=15;
 Gama(4)=7; Gama(9)=17;
 Gama(5)=9; Gama(10)=19;
 Gama(11)=21

Lh1(1)=2; Lt(1)=L2m;
 Lh1(2)=4; Lt(2)=L2m/4;
 Lh1(3)=6; Lt(3)=L2m/6;
 Lh1(4)=8; Lt(4)=L2m/8;
 Lh1(5)=10; Lt(5)=L2m/10;
 Lh1(6)=12; Lt(6)=L2m/12;

alpha=pi/6;
 Beta=-pi/4;

% alpha=pi/2;
 % Beta=+pi/2;

% The Electromagnetic torque versus the space angle
 %=====

```

clc;
Tem2t=0;
% for ii=1:1:n                    % time cycle
for ii=1:1:n-2
    sum22=0;
    ii=ii'
    sum1x_r=0; sum2x_r=0; sum3x_r=0;
for ni=1:2:N_I    %Current-harmonic cycle
    K_ni=Hi(ni+1)/Im1;
    sum11=0;
    ps_ni=psi_i(ni+1);
    if ni==1 ps_ni=ps_s1; else ps_ni=abs(ps_ni); end
    sum11_r=0; sum22_r=0; sum33_r=0;
for ng=1:1:N_g    % Winding factor cycle
    q=slot/(p*m);
    tay=slot/p;
    yai=tay-1;
    Gama_m=(2*pi)/slot;
    Gama_el=Gama_m.*p/2;
    Kpn=sin(ng*(yai/tay)*(pi/2));
    Kdn=(sin(ng*q*Gama_el./2))/(q*sin(ng*Gama_el./2));
    Kw(ng)=Kpn.*Kdn;
    A1=cos((Gama(ng)-ONi(ni))*wt);
    A2=cos((Gama(ng)+ONi(ni))*wt);
    A3=cos(ps_ni);
    A4=sin(ps_ni);
    X1_t= Kw(ng)*Kb(ng)*(A1*A3-A2*A4);
    sum11=sum11+X1_t;    % PM torque
    
```

%***** Rel*****

```

sum1r=0; sum2r=0; sum3r=0;
for il=1:1:N_l% Inductance harmonics
    Lh=Lh1(il);
    Kl=Lt(il)/L2m;
    
```

X1_r=(K_ni^2./Gama(ng))*Fmor.*(sin(2*(ONi(ni)*wt-Gama(ng)*alpha))-sin(2*(ONi(ni)*wt+Gama(ng)*alpha)));

```
sum1r=sum1r+X1_r;
X21_r=(K_ni^2./Gama(ng))*Fm2r.*(sin(2*(ONi(ni)*wt-Gama(ng)*alpha))-sin(2*(ONi(ni)*wt+Gama(ng)*alpha)));
X2_r=Kl.*X21_r.*cos(2*Lh*(alpha+Beta));
sum2r=sum2r+X2_r;
X34_r=(cos(ONi(ni)*wt-Gama(ng)*alpha)).*(cos(ONi(ni)*wt-Gama(ng)*alpha));
X35_r=(cos(ONi(ni)*wt+Gama(ng)*alpha)).*(cos(ONi(ni)*wt+Gama(ng)*alpha));
X36_r=2*(cos(2*ONi(ni)*wt)+cos(2*Gama(ng)*alpha));
X41_r=2*Fm2r.*Kl*Lh*(K_ni^2./Gama(ng)^2)*(X34_r+X35_r-X36_r);
X4_r=X41_r.*sin(2*Lh*(alpha+Beta));
sum3r=sum3r+X4_r;
end % L(h)
sum11_r=sum11_r+sum1r;
sum22_r=sum22_r+sum2r;
sum33_r=sum33_r+sum3r;

%***** Rel*****
end %Kw
sum1x_r=sum1x_r+sum11_r;
sum2x_r=sum2x_r+sum22_r;
sum3x_r=sum3x_r+sum33_r;

sum22=sum22+K_ni.*sum11; % PM torque

end% Ki
Tem2r= sum1x_r+sum2x_r-sum3x_r; % Rel Torque
% Tem2r=0;
% sum22=0;
Tem2=Fmo.*sum22;
Tem2t=Tem2+Tem2r;

end % t
[wt, Tem2t]'
T_av=mean(Tem2t);
T_av=T_av,

S=input('Press a key');
%=====Torque performance=====

for ii=1:1:n-nx
plot((w*t*180/pi), Tem2r , 'color', 'g', 'linewidth', 2, 'linestyle', '-' );
hold on;
plot((w*t*180/pi), Tem2 , 'color', 'R', 'linewidth', 2, 'linestyle', '-' );
hold on;
plot((w*t*180/pi), Tem2t , 'color', 'B', 'linewidth', 1, 'linestyle', '*' );
end

xlabel('Alpha, dg', 'fontweight', 'Bold');
ylabel('Torque, Nm', 'fontweight', 'Bold') ;
title(' Torque performance ', 'Fontweight', 'Bold');
% legend('with curent -harmonic spectrum');
grid on;
hold on;
S=input('Press .....');

%=====START F F T - Torque=====

clc;
N=1024;
% t=0:0.02/N:0.02;
% x=8*sin(2*pi*8*f1*t)+4*sin(2*pi*4*f1*t);
t=0:(0.02/N):0.02;
```

```

    Y_m=fft(Tem2t,N);
    for ji=1:1:(N/2);
        Ha_m=real(Y_m(ji));
        Hr_m=imag(Y_m(ji));
        Hq_m=sqrt(Ha_m^2+Hr_m^2);
        if ji==1 Hm(ji)=Hq_m*1/N; else
            Hm(ji)=Hq_m*2/N;
            end;
        % N_hm(ji)=(ji-1)*2 ;
        N_hm(ji)=(ji-1) ;

        if Hm(ji)<0.0 Hm(ji)=0.0; end;
    end;
% [N_hm, Hm]'
    ppy1=0;
    ppy1=Hm.*conj(Hm)/N;
    plot(N_hm(1:N/2),Hm(1:N/2));
% bar(N_hm(1:N/2),Hm(1:N/2));
    hold on;
    pause;
    hold off;
    S=input('Press a key');
    %===== Toque-harmonic file=====
    Q5=[N_hm;Hm];
    fid =fopen('Trq_har.M','w');
    fprintf(fid,'%12.8f %10.5f\n',Q5);
    fclose(fid);

%===== END F F T =====

% time cycle
    sum1=0; Irms=0; TCR=0;
    for ni=1:2:N_I %Current-harmonic cycle
        I_eff=Hi(ni+1)/sqrt(2);
        sum1=sum1+I_eff.^2;
    end% Ki
    Irms=sqrt(sum1);
    TCR=T_av/Irms;
    %=====
    sum1=0;TRF=0;
    for ji=1:2:(N/2);
        Tmn=(Hm(ji)/T_av).^2;
        sum1=sum1+Tmn;
        sum1=sum1,
    end
        TRF=sqrt(sum1-1);
        TRF=TRF,
% S=input('Press a key....');

    Pcu=R*Irms.^2;
    Pout=T_av.*speed/9.549;
    Ief1=Iml/sqrt(2);
    HF=sqrt((Irms./Ief1)^2-1);
    Irms=Irms,
    TCR=TCR,
    T_av=T_av,
    Pcu=Pcu,
    Pout=Pout,
    HF=HF,
    S=input('Press a key');

```



```

L_A1=0; L_A2=0; L_Ad1=0;L_Ad2=0;

for il=1:1:N_LT

    X_A1=Ltx(il)*cos(N_rt*al1);
    X_A2=Ltx(il)*cos(N_rt*al2);
    X_Ad1=-Ltx(il)*N_rt*sin(N_rt*al1);
    X_Ad2=-Ltx(il)*N_rt*sin(N_rt*al2);

    sum_A1=sum_A1+X_A1;
    sum_A2=sum_A2+X_A2;
    sum_Ad1=sum_Ad1+X_Ad1;
    sum_Ad2=sum_Ad2+X_Ad2;

end

L_A1=Lox+sum_A1;
L_A2=Lox+sum_A2;
L_Ad1=sum_Ad1;
L_Ad2=sum_Ad2;
%=====
X1=Rx/L_A2;
X2=L_Ad2/L_A2;
X3=Rx/L_A1;
X4=L_Ad1/L_A1;
X5=Vx_A1/L_A1+Vx_A2/L_A2;
Y1=1+X1.*da/2+X2.*da/2;
Y2=1-X3.*da/2-X4.*da/2;
Y3=X5.*da/2;
Ia2=Ia1*(Y2/Y1)+Y3/Y1;
Ia1=Ia2;
IZ(jz)=Ia2;

end %J
% ALFX(M)=al2*180/pi;

end % for
Ia2=Ia2,
N_zu=jz-2;
% [ ALFU,U1];
N_zu=N_zu,
S=input('Press a key....');
clc;
%=====
Q9=[ALFZ;IZ];
fid =fopen('Cur-dc.M','w');
fprintf(fid,'%12.8f %10.5f\n',Q9);
fclose(fid);

%=====
I_av=mean(IZ);
I_av=I_av,
S=input('Press a key....');
clc;
for jz=1:1:Nzt-1
    IZ(jz+Nzt-1)=IZ(jz);
    ALFZ(jz+Nzt-1)=180+ALFZ(jz);
end
for jz=1:1:2*Nzt-1
plot(ALFZ ,IZ , 'color','r','linewidth',2,'linestyle','- ');
end
    
```

```

        xlabel('alpha ,dg','fontweight','Bold');
        ylabel('Current ,A','fontweight','Bold') ;

title(' Brushless DC motor Current','Fontweight','Bold');
grid on;
hold on;
s=input(' Press.....');
hold off;
%=====
clc;
Nzt=Nzt,
    n=2*Nzt;%Is=20; Kw1=0.94;
    Kw1=0.97;
    Tr=0;Te=0; Tem1=0;
alpha=0:2*pi/n:2*pi;
alpha(1)=0.0;
    N_kw=Kw1*Nphd;
    beta=-0.0; Is=0;
    %Is=9;
    % beta=0;
% Fsx=N_kw.*Is; % dc current
for ii=1:1:n-2

    Is=IZ(ii);% wessles model
    ald=alpha*180/pi;
    Fsx=N_kw.*Is; % dc current
% Fsx=Fsx,
    X1=(-Fsx.^2)*(G2.*sin(2*(alpha-tita2))+G4.*sin(4*(alpha-tita4)));
    A=2*Go+(2*G2./3)*cos(2*tita2)-(2*G4./15)*cos(4*tita4);
    B=(4*G2./3)*sin(2*tita2)-(8*G4./15)*cos(4*tita4);
    X2=Fsx*Fr*(A.*sin(alpha)-B.*sin(alpha));
    Tr=X1 ;
    Te=abs(X2) ;
    Tem1=Tr+Te;
    %===== Total Torque S1, S2, & S3
    Tem2=Fmo.*sum22+Tem2r;
    Tem_tot=Tem2+Tem1;

end
Tav1=mean(Tem1);
    Tav_tot=mean(Tem_tot);

Tav1=Tav1,
Tav_tot=Tav_tot,
s=input(' Press.....');
clc;
    for ii=1:1:n-2
        plot(alpha*180/pi ,Tr ,'color','g','linewidth',2.0,'linestyle','-' );
        hold on;
        plot(alpha*180/pi ,Te,'color','r','linewidth',2.0,'linestyle','-' );
        hold on;
        plot(alpha*180/pi ,Tem1,'color','B','linewidth',1.0,'linestyle','*' );
    end

    xlabel('alpha ,dg','fontweight','Bold');
    ylabel('Torque ,Nm','fontweight','Bold') ;

title(' Brushless DC motor- A1-A2; B1-B2 ','Fontweight','Bold');
% legend('Tr-green,Te-red,Temtot-blue');
grid on;
hold on;

```



```
% DELTAM(M)=ALFA(2*M)-ALFA(2*M-1);  
%ALFAD(M)=ALFAM(M)*180/pi;  
% DELTAD(M)=DELTAM(M)*180/pi;  
% if M==NPT  
%ALFAM(M)=pi;  
% DELTAM(M)=pi-ALFA(2*M-1);  
%ALFAD(M)=ALFAM(M)*180/pi;  
% DELTAD(M)=DELTAM(M)*180/pi;  
%NPT=NPT+1;  
%else NPT=NPT;end  
end
```